

Distribution Agreement

In presenting this thesis or dissertation as a partial fulfillment of the requirements for an advanced degree from Emory University, I hereby grant to Emory University and its agents the non-exclusive license to archive, make accessible, and display my thesis or dissertation in whole or in part in all forms of media, now or hereafter known, including display on the world wide web. I understand that I may select some access restrictions as part of the online submission of this thesis or dissertation. I retain all ownership rights to the copyright of the thesis or dissertation. I also retain the right to use in future works (such as articles or books) all or part of this thesis or dissertation.

Signature:

Brian S. Wakeman

Date

Identification and characterization of MHV68 and KSHV ORF50 transcripts:
A potential role in type I interferon evasion

By
Brian S. Wakeman
Doctor of Philosophy

Graduate Division of Biological and Biomedical Science
Immunology and Molecular Pathogenesis

Samuel H. Speck
Advisor

Brian Evavold
Committee Member

Arash Grakoui
Committee Member

Jacob Kohlmeier
Committee Member

Anice C. Lowen
Committee Member

Mehul S. Suthar
Committee Member

Accepted

Lisa A. Tedesco, Ph.D.
Dean of the James T. Laney School of Graduate Studies

Date

Identification and characterization of MHV68 and KSHV ORF50 transcripts:
A potential role in type I interferon evasion

By

Brian S. Wakeman
B.S., Wake Forest University, 2006
M.S., University North Carolina Greensboro, 2008

Advisor: Samuel H. Speck, PhD

An abstract of
A dissertation submitted to the Faculty of the
James T. Laney School of Graduate Studies of Emory University
in partial fulfillment of the requirements for the degree of
Doctor of Philosophy
in Graduate Division of Biological and Biomedical Science
Immunology and Molecular Pathogenesis
2015

Abstract
Identification and characterization of MHV68 and KSHV ORF50 transcripts:
A potential role in type I interferon evasion

By Brian S. Wakeman

Gammaherpesviruses are a lymphotropic subfamily of *Herpesviridae*, characterized by their ability to establish a lifelong infection within a host. The human gammaherpesviruses are further subdivided into the genera lymphocryptovirus containing Epstein-Barr (EBV or HHV-4), and rhadinovirus containing Kaposi's Sarcoma-Associated Herpesvirus (KSHV or HHV-8). Human gammaherpesviruses demonstrate widespread infectivity resulting in approximately 90% of the world population showing signs of latent EBV infection, and to a lesser extent KSHV infection. While these high infectivity rates are hypothesized to shape the overall global human immune profile, they are usually without major consequences in healthy individuals. This lack of consequences however changes in immunocompromised individuals and those experiencing secondary infections, left untreated EBV and KSHV have been associated with lymphoproliferative disease and lymphomagenesis.

Complicating studies of gammaherpesviruses is the highly host specific nature of human infection which results in the use of an animal model utilizing Murine Herpesvirus-68 (MHV68). MHV68 shares large sequence homology with both KSHV and EBV, and one of the most highly conserved genes is that of Orf50, which encodes the protein RTA (Replication and Transcriptional Activator), which acts as a switch between acute and latent infection. The importance of RTA within the viral lifecycle makes it a prime target for drug therapeutics and other potential medical interventions such as vaccines resulting in a critical need for further study and investigation.

In this study, we identified three previously unknown MHV68 Orf50 transcripts driven by two previously unknown promoters. We demonstrate that these previously unidentified transcripts retain the ability to drive lytic replication in absence of the previously known transcripts as well as reactivate latently infected virus; however this ability is only observed in the absence of a type I interferon response. Further we identified three previously unknown KSHV transcripts driven by two previously unknown promoters. Unlike MHV68 these KSHV transcripts result in unique isoforms of RTA. These unique isoforms, while maintaining many similar characteristics of known RTA, result in a different viral gene expression profile. These studies further the understanding of the essential lytic protein RTA and help shed light on the complex process regulating the lytic/latent cycle.

Identification and characterization of MHV68 and KSHV ORF50 transcripts:
A potential role in type I interferon evasion

By

Brian S. Wakeman
B.S., Wake Forest University, 2006
M.S., University North Carolina Greensboro, 2008

Advisor: Samuel H. Speck, PhD

A dissertation submitted to the Faculty of the
James T. Laney School of Graduate Studies of Emory University
in partial fulfillment of the requirements for the degree of
Doctor of Philosophy
in Graduate Division of Biological and Biomedical Science
Immunology and Molecular Pathogenesis
2015

Acknowledgements

I first would like to thank my mentor Dr. Sam Speck for all of his guidance, wisdom, and support in the completion of this dissertation work. His style of mentoring has allowed me to grow and become the type of independent thinking scientist I am today. He is always there when you need him but allows you to solve problems on your own and for that I will forever be thankful. I would also like to thank my lab members past and present. Many people have passed through the lab from the time I entered and each one of them I consider a friend and colleague. From help with designing experiments to doing actual lab work the support the Speck lab shows each other is tremendous. Even long after leaving lab I must thank former members for taking time to help solve problems when they have no obligation to do so. I would also like to thank my committee. Though we had few meetings their guidance and support has helped shape this dissertation to what it is today. Their doors are always open to discuss whatever problems I may be encountering and for that I am grateful. Finally I would like to thank my friends and family. Graduate school is a long and tedious process and without them I would not have made it through. To my parents I say thank you for supporting me well beyond anyone should. I could not ask for better role models. Finally I would like to thank Luci; you have been through pretty much all of this with me. You are always my biggest fan, there to give me encouragement and support and I love you for it.

TABLE OF CONTENTS

Chapter 1: Introduction	1
1.I. General background	
i. Herpesviridae.....	1
ii. Epstein-Barr Virus (EBV).....	5
iii. Kaposi's Sarcoma-Associated Virus (KSHV).....	7
iv. Murine Herpesvirus 68 (MHV68).....	10
1.II. The Replication and Transcriptional Activator (RTA) protein	
i. Function.....	15
ii. Transcriptional activation by RTA and its regulation.....	18
1.III. Type I interferon response	
i. General background.....	21
ii. Type I interferon effect.....	23
iii. Type I interferon effect in gammaherpesviruses.....	25
1.IV. Figure legends	29
1.V. Figures	30
Chapter 2: Identification of alternative transcripts encoding the essential murine gammaherpesvirus lytic transactivator RTA	32
2.I. Abstract	34
2.II. Introduction	36
2.III. Materials and Methods	39
2.IV. Results	50
2.V. Discussion	66
2.VI. Figure legends	71
2.VII. Figures	77

Chapter 3: Identification of novel KSHV Orf50 transcripts: discovery of new RTA isoforms with variable transactivation potential.....	87
3.I. Abstract.....	89
3.II. Introduction.....	90
3.III. Materials and Methods.....	93
3.IV. Results.....	100
3.V. Discussion.....	110
3.VI. Figure legends.....	116
3.VII. Figures.....	120
Chapter 4: Conclusions and Future Directions.....	127
4.I. The MHV68 exon N3, exon N4, exon N5 and their promoters.....	128
4.II. Type I interferon sensitivity.....	133
4.III. The new KSHV transcripts and their promoters.....	137
4.IV. Summary.....	139
4.V. Figure legends.....	140
4.VI. Figures.....	143
Literature Cited.....	149

LIST OF FIGURES and TABLES

Chapter 1:

1. Depiction of kinetics of MHV68 lytic and latent infection when administered through i.n. challenge
2. Schematic illustrating known RTA splicing in the gammaherpesvirus family

Chapter 2:

1. Genomic Alignment of Orf50/BRLF1/Rta region from MHV68, EBV, KSHV, and HVS gammaherpesviruses illustrating the conserved organization of gene 50 transcription
2. Promoter deletions within the MHV68 E0 250bp promoter region
3. Generation of MHV68 G50DbIKo and G50DbIKo.MR viruses
4. G50DbIKo virus replicates *in vitro* in Vero-Cre cells, but fails to replicate in NIH 3T12 fibroblasts
5. G50DbIKo virus fails to replicate *in vitro* when IFN α is present
6. Single-step growth analyses of the G50pDbIKo mutant, and analysis of the kinetics of RTA expression
7. RACE analyses reveal three additional G50 exons upstream of E0
8. Promoter activity in the region immediately 5' to MHV68 N3, N4, and N5 exons
9. Immunoblot analyses of RTA protein expression levels in WT and G50DbIKo infected NIH 3T12 fibroblasts, C57BL/6 MEFs, and 129S2/SvPas.IFN- α / β R^{-/-} MEFs
10. G50DbIKo virus exhibits a severe reactivation defect and a moderate latency defect *in vivo*
11. Infection of 129S2/SvPas.IFN- α / β R^{-/-} mice with G50DbIKo virus does not result in lethality as seen with WT virus despite the presence of high viral titers in the lungs
12. G50DbIKo virus establishes latency and reactivates to similar levels as WT Virus when used to infect 129S2/SvPas.IFN- α / β R^{-/-} mice *in vivo*
13. Promoter activity in the region immediately 5' to the MHV68 proximal promoter and proximal promoter deletion

Table 1. Summary of virus latency and reactivation

Chapter 3:

1. RACE analyses and primer walking reveal the existence of six G50 exons upstream of exon 2
2. Upstream exons extend the KSHV G50 open reading frame to form unique RTA isoforms.
3. Promoter deletions of the four G50 promoters identify minimal promoter length as well as activity in various cell types
4. Transactivation of Orf50 promoters by isoform 1 (E1-E2) and isoform 4 (N5-E2) RTA
5. Promoter truncation from 1000bp to 100bp within the KSHV E1, E0A/B, N3/4 and N5 promoters showing essential region required for E1-E2 isoform 1 RTA transactivation
6. KSHV Orf50 promoter region transactivation by XBP-1, transactivation by IL-4, and inhibition by IFN γ
7. Promoter activity of various KSHV Orfs transactivated by either E1-E2 isoform 1 RTA or N5-E2 isoform 4 RTA
8. KSHV b-ZIP and PAN promoter activity when transactivated by E1-E2 isoform 1 RTA or N5-E2 isoform 4 RTA in virus containing cells

Chapter 4:

1. IL-4 promotes viral replication and antagonizes IFN γ suppression of viral replication through the Orf50 promoter
2. G50E1SaKo virus displays a growth defect *in vitro* when IFN α is present
3. G50N4/N5pKo virus exhibits a reactivation defect while the Orf47.Stop virus displays a hyper reactivation defect *in vivo*
4. G50Db1Ko virus displays a growth defect *in vitro* when PKR or RNaseL is functional
5. Immunoblot analysis of eIF α phosphorylation levels in WT or G50Db1Ko virus infected NIH 3T12 fibroblasts
6. Generation and infection of 129S2/SvPas.IFN α / β R $^{-/-}$ chimeric mice.
7. KSHV isoform 1 and isoform 4 RTA show varying transactivation potential on viral promoters

Chapter 1: Introduction

1.I General Background

1.I.i. *Herpesviridae*

Viruses are complex, unique infectious agents, displaying a wide range of host and cellular tropism, genetic organization, and disease outcomes. Viruses are as old as life itself, co-evolving through the years with their hosts in what amounts to an arms race at the cellular level. Humans have evolved remarkable abilities to deal with the ever present threat viral infection poses, from the ancient innate immune system, to the more complex adaptive immune response, the back and forth between viruses and the human immune system has resulted in a tug and pull that is essential for our existence. One such virus family, *Herpesviridae*, has been evolving with humans for millions of years with modeling placing the alphaherpesvirus varicella-zoster virus (VZV) at over 400 million years old (85).

Herpesviruses as a family are double-stranded DNA viruses with large and complex genomes ranging between 120 to 250Kb in size, and encoding over 70+ genes. The herpesvirus virion consists of linear DNA wrapped in an icosahedral protein capsid, which itself is surrounded by a tegument consisting of various proteins and viral mRNAs which are thought to initiate viral replication upon host cell entry. To aid in entry, the outer layer of the virion is a lipid bilayer envelope which contains various viral glycoproteins used in viral entry and cellular fusion. Three to four of these glycoproteins are essential for viral entry. The three known essential glycoproteins conserved amongst all herpesviruses are designated gB, gH, and gL with gB containing the highest degree of homology amongst all herpesviruses.

Upon cellular binding entry occurs through fusion of the virion lipid bilayer with the cellular membrane. After binding the viral capsid travels to a nuclear pore where the linear viral DNA is released into the nucleus and circularizes. Gene transcription occurs through viral DNA transcription into viral mRNA using host machinery and RNA polymerase II. This early viral gene transcription and the genes transcribed are known as immediate-early lytic gene expression. The transcribed viral mRNA leaves the nucleus as if it were host mRNA and is translated within the cytoplasm resulting in the generation of immediate-early viral proteins. Many of these proteins act as transcription factors in a cascade of viral gene expression. The proteins traffic back to the nucleus where they bind viral promoters, along with host cellular transcription factors, resulting in a second round of viral mRNA transcription and translation. This second round of transcription is known as early gene transcription. The products of early gene transcription are translated and aid in viral inhibition of host defenses and shutdown of normal host cellular processes allowing for easier hijacking of the transcription and translation pathways. Finally viral DNA synthesis occurs at lytic origins of replication and viral genomes are transcribed as long sequences through a process known as rolling circle replication. This provides the necessary template for final late gene expression. Many of the late genes are viral structural proteins such as glycoproteins and provide the necessary framework for viral capsid assembly. Full length viral DNA is packaged within empty capsids that have entered the nucleus and go on to form nucleocapsids; these nucleocapsids associate with segments of the nuclear membrane where various viral tegument and envelope proteins have bound and accumulated. The association with these proteins results in envelopment by budding through the nuclear membrane. Mature virions are released from the cell by exocytosis, but often virions accumulate in the endoplasmic reticulum overwhelming cellular stability. When enough virus has

accumulated within a cell, the cells will lyse releasing all accumulated mature virions. Mature virions go on to infect other healthy cells and continue the process of lytic replication.

Herpesviruses display incredible worldwide distribution and have been discovered in many vertebrate species from non-human primates to ticks feeding on reptiles (66). Herpesviruses have two very interesting features: first viruses display a very narrow host range usually resulting in a single species infection. Second, all herpesviruses are characterized by their ability to infect and persist for the lifetime of the host. This lifelong infection is the result of a process named latency in which the virus establishes a noncytopathic infection resulting in limited viral gene expression and the absence of viral progeny. This latent infection is often cellular specific in which latency is established in a single unique subset of cells. Despite entering latency virally infected cells can once again enter the lytic cycle of gene expression which results in the generation of infectious viral progeny through a process known as reactivation. It is believed that despite well established latency, there are constant sporadic viral reactivation events which lead to limited viral replication and reseeding of the latency reservoir. Reactivation from latency can occur for a variety of reasons, and the virus has evolved many ways to sense the environment in which it resides. Sporadic reactivation can be triggered from natural cellular turnover such as apoptosis to the sensing of an opportunistic environment caused by a secondary infection. Despite these sporadic reactivation events herpesviruses latency is unique and differs from other chronic acute infections. With minimal viral gene expression the viral genome is maintained as an episome within the host nucleus, replicating when the cell replicates using host DNA polymerase as opposed to the viral DNA polymerase used during lytic infections. At present time there has been only one identified herpesvirus species, HHV-6, that

has been shown to actually integrate in the host genome, though the process can't be ruled out amongst other species (119).

Herpesviruses are found within birds and mammals can further be divided into three different subfamilies: alpha, beta, and gamma. All herpesvirus subfamily members share similar viral characteristics related to establishment of latency, reactivation, and viral replication as mentioned above. They do differ greatly in sequence homology, unique subsets of genes, and most importantly cellular tropism. Alphaherpesviruses include the human viruses Varicella-Zoster Virus (VZV), which leads to chickenpox and shingles, and Herpes Simplex Viruses-1 and 2 (HSV-1 and HSV-2), which leads to genital herpes and cold sores. Alphaherpesviruses are categorized by their ability to infect and establish latency within neurons. Betaherpesviruses include Human Herpesvirus-6 and 7 (HHV6 and HHV7), which are associated with a range of secondary conditions such as rash, fever, and respiratory disease. Betaherpesviruses are better known for human cytomegalovirus (hCMV) and its model of study murine cytomegalovirus (mCMV). hCMV is associated with complications during pregnancy resulting in hearing loss as well as a range of complications in immunocompromised individuals. Betaherpesviruses express broad cellular tropism, but hCMV is most often associated with salivary glands. The final subfamily of herpesviruses is the gammaherpesviruses which include the human viruses Epstein-Barr Virus (EBV), which is associated with infectious mononucleosis during primary infection, as well as Kaposi's Sarcoma-associated Herpesvirus (KSHV) which often is asymptomatic for immunocompetent individuals. All gammaherpesviruses are associated with infection and establishment of latency in lymphocytes. It is also worth noting murine gammaherpesvirus-68 (MHV68), a naturally occurring rodent gammaherpesvirus, is used extensively as a model of gammaherpesvirus infection and the subject of a majority of the work discussed.

1.1.ii Epstein-Barr Virus (EBV)

Epstein-Barr virus was the first gammaherpesvirus discovered through observations by Michael Epstein and Yvonne Barr in 1964 and is a member of the lymphocryptovirus genus (63). Later it was discovered that EBV was associated with infectious mononucleosis as well as exhibited the ability to transform B cells into a continuously proliferating cell line known as LCLs (93, 94, 179). This discovery of cellular transformation was the first known incidence of an oncogenic virus and the association of viral infection with cancer. What made this discovery even more fascinating is that 95% of the world's population is infected with EBV by adulthood. EBV takes advantage of the host's own immune system to infect, replicate and establish latency in B-cells, a cellular compartment which often times has low turnover and itself can persist for the lifetime of a host (104, 162). Often a primary infection of EBV will go unnoticed or assumed to be a common viral infection resulting in cold like symptoms. However EBV requires a strong T-cell response to control initial infection and if this response is overwhelming the resulting immunopathology leads to a condition known as infectious mononucleosis. Primary infection resulting in infectious mononucleosis symptoms occur in less than 30% of individuals infected more so in those with infection delayed until adolescence. Regardless of symptoms associated with primary infection, all individuals infected remain so, as EBV establishes lifelong latency within the memory B-cell compartment.

Though primary infection by EBV appears to have no infectivity preference between naïve and memory B cell populations, establishment of latency is found to be concentrated in IgD⁻CD27⁺ memory B cell subsets (8, 96). The establishment of EBV latency is associated with a limited set of viral gene products consisting of three latency membrane proteins (LMP 1,2A and 2B) as well as six Epstein-Barr nuclear antigens (EBNA 1, 2, 3A, 3B, 3C and LP). Though

primary EBV infection is self limiting and establishment of latency itself is unproblematic, together the expression of these EBV proteins is what provides the basis of cellular transformation. Although some latency associated proteins such as LMP-1 alone are oncogenic, cellular transformation requires multiple EBV latency gene expression. LMP-1 mimics a constitutively active form of the CD40 receptor allowing for CD4 T cell help and differentiation into memory B cells and plasma cells (61, 65, 125). EBNA-1 is responsible for binding viral DNA and maintaining the viral genome during cellular division while EBNA-2 mimics the Notch signaling pathway and increases cellular proliferation (92, 97, 136, 294). EBV is unique in that it can establish three different latency programs and these programs differ in the latency genes expressed. It is believed that EBV progresses in order through Latency III to Latency II and finally Latency I, which also coincides with decreased latency gene expression (121, 221).

Like all herpesviruses EBV retains the ability to reactivate from latency and enter an acute phase of replication. For EBV it has been shown that stimulation of the B cell receptor is enough to trigger reactivation from latency. EBV contains two immediate-early lytic genes known as BRLF1 (RTA) and BZLF1 (ZTA) (123, 199, 212, 287). These two lytic proteins function as transcriptional activators of various cellular and viral genes, and expression of each alone is enough to reactivate cells from latency (45, 91, 99, 122, 199, 249, 287). Through binding to specific ZTA or RTA response elements found within viral gene promoters these two lytic genes are able to start the cascade of gene expression. It is important to note that while each individual protein can initiate viral replication alone, the expression of either ZTA or RTA results in the expression of the other (86, 227, 287). While *in vitro* BCR crosslinking is enough to reactivate latent cells indicating that *in vivo* activation of latently infected cells may result

from B cell exposure to antigen, many other external triggers such as cellular stress, inflammation, and cytokines may also trigger reactivation.

While this lifelong infection with EBV is uneventful to the majority of individuals infected, it has been associated with a variety of life-threatening diseases. EBV has been linked with endemic Burkitt's lymphoma, Hodgkin's lymphoma, nasopharyngeal carcinoma, T cell lymphomas, and lymphomas associated with immunocompromised patients. All related EBV malignancies demonstrate EBV latency genes within solid tumors and enhance immune responses, mostly antibody titers. Endemic Burkitt's lymphoma is connected with sub-Saharan Africa and coinfection with malaria (207, 246). Though non-EBV associated Burkitt's exists all cases are characterized by the translocation of c-myc (191). Like Burkitt's, Hodgkin's lymphoma can also be unassociated with EBV. Hodgkin's lymphoma that is EBV associated may result from the expression of EBV latency genes that prevent the apoptosis of infected cells leading to the accumulation of mutations that promote lymphoma (115). Nasopharyngeal carcinoma is highly endemic to Southeastern Asia and is the result of EBV transformation occurring during epithelial infection and latency (198). Finally, lymphomas related to immunocompromised patients, either through the result of HIV infection or immune suppression drugs taken for transplant, are the result of EBV outgrowth from the lack of T cell associated control (30, 283)

1.1.iii Kaposi's Sarcoma-Associated Herpesvirus (KSHV)

Unlike EBV the discovery of KSHV occurred much more recently. This recent history is despite the fact that Kaposi's Sarcoma, for which the virus bares its namesake, was first described in 1872 by a dermatologist named Moriz Kaposi (116). Despite this discovery there was much controversy surrounding the causative agent of the observed Kaposi's sarcoma,

especially upon observations made during the AIDS epidemic that 50% of AIDS patients reported development of Kaposi's sarcoma (216). It wasn't until the work of Yuan Chang and Patrick Moore in 1994, who successfully isolated KSHV from a KS tumor, that KSHV was finally identified (36, 165). This discovery provided the foundation for the knowledge we have now obtained about KSHV. First, despite being a gammaherpesvirus subfamily member it differs from EBV in that it is of the genus rhadinovirus instead of the genus lymphocryptovirus. One difference of many between the two is that rhadinoviruses have been observed in wide range of mammalian hosts while lymphocryptovirus have only been identified in primates. One reason for the recent discovery of KSHV is because primary infection in healthy individuals is completely asymptomatic, showing no signs of infection unlike EBV. Due to this, the route and nature of primary KSHV infection is relatively unknown. It is known that like all herpesviruses once an individual becomes infected with KSHV they will remain infected for life. It is also known that the seroprevalence of KSHV is much lower than the 95% observed in EBV, and there is a range dependent on geographical location. The low range of seroprevalence is 2-4% found in the majority of locations, with that range increasing with up to 40% of individuals infected in sub-Saharan Africa (21, 211).

While a hallmark of EBV infection is its ability to transform B cells, so far KSHV has failed to generate immortalized B cell lines. This is further supported by the lack of KSHV homologs to EBV genes that have been identified as requirements for immortalization. Despite the lack of these homologs, KSHV encodes several unique genes that play a role in the development of clinical disease and oncogenesis. One unique gene is the latency-associated nuclear antigen (LANA) which acts like EBNA-1 by tethering the viral genome to cellular chromosomes. This allows the virus to remain latent and replicate as the infected cell undergoes

replication. LANA differs in its ability to alter various cellular pathways which contribute to oncogenesis. For example LANA has the ability to associate with p53 and block p53's ability to mediate transcription and apoptosis (70, 117). In addition to LANA, unique KSHV genes include the expression of a cyclin D homolog (v-cyclin), Kaposin family of proteins, viral interferon regulatory factors (IRF), a Flice inhibitory protein (FLIP) homology (v-FLIP), and finally a membrane associated protein K1. All of these proteins exhibit potential oncogenic properties; v-cyclin has the ability to promote cell cycle progression and overcome senescence (113, 290), Kaposin proteins have been shown to inhibit the degradation of cytokine signaling such as GM-CSF (158), vIRF proteins block the type 1 and 2 interferon response as well as suppresses p53 (72, 173, 223), v-FLIP inhibits cellular apoptosis despite FAS-induced signaling (15), and K1 encodes a membrane protein that mimics constitutively active BCR signaling (133, 134). KSHV also differs in its ability to reactivate from latency as it lacks a BZLF1 homolog and only encodes one immediate-early lytic gene Orf50 (RTA). Despite this difference, reactivation and the properties of Orf50 are similar to those of BRLF1 previously described and will be elaborated on later in this chapter.

Like EBV, infection with KSHV results in a self-limiting uneventful primary infection in immunocompetent hosts. This, also like EBV, is not the case in individuals who are immunocompromised like those infected with HIV. Diseases associated with KSHV are Kaposi sarcoma (KS), primary effusion lymphoma (PEL), and multicentric Castleman's disease (MCD). KS is marked by reddish brown and purple lesions of the skin, is highly associated with AIDS, and is an endothelial-associated vascular tumor (213). PEL is a unique form of Non-Hodgkin's lymphoma that is also highly associated with AIDS patients. PEL cells come from a clonally expanded B cell population and may be KSHV singularly infected or EBV/KSHV infected (7,

101, 217). Finally, MCD is only associated with KSHV in its plasmablastic variant and is associated with increased expression of IL-6 (230).

1.1.iv Murine Herpesvirus 68 (MHV68)

While *in vitro* cell culture systems exist for the study of EBV and KSHV, their narrow host tropism prevents extensive *in vivo* studies from being conducted. While some studies have been conducted using chimeric mice and humanized mouse models, these studies are severely limited especially in the context of host immune response to viral infection. To overcome this obstacle an animal model was required to investigate primary infection, establishment of latency, and reactivation in the context and progression of a naturally occurring infection. There are various non-human primate gammaherpesviruses such as herpesvirus saimiri (HVS) and rhesus lymphocryptovirus (RLV) that have been used to generate limited data from *in vivo* studies, but these studies are small and complicated by cost and facilities needed to house non-human primates (1, 163, 168). For these reasons the discovery of a robust small-animal model was necessary for the field. Murine gammaherpesvirus 68 (MHV68) has emerged as the leading small-animal model for *in vivo* gammaherpesvirus studies. MHV68 was isolated in 1980 from bank voles and yellow-necked field mice located in Slovakia (19). Further studies have identified wood mice as the major endemic reservoir for MHV68 infection, while also identifying another related gammaherpesvirus (WMHV) (18, 103).

While the natural course of infection in wild animals is unknown, MHV68 is able to readily infect laboratory strains of mice. Currently the natural route of infection is unknown in MHV68 transmission. Many studies have been conducted to elucidate an answer but results have been inconclusive. Some evidence suggests the natural route of transmission may be through

intranasal (I.N.) infection while more recent evidence points towards a sexual route of infection (69, 175). Largely intranasal infection in laboratory settings has been adopted as the standard route of infection for experiments. Upon intranasal infection with MHV68 there is an acute phase of replication that occurs in the alveolar epithelial cells of the respiratory tract (242). This acute phase replication is detectable by day 4 in the lungs by plaque assay, with viral titers peaking around day 9, and becoming undetectable by 12 days postinfection (Fig.1). While acute phase replication occurs in the lungs it has also been detected in salivary glands, thymus, and omentum (82, 106, 160). From the lungs the virus traffics to distal organs like the spleen by infecting either resident B cells of the lung or circulating B cells. The importance of B cells for viral trafficking has been shown with μ MT mice which lack B cells. Infection in these animals results in a failure of the virus to traffic from the lungs and establishing latency (251, 262). After the virus leaves the lungs and travels to the spleen, establishment of latency begins in which viral genes are silenced, occurring between days 12 to 18 postinfection. At day 18 almost no lytic virus is detectable in the spleen, this is despite the fact that 1 in 100 splenocytes contain MHV68 latent genomes and approximately 1 in 5000 splenocytes are capable of reactivating in tissue culture (267). These numbers represent that absolute peak of infection and latency in the spleen, as latency will retract through an unknown mechanism to a predetermined latency set point. While at 42 days postinfection, lytic reactivation from splenocytes is undetectable with current methods; thus, it is hypothesized that sporadic reactivation occurs throughout the lifetime of infection. It is believed that latently infected B cells are poised to reactivate upon external stimulation either through BCR signaling or environmental triggers (73, 169).

While intranasal inoculation is used in what is considered a “natural” route of infection other times an intraperitoneal (I.P.) route of infection is used for study. This route is used

because the other site of latency has been determined to be the peritoneum where the major cell types harboring latent MHV68 virus are macrophages and dendritic cells (263). While establishment of latency in the peritoneum occurs following intraperitoneal and intranasal routes of infection, the initial seeding and reactivation is higher in PECs (peritoneal exudates cells) following intraperitoneal infection. In the peritoneum MHV68 is also able to establish latency by day 18 just as it is seen in splenocytes. One variation of this is that reactivating virus can be measured out 3 to 6 months postinfection (263). This later measurement of reactivation is hypothesized to occur because of the cellular environment in which latency is occurring. While splenocytes and a memory B cell population are somewhat self contained, PECs are much more readily exposed to the environmental conditions of the host. Despite difference in reactivation, the “latency pool” remains fairly stable in both PECs and splenocytes throughout the lifetime of a host. It is also important to note that the inoculation dose has no bearing on the establishment of the “latency pool”. A higher dose or lower dose of infection results in altered kinetics in the establishment of latency, but these altered kinetics result in the same levels of latency overtime as the latency pool contracts to what appears to be a particular viral latency set point. At this time it is unknown what triggers and determines the latency set point as well as how this set point is maintained overtime.

Like both EBV and KSHV, MHV68 is a member of the gammaherpesvirus family, but is more closely related to KSHV, being a member of genus rhadinovirus. The complete genome of MHV68 was sequenced in 1997 and revealed a high degree of homology between both EBV and KSHV not only in genes but genomic structure as well (255). All of these genomes are between 150-182 Kb in size, and the genes are organized by lytic and latent regions which allows for a cascade of gene expression to occur. All of the genomes contain GC-rich sequences at the ends

of the genome which repeat, and are referred to as terminal repeat regions. All of the genomes also encode several unique mRNA and tRNAs whose function is still being determined. There is a high degree of conservation among viral Orfs which encode the major structural and capsid proteins of the viruses. This is also true for viral specific genes like those that encode the viral DNA polymerase and are involved in viral replication. The ability of MHV68 to infect many different cell lines, as well as its use in an animal model, has allowed for the function of many of these MHV68 Orfs and subsequently there KSHV and EBV homologs to be determined (166, 229).

Despite some difference in the viral genomes, MHV68 infection in a mouse is very similar to gammaherpesvirus infection observed in humans. During primary infection with MHV68 a mononucleosis-like syndrome is observed in which there is a large expansion of lymphocytes (226). This expansion of lymphocytes is also marked by splenomegaly, which is a symptom often seen during primary EBV infection in response to the replicating virus. Another hallmark of EBV infection is the clonal expansion of a CD8+ T cell population through the activation of TCRs (27). This clonal CD8+ T cell expansion is also seen during MHV68 infection and is induced by the non-homologous M1 gene (64, 129). The clonally expansion is seen approximately 28 days postinfection and peaks by day 42. This clonal expansion results in nearly 50% of all CD8+ T cells having a V β 4 subtype. Another important similarity between MHV68 and the human gammaherpesviruses is that acute infection takes place in epithelial and endothelial cells and that latency occurs in lymphocytes. It is believed that MHV68 models the same track of infection as EBV and KSHV where the virus acutely replicates at the site of infection before trafficking to sites of latency. The sites of latency for both EBV and MHV68 have been determined to preferentially be the memory B cell population, more specifically the

IgD⁻, CD27⁺ class-switched memory B cells population (32, 262, 267). One historical criticism of the MHV68 model is the lack of tumorigenesis observed in infection with MHV68. This however would be a rare occurrence due to the fact that, like EBV and KSHV, the virus is well controlled in an immunocompetent individual. In these individuals the virus acutely replicates, seeds a latency reservoir and is controlled well for the lifetime of infection. Like immunocompromised individuals, mice with deletions to key immunoregulatory or tumor suppressor genes are actually prone to MHV68 tumorigenesis. One such example is mice that lack β 2-microglobulin in a BALB/C background, where infection with MHV68 has been shown to result in lymphomas and a type of lymphoproliferative disease (209, 241, 244, 250). Recently it has also been shown that MHV68 can result in the immortalization of fetal-liver derived B cells and that injection of these immortalized B cells results in tumorigenesis (145, 146).

Many of the *in vitro* experiments conducted with EBV and KSHV have been confirmed *in vivo* using the MHV68 system. This has allowed for a deeper understanding of genes related to transformation mentioned in previous sections. While related to both EBV and KSHV, homology is greater with the KSHV genome due to the fact MHV68 is a rhadinovirus. This means that certain genes are found in both KSHV and MHV68 that are not found in EBV. Genes like LANA, v-Cyclin, and K3 are all encoded by both KSHV and MHV68. Like KSHV LANA is responsible for maintaining the viral genome as an episome during latency and viruses lacking LANA are severely impaired in the establishment of latency in the spleen following intranasal infection (68, 167). MHV68 v-Cyclin is similar to KSHV v-Cyclin in that it deregulates normal cell cycle progression but does differ in cellular CDK targets (98, 222). Finally MHV68 K3 is similar to KSHV K3 and K5 as it inhibits antigen presentation by MHCI and helps to avoid the host CD8 T cell response (44). While MHV68 is highly similar in structure, proteins, and viral

life cycle there are unique genes found within the MHV68 genome. These genes are labeled as M genes throughout the genome and have no known human gammaherpesvirus homologs. This is not to say that they do not represent pathways that are also manipulated by the human viruses. For example MHV68 encodes an M2 protein that is critical in the establishment of latency as well as reactivation from latency (95, 110). This critical role M2 plays is mediated by its ability to drive B cell proliferation through increased expression of IL-10 (201, 224). Though EBV does not encode an M2 gene product it does encode an IL-10 homolog indicating that manipulation of this pathway is shared across gammaherpesviruses (102, 236). The most important genes that can be studied using MHV68 are those that are homologous between all three viruses, MHV68, KSHV and EBV. This allows studies done in MHV68 to be applied to both human viruses. One of these genes is Orf50, the Orf that encodes the Replication and Transcriptional Activator (RTA) protein. This gene is conserved between all three viruses and is critical for replication and reactivation from latency. This critical gene is the focus of the work presented in this dissertation where it is investigated in the context of both MHV68 and KSHV.

1.II. The Replication and Transcriptional Activator (RTA) protein.

1.II.i Function

The MHV68 Orf50 gene, also known as RTA/Orf50 in KSHV and BRLF1 in EBV, is one of the most highly conserved genes among gammaherpesviruses. This high degree of conservation is because of the critical nature of the RTA protein, and its requirement for lytic replication during acute phase infection as well as viral reactivation from latency. RTA is the master regulator of the lytic cascade of gene expression, and the expression of MHV68 and KSHV transcripts are insensitive to cyclohexamide indicating that RTA is an immediate-early

gene (149, 240). More important than reactivation from latency is RTA's ability to promote general viral replication during the course of the initial primary infection. Viruses lacking RTA fail to replicate both *in vitro* and *in vivo* demonstrating the extreme importance of RTA in viral fitness (190, 272, 276). This points to the role that transcription of the RTA gene has upon immediate entry within a host cell and its role as a transcriptional activator of viral promoters. Without the expression of RTA and its binding to cellular promoters, downstream early and late viral genes fail to be expressed. Despite this initial critical nature during primary infection RTA also remains important for reactivation from latency following a similar cascade of gene expression, and the ectopic expression of RTA alone in certain gammaherpesvirus cell lines is enough to induce lytic reactivation from latency (14, 199, 205).

The highly conserved nature of RTA-coding region is not just in function but also in genomic location as well as organization. It had previously been shown that EBV, KSHV, and MHV68 all encode a two exon RTA, containing Exon 1 which in turn splices out a large intron while splicing to Exon 2. For the rhadinoviruses the ATG coding region of RTA is located upstream in the Exon 1 promoter. The promoter drives transcription from Exon 1, and the splicing of Exon 1 to Exon 2 extends the Exon 2 open reading frame. EBV differs from the rhadinoviruses in that the ATG coding region begins in Exon 2. The promoter however like KSHV and MHV68 is located upstream of Exon 1, and drives the transcription of an E1-E2 transcript where a large 5' untranslated region then exists upstream of the ATG initiation site within Exon 2. (Fig. 2). This Exon 1 to Exon 2 splicing was the only known RTA Exons until recently it was discovered that an upstream Exon identified as Exon 0 exists in all three viruses (81). This Exon 0 is driven by a unique and different promoter than Exon 1 and was appropriately named the distal promoter. Transcription from this promoter is actually found to

differ between MHV68 and KSHV. In MHV68 Exon 0 is spliced to Exon 1 which in turn splices to Exon 2. So far no Exon 0 to Exon 2 transcripts has been identified. The splicing of Exon 0 to Exon 1 does not extend the open reading frame of RTA and therefore the RTA protein generated remains the same between transcription driven off the distal or proximal promoter. This is different than what is found in KSHV where Exon 0 does not splice to Exon 1 but instead directly splices to Exon 2 (Fig. 2). This splicing out of Exon 1 results in a unique extension of the open reading frame and therefore the protein generated varies slightly between transcription driven by the distal and proximal promoter. Using MHV68 it has been shown that the newly identified transcripts are capable of driving lytic replication in the absence of the previously described proximal promoter transcript. The deletion of the proximal promoter does result in lower levels of latency as well as an inability to reactivate from latency in splenocytes (81). Surprisingly reactivation is unaffected in PECs which may indicate a role for different RTA promoters dependent on the type of cell infected (81). Even with the recent discovery of previously unidentified transcripts, the Orf50 region remains organized in a compact fashion located relatively in the middle of the genome. The Orf50 region lies in the middle of the Orf48 and Orf49 genes who are located on the opposite strand and transcription takes place in reverse orientation that that of RTA. The high degree of overlap between all three Orfs complicates manipulation of the region for experimental purposes as any mutations generated may be deleterious to transcripts running in the opposite direction. In fact transcriptional interference from opposite strands has been demonstrated in EBV for playing a role in the establishment and control of latency, and a similar role for Orf48 and Orf49 may exist to help regulate RTA (196, 270).

1.II.ii Transcriptional activation by RTA and its regulation

The conserved nature of RTA described above in its ability to control viral replication, reactivation from latency, and genomic organization points to RTA having a conserved role in its ability to act as a transactivator of other viral genes. It also points to RTA having a similar method of regulation amongst all gammaherpesviruses. One such factor of regulation is the ability of RTA to respond to the plasma cell-specific transcription factor XBP-1. This factor has been shown to upregulate KSHV, EBV and MHV68 RTA expression *in vitro* (48, 144, 156, 268, 285). The utilization of this highly cell specific transcription factor is a perfect example of gammaherpesviruses manipulating the environment in which they infect. As mentioned previously, the virus preferentially infects a memory B cell population. To do this the virus hitches a ride to the site of B cell expansion, the germinal center, in which B cells undergo rapid proliferation and expansion in response to antigen. Currently it is unknown if the virus specifically targets gammaherpesvirus antigen specific B cells or targeting is random. Either method results in the virus hijacking the B cell pathway and if the B cell is moved towards differentiation into a plasma cell the virus rapidly begins to produce viral progeny. This move from a B cell to a plasma cell requires the transcription factor XBP-1, so it is intuitive the virus would develop a way for the critical replication protein RTA to respond to this B cell differentiation. While *in vitro* studies have been very conclusive in the ability of the RTA promoter to respond to XBP-1, *in vivo* studies have not. Studies conducted using MHV68 in XBP-1 conditional knockout mice showed no effect on the lack of XBP-1 and the ability of the virus to replicate or reactivate from latency (156). This difference between *in vitro* and *in vivo* studies illustrates the importance of the MHV68 model and points to there being many more factors at play in XBP-1's ability to control RTA expression.

Other factors regulating the expression of RTA are cellular stress proteins. It is believed that the virus remains latent until some secondary event occurs which can trigger reactivation. The ability to respond to these events is critical for the gammaherpesvirus lifecycle and therefore the RTA promoter has been found to respond to many different cellular events beyond differentiation as mentioned above. One event would be oxidative stress and a low oxygen environment like the ones found in tumors, which is interesting in the context of gammaherpesviruses and their transforming properties. One transcription factor of stress is the hypoxia inducible factor (HIF), and it has been shown that the RTA promoter of gammaherpesviruses contain HIF-responsive elements (26, 90, 112, 195, 279, 289). The ability to respond to stress is important as the virus has the ability to sense the cellular environment and determine if reactivation from latency is ideal. Conditions in which the host is weakened from a secondary infection are ideal for reactivation and advantageous.

A very important component of RTA is its own ability to act as a transcription factor and target the up regulation of viral genes. Since RTA acts as one of the first proteins translated its main function in infection or reactivation from latency is to “awaken” other viral genes. Once translated the RTA protein traffics back to the nucleus where it binds to RTA Response Elements (RREs) found on many different viral promoters. The binding of RTA often induces a promoter anywhere from 10-1000 fold over resting activity. While RREs are more homologous within the MHV68 genome, they appear to be more fluid in the KSHV genome though attempts to determine consensus RREs have been undertaken. As you can imagine early lytic genes are primary targets of RTA transactivation and it has been shown that Orf57 and K8 are both upregulated by RTA (25, 189). It has also been shown that RTA often work in a feedback loop of activation and that activation of a downstream gene can often then bind RTA promoters and lead

to the generation of additional RTA. This binding of the RTA promoter is often in cooperation with cellular transcription factors, and it has been shown that RTA promoters can be activated by CBP/p300, AP-1 and SP-1 binding (67, 88, 142, 243, 280). Another factor that is upregulated by RTA and in turn also then cooperates with RTA is the KSHV K-bZIP protein. It has been shown that RTA can bind the K-bZIP promoter and this results in a significant increase in promoter activity, while in turn K-bZIP can function to eliminate the effect RTA has on other promoters, for example Orf57 (280). Complicating this is Orf57 upregulation by RTA leads to cooperation of Orf57 with RTA to regulate RTA's own promoter (55, 154). This highlights the complex nature of RTA where it can bind to different RREs leading to the increased expression of downstream genes, these downstream genes can then in turn upregulate or downregulate different genes themselves sometimes enhancing or decreasing the effect RTA has. There have been many other genes that have been identified that directly respond to RTA, this makes lytic replication and reactivation that much more complicated of a web. It has been shown that V-cyclin is upregulated by RTA, Orf73 is downregulated, Orf49 is upregulated and feeds back on RTA, Orf18 is upregulated, and the MHV68 M1 gene is upregulated in a synergistic fashion with IRF4 (4, 89, 100, 137, 181, 182). This complex regulation, downregulation and upregulation illustrates the reason why the Orf50 region is controlled by multiple promoters, transcriptional splicing, transactivators and silencers, as well as epigenetic regulations such as DNA methylation and histone acetylation (81, 83, 141, 170, 278). Without this careful control and regulation gammaherpesviruses would be unable to establish latency as well as be unable to sense the microenvironment around them leading to reactivation.

1.III. Type I interferon response

1.III.i General Background.

There is a constant struggle between host and pathogens in an attempt by pathogens to establish a productive infection. The reason why many of these attempts fail is the ability of the host to recognize foreign invaders and generate an appropriate response. For humans this response consists of three phases. Phase one is the ability of the body to simply prevent infection through physical barriers such as skin and mucous. The easiest way to prevent infection is to never allow it to enter the body. The second phase is the innate immune system which is the evolutionary distant immune response and considered the immediate response to infection. The innate immune response controls the initial infection allowing for more efficient control and clearance. While often the innate immune response is not enough to clear the infection, it is critical in preventing a widespread established infection from occurring. The final phase is the adaptive immune response; this response is evolutionarily newer than the innate immune response and is critical for clearance and long term control of an infection. Also important is the adaptive immune responses ability to form memory to a given pathogen; this memory often assures a secondary infection with the same or similar pathogen is mild to non-existent. In this discussion we will be focusing on the innate immune system which is comprised of many different response and cell types. Critical to these responses is the release of cytokines, and important for this work the release of type I interferons. While classified as an innate immune response type I interferons share an increasingly observed functional link to the adaptive immune response.

While the immune system can recognize bacteria and fungi which contain easily distinguishable microbe-specific components, viruses pose a unique set of problems in that they

are compromised almost entirely of adopted host components. One way that has evolved to detect viral infection is through nucleic acid recognition, specifically pattern recognition to help aid in the recognition of host-derived RNA and DNA from that of virus derived. Sensors to detect these patterns have been compartmentalized in areas in which viral replication exists such as extracellular fluid and lysosomes, also to aid this is host nucleic acids which eliminate self nucleic acids from the areas in which viruses are found (12, 282). Signaling of viral infection however does not require a cell to be infected, as certain innate immune cells such as macrophages and dendritic cells can engulf pathogens and stimulate a cytokine response without infection. One of the most important components to viral detection is Toll-like receptor (TLR) signaling, where several TLRs can distinguish different viral components. TLR3 is known to recognize double-stranded RNA, TLR 7 and 8 detect single stranded RNA, and finally TLR9 recognizes unmethylated CpG DNA (13, 57, 172, 184). In addition to TLR sensing of viral infection, cells also use an intracellular system of recognition mediated by RIG-I, MDA5, and a viral DNA sensor to trigger innate signaling (203, 238, 248). While sensing can occur on many cell types, key innate immune cells such as macrophages and dendritic cells are key to sensing viral infection and the generation of a primary immune response. One specialized subset of cells, plasmacytoid dendritic cells (pDCs) are responsible for the generation of large concentrations of type 1 IFNs in response to signaling (24, 43).

The type I interferon (IFN) family is a critical outcome of viral surveillance. IFNs can affect many cells and have strong antiviral and inhibitory effects that aid in first line defense and signaling of infection. The IFN family consists of two main classes of cytokines which are type I IFNs and type II IFN, as well as several less common family members (193, 194). While Type II interferons only contain one type, IFN γ , type I interferons can be divided into two main effectors

IFN α and IFN β , while IFN α is then further subdivided into 13 subtypes. Despite all the various subtypes, type I interferons only bind a single common cell-surface receptor known as the type I IFN receptor. The type I IFN receptor is composed of two distinct subunits and these subunits are associated with JAK/STAT signaling (50). The binding of type I interferons to the receptor results in classical JAK/STAT signaling as well as a downstream cascade of associated signaling. This cascade of signaling results in the induction and expression of hundreds of genes associated with type I IFNs (56). The classical pathway observed for Type I IFN signaling is the binding of IFN α or IFN β to the IFN α/β R which results in the autophosphorylation of JAKs and their activation, this leads to the phosphorylation and activation of STATs such as STAT1, 2, 3 and 5, after activation STATs form dimers and translocate to the nucleus where they bind STAT specific binding sequences found in the promoters of IFN-stimulated genes (ISGs) (49, 50, 225, 234). It is these ISGs that are critical for the antiviral response type 1 IFN signaling plays during infection.

1.III.ii Type I interferon effect

As mentioned above viral sensing leads to the generation of type 1 IFNs. IFN α and IFN β , bind to type I IFN receptors found on cells which in turn generates a signaling pathway which leads to the upregulation and expression of hundreds of genes. The type I IFN response works in an autocrine and paracrine manner effecting the cell that produces it as well those around it, this allows the production of type 1 interferon to generate an “antiviral state” (252). Antiviral state is a relatively simple term to describe the resulting effect of a very complex process with the ultimate goal to inhibit viral replication and spread. As type I interferons stimulate hundreds of genes there are a wide range of effects shown. One such well known effect is the induction of

2'5' oligoadenylate synthase (OAS) which has the ability to activate the stable nuclease RNaseL. The activation of RNaseL results in the degradation of viral RNA as well as host RNA (33, 127). This is an important concept as a lot of type I interferon effects are deleterious not only to viruses but the host cell in which they reside, a cut off the hand to save the head mentality. Another well known effect is the induction of the antiviral effector gene protein kinase R (PKR), which leads to the phosphorylation of the critical translation factor eIF2 α . This results in the inability of eIF2 α to be recycled within the pathway resulting in an inhibition of both viral and host protein translation (118, 171, 281). While direct effects of type I interferons provide cells with an antiviral state to inhibit viral replication and spread, this alone is not enough to confer protection. Type I interferons however have been shown to be involved in non-direct effects that are also critical to the viral immune response.

One such type I interferon non-direct result is the induction of a cellular apoptotic state in which cells treated with type I interferons are more susceptible to apoptosis (38, 40). Induction of an apoptotic state allows infected cells to rapidly enter a death pathway before viral machinery can begin to produce new viral progeny. In responding to type I interferon, surrounding unaffected cells are primed and ready to respond if they should encounter virus. Another effect that type I interferons have is their interplay with the adaptive immune system. While type I interferon is an immediate response to viral infection it has the ability to shape the long term immune response. Two particular cell types that are affected by the type I interferon response is natural killer cell (NKC) and cytotoxic T cells (CTLs). Like infected cell responses, type I interferons can play a direct and indirect role in the adaptive immune response. Type I interferon has been shown to directly activate NK cells and increase their cytotoxic properties (76, 153). Type I interferons induce the production of IL-15 resulting in an indirect role in recruitment,

proliferation and maintenance of NK cells and memory CD8 T cells (277). Interestingly recent work has shown that type I interferons also play a role during chronic infections and actually may have an inhibitory effect on certain cell type. Type I interferons have been shown to induce suppressive factors such as IL-10 and PDL1 (16, 159) It is clear that the type I interferon response is a critical pathway in the immune response to viral infection. Type I interferons are stimulated in response to infection and directly and indirectly effect cells. Type I interferons also play an important role in shaping the adaptive immune system environment. Much is now known about this role and an excellent review by Donlin and Ivashkiv delves into this as well as a review by Trinchieri (108, 247).

1.III.iii Type I interferon effect in gammaherpesviruses

Type I interferons play a critical role in the host immune response to viral infection as described above. For this reason many viruses have evolved to counter and take advantage of the type I interferon pathway. Gammaherpesviruses is one virus that has developed multiple strategies for dealing with the type I interferon response. While type I interferons are unable to successfully control infection and prevent replication of gammaherpesviruses they do play a critical role and high levels are produced during infection (59, 219, 264). The triggering of the type I interferon response occurs immediately upon cellular infection most likely by the binding of viral glycoprotein to the cellular surface. In KSHV it has been shown that the glycoprotein K8 alone is enough to stimulate a response (192). *In vivo* studies using MHV68 have shown that the type I interferon response is necessary to control acute infection, and that animals deficient in type I interferons rapidly succumb to infection (117, 131). Further the administration of type I interferons during infection greatly enhances the gammaherpesviruses humoral immune response

(6). While type I interferon response is critical for initial control of infection it is also essential for control of reactivation from latency (10, 245).

While type I interferon response is critical for control of primary viral infection and reactivation from latency, gammaherpesviruses have evolved many pathways to evade this response. The evasion of this pathway in immunocompetent individuals demonstrates that type I interferon response is critical but not sufficient to control infection. Since it has been demonstrated that binding alone of the virus is enough to generate a response the virus has evolved ways to immediately inhibit the type I interferon response. One such response is initiated by Orf45 which has been found within the virion of KSHV and MHV68 (22) (293). Orf45 restricts the type I interferon response by targeting the interferon pathway, specifically IRF-7 by targeting phosphorylation and translocation to the nucleus (220, 291, 292). Another virion associated protein, Orf64, has also been shown to inhibit the immediate type I interferon response by targeting the ubiquitination pathway of RIG-I (84, 107). Finally, the tegument protein Orf36 in MHV68 with homology to the EBV BGLF4 protein inhibits the type I interferon response by binding to IRF3 preventing it from interacting with its cotranscriptional activator CBP, which prevents binding and upregulation of the IFN β promoter (105, 257).

Virion associated proteins provide immediate suppression of the type I interferon response, additional proteins provide suppression once acute infection has occurred as well as reactivation from latency. While Orf45, Orf64, and Orf36 remain important for suppression from the virion, proteins such as RTA, RIF, and K-bZIP are also required for type I interferon evasion. RTA, which is discussed in detail above, is an immediate-early protein essential for viral replication. Since RTA is essential for replication and also triggers the lytic cascade of gene expression it is reasonable to think RTA would target the type I interferon pathway to inhibit the

anti-viral state. To do this RTA directly targets IRF3 and 7 which leads to the proteasomal degradation through actions as an ubiquitin E3 ligase (286). It has also recently been discovered that RTA may target TRIF in a similar manner, leading to its degradation and a reduced response (3). RIF (Orf10) is different that most gammaherpesviruses type I immune evasion strategies in that instead of targeting IRF3 and 7 it targets the signaling pathway. To inhibit the signaling pathway, RIF forms inhibitory complexes with JAKs and STAT2 resulting in impairment of STAT phosphorylation (17). The K-bZIP protein binds to the IFN- β promoter preventing the IRF3 complex from binding (138).

While many type I interferon immune evasion strategies are conserved among all gammaherpesviruses, additional pathways unique to each virus exist. The Orf54, M2, and viral IRFs are also important in targeting type I interferons. MHV68 Orf54 targets the degradation of the type I interferon receptor (IFNAR1) through an unknown mechanism, and appears critical for normal replication in an immunocompetent mouse (132). The MHV68 M2 gene is unique in that it is a latency associated gene and targets both STAT1 and STAT2 for downregulation (147). Finally, KSHV encodes several viral IRFs -1, 2, 3, and 4 homologs of cellular IRFs that function to downregulate the type I interferon response (5, 71, 114, 135, 148, 164). These viral IRFs function to compete with cellular IRFs, bind transcription factors to form inhibitory complexes, as well as directly bind IRFs and prevent their function.

It is clear that gammaherpesviruses have evolved many different ways to deal with the type I interferon response, demonstrating the important nature of overcoming this initial immune response in establishment of infection. What is interesting is the hijacking of this pathway by the virus in establishment of latency and control of the replication cycle. While a large type I interferon response would be considered detrimental, the lack of one is as well.

Gammaherpesviruses have evolved type I interferon responsive promoters in an effort to hijack the signaling used by interferon. Additionally type I interferon is critical in containing viral reactivation and the viruses at times may require a type I interferon response to enter latency, or a lack of one to reactivate. This yin and yang of evasion and acceptance can be seen in EBV in which the viral SM protein induces STAT1 and interferon stimulated gene expression (214). Also the latent gene LMP1- induces an antiviral state to help secure a latent phenotype while at times also subverting the type I interferon response by targeting phosphorylation (74, 288). Overall the type I interferon response is a critical pathway that is subverted by many different mechanisms encoded by gammaherpesvirus genes. This pathway plays a role during primary infection, latency, and reactivation making it a critical component to the viral life cycle.

1.IV. FIGURE LEGEND

Figure 1. Depiction of kinetics of MHV68 lytic and latent infection when administered through i.n. challenge. Dark shaded area represents lytic replication which occurs in the lungs and spleen and is detectable by plaque assay by day 4 postinfection. Acute replication is cleared by 16 to 18 days postinfection. Light shaded area represent latent infection which is detected by a limiting dilution PCR assay. Latency remains with a host for life and is maintained as a set viral load, characterized by the absence of lytic viral replication.

Figure 2. Schematic illustrating known RTA splicing in the gammaherpesvirus family. A promoter upstream of Exon 1 (indicated by the small arrow) drives expression of a transcript containing Exon 1 spliced to Exon 2. A promoter upstream of Exon 0 (indicated by the small arrow) drives expression of a transcript containing Exon 0 splice to Exon 1 spliced to Exon 2 only in MHV68. The promoter upstream of Exon 0 drives Exon 0 splicing to Exon 2 and does not splice through Exon 1 in both KSHV and EBV.

1.V. FIGURES

1. Depiction of kinetics of MHV68 lytic and latent infection when administered through i.n. challenge
2. Schematic illustrating known RTA splicing in the gammaherpesvirus family

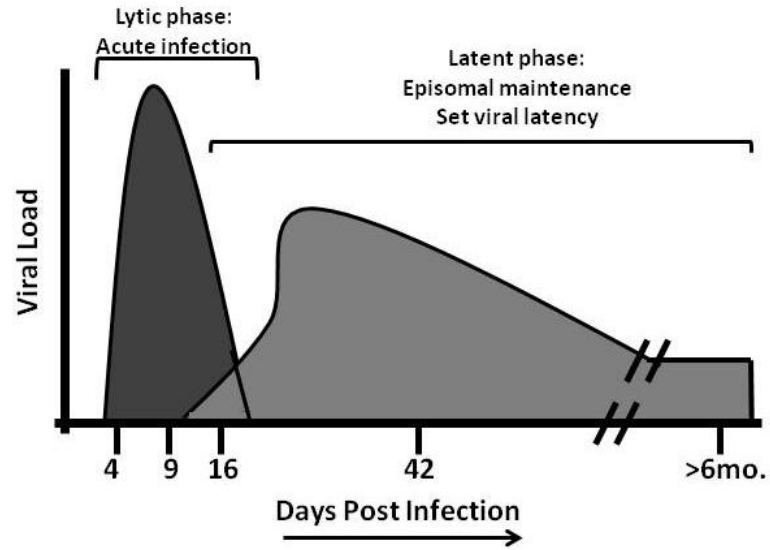


Figure 1

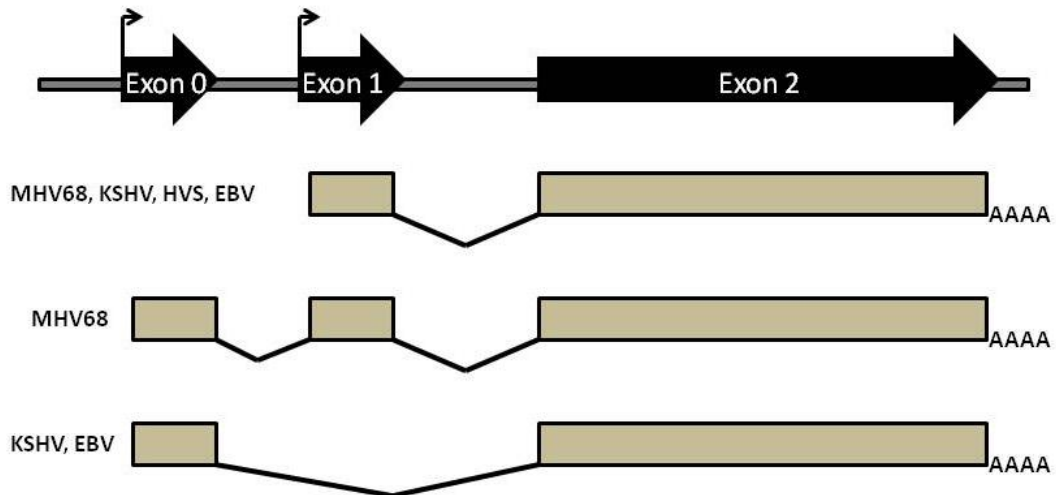


Figure 2

Chapter 2: Identification of alternative transcripts encoding the essential murine gammaherpesvirus lytic transactivator RTA

2.I. Abstract

2.II. Introduction

2.III. Materials and Methods

2.IV. Results

2.V. Discussion

2.IV. Figure legends

2.VII. Figures and Tables

1. Genomic Alignment of Orf50/BRLF1/Rta region from MHV68, EBV, KSHV, and HVS gammaherpesviruses illustrating the conserved organization of gene 50 transcription
2. Promoter deletions within the MHV68 E0 250bp promoter region
3. Generation of MHV68 G50DbIKo and G50DbIKo.MR viruses
4. G50DbIKo virus replicates *in vitro* in Vero-Cre cells, but fails to replicate in NIH 3T12 fibroblasts
5. G50DbIKo virus fails to replicate *in vitro* when IFN α is present
6. Single-step growth analyses of the G50pDbIKo mutant, and analysis of the kinetics of RTA expression
7. RACE analyses reveal three additional G50 exons upstream of E0
8. Promoter activity in the region immediately 5' to MHV68 N3, N4, and N5 exons
9. Immunoblot analyses of RTA protein expression levels in WT and G50DbIKo infected NIH 3T12 fibroblasts, C57BL/6 MEFs, and 129S2/SvPas.IFN- α/β R^{-/-} MEFs
10. G50DbIKo virus exhibits a severe reactivation defect and a moderate latency defect *in vivo*
11. Infection of 129S2/SvPas.IFN- α/β R^{-/-} mice with G50DbIKo virus does not result in lethality as seen with WT virus despite the presence of high viral titers in the lungs
12. G50DbIKo virus establishes latency and reactivates to similar levels as WT Virus when used to infect 129S2/SvPas.IFN- α/β R^{-/-} mice *in vivo*
13. Promoter activity in the region immediately 5' to the MHV68 proximal promoter and proximal promoter deletion

Table 1. Summary of virus latency and reactivation

*All material in this chapter has been previously published (256)

Identification of Alternative Transcripts Encoding the Essential Murine Gammaherpesvirus Lytic Transactivator RTA

Brian S. Wakeman,^a L. Steven Johnson,^b Clinton R. Paden,^a Kathleen S. Gray,^a
Herbert W. Virgin,^b and Samuel H. Speck^a

Emory Vaccine Center and Department of Microbiology & Immunology, Emory University
School of Medicine, Atlanta, Georgia, USA^a;
Department of Pathology and Immunology, Washington University School of Medicine,
St.Louis, Missouri, USA^b

All figures were generated by Brian Wakeman with exceptions noted below

Figure 2. Help was conducted by Kathleen Gray in generation of distal promoter constructs
Figure 7. RACE transcripts were confirmed and analyzed in collaboration with L. Steven
Johnson and Herbert W. Virgin.

2.I. ABSTRACT

The essential immediate-early transcriptional activator RTA, encoded by gene 50, is conserved among all characterized gammaherpesviruses. Analyses of a recombinant murine gamma-herpesvirus 68 lacking both of the known gene 50 promoters (G50pDblKO) revealed that this mutant retained the ability to replicate in the simian kidney epithelial cell line Vero, but not in permissive murine fibroblasts following low MOI infection. However, G50pDblKo replication in permissive fibroblasts was partially rescued by high MOI infection. In addition, replication of the G50pDblKO virus was rescued by growth on MEFs isolated from $\text{IFN}\alpha/\beta\text{R}^{-/-}$ mice, while growth on Vero cells was suppressed by the addition of $\text{IFN}\alpha$. 5' rapid amplification of cDNA ends (RACE) analyses of RNA prepared from G50pDblKo and wild-type MHV68 infected murine macrophages identified three novel gene 50 transcripts initiating from 2 transcription initiation sites located upstream of the currently defined proximal and distal gene 50 promoters. In transient promoter assays neither of the newly identified gene 50 promoters exhibited sensitivity to $\text{IFN}\alpha$ treatment, although RTA levels were lower in $\text{IFN}\alpha$ -responsive cells infected with the G50pDblKo mutant. Infection of mice with the MHV68 G50pDblKo virus demonstrated that this mutant virus was able to establish latency in the spleen and peritoneal exudates cells (PECs) of C57Bl/6 mice with about 1/10 the efficiency of wild-type virus or marker rescue virus. However, despite the ability to establish latency, the G50pDblKo virus mutant was severely impaired in its ability to reactivate from either latently infected splenocytes or PECs. Consistent with the ability to rescue replication of the G50pDblKO mutant by growth on type I interferon receptor null MEFs, infection of $\text{IFN}\alpha/\beta\text{R}^{-/-}$ mice with the G50pDblKo mutant virus demonstrated partial rescue of: (i) acute virus replication in the lungs; (ii) establishment of latency; and (iii) reactivation from latency. The identification of additional gene 50/RTA transcripts highlight the complex mechanisms involved in controlling expression

of RTA, likely reflecting time dependent and/or cell-specific roles of different gene 50 promoters in controlling virus replication. Furthermore, the newly identified gene 50 transcripts may also act as negative regulators that modulate RTA expression.

2.II. INTRODUCTION

Herpesviruses are large double-stranded DNA viruses. The hallmark of all herpesvirus infection is their ability to persist latently for the lifetime of the host, which is marked by sporadic virus reactivation, replication, and virus shedding. The herpesvirus family is divided into three classes; α -, β -, and γ -herpesviruses. While both α - and β -herpesviruses generally exhibit broad tropism and the ability to infect a range of cell types, γ -herpesviruses are unique in that they are mainly lymphotropic, infecting and establishing latency in T or B lymphocytes. γ -herpesviruses are also unique in that they are associated with a variety of lymphomas. Kaposi's sarcoma-associated virus (KSHV) is associated with tumor development in its namesake Kaposi sarcoma, as well as multicentric Castleman's disease and primary effusion lymphoma. Epstein-Barr Virus (EBV) is tightly associated with the development of several human malignancies including, nasopharyngeal carcinoma, Hodgkin's lymphoma, Burkitt's lymphoma, and post-transplant lymphoproliferative disease (284). Though both KSHV and EBV associated malignancies are rare, their prevalence is elevated in people who are immunocompromised either via immunosuppressive therapies, or HIV infection (46, 47, 197).

While *in vitro* cell culture systems exist to study the two human gammaherpesviruses, EBV and KSHV, these viruses have a narrow host tropism which severely limits *in vivo* studies. This has generated a need for robust small animal models to further investigate primary viral infection, establishment of latency, and reactivation in the context of natural infection. Murine gammaherpesvirus 68 (MHV68) has emerged as the leading animal model for characterizing γ -herpesvirus pathogenesis *in vivo*. MHV68 is a natural pathogen of wild murid rodents and readily infects laboratory strains of mice (233). Complete sequencing of the MHV68 genome revealed extensive homology to both EBV and KSHV (255). MHV68 infects multiple organs,

establishes latency in the spleen and lymph nodes, is primarily lymphotropic, and is associated with development of lymphoproliferative disease and lymphomas (9, 131, 146).

An area of the MHV68 genome that is well conserved in both sequence homology and function is the gene 50 region, which encodes the essential immediate-early viral transcriptional activator RTA (also known as R or BRLF1). Notably, the MHV68, KSHV and EBV gene 50 transcripts exhibit similar splicing patterns, promoters, and genome location (Figure 1). Furthermore, ectopic expression of RTA in MHV68, HVS, KSHV, and EBV latently infected cells is capable of driving virus reactivation (199, 239), mediated through RTA activation of viral lytic cycle-associated gene promoters (4, 149, 189, 274). RTA feeds into many different lytic and latent gene pathways acting as both a positive and negative regulator of gene transcription. The many important functions exhibited by RTA make it one of the most tightly regulated genes in γ -herpesviruses where control is established through the use of alternative splicing, epigenetic modifications, feedback loops, and multiple promoters.

Recently we identified a new RTA promoter, which we named the distal gene 50 promoter (81). Notably, we previously showed that this promoter is also present in KSHV and EBV (Fig. 1). The transcript initiated from the distal promoter encodes an 181bp exon (E0) at coordinates bp 65909 to 66089 in the MHV68 genome, which splices to the E1 exon located at coordinates bp 66509 to 66796 and then splices to exon 2 at coordinates bp 67662 to 69462. Notably, we have shown that a proximal gene 50 mutant virus is able to replicate, establish latency in both splenocytes and PECs, and reactivate from PECs, suggesting that the distal promoter is functional (81). However, the proximal promoter mutant is defective in reactivation from splenocytes (81).

Here we demonstrate that the expression of RTA can be driven from multiple previously unknown promoters upstream of the distal promoter. These promoters encode three new exons, two of which represent extensions of exon 0 and the other a completely unique exon. To further characterize these promoters we generated a MHV68 mutant lacking both the proximal and distal gene 50 promoters (G50DbIKo). We show the G50DbIKo virus retains the ability to replicate to similar levels as WT virus, but only in the absence of a type 1 interferon response. Furthermore, we show that the G50DbIKo virus is extremely sensitive to type 1 interferons both *in vitro* and *in vivo*. We also show that despite the replication defect observed in the presence of a type I interferon response, the G50DbIKo virus established a latent infection in both splenocytes and PECs – although it was unable to reactivate from either splenocytes or PECs. Importantly, the replication and latency defects exhibited by the G50DbIKo mutant were largely rescued by infection of mice lacking a type I interferon response. Finally, despite the sensitivity of the G50DbIKo mutant virus to type I IFNs, we show that the newly identified promoters themselves are not directly sensitive to IFN α - indicating that type I IFNs likely act downstream of RTA transcription.

2.III. MATERIALS AND METHODS

Generation of G50DblKo and G50DblKo.MR viruses. The MHV68.G50DblKo virus was generated using the galK-mediated Red recombineering method as described previously (187, 260). Briefly, we introduced the MHV68 BAC into the galK strain of bacteria SW102 where the galK was inserted into the Orf50 locus. To generate the Orf50 galK swap we amplified the galK gene from the plasmid pGalK using the primers GalK-G50-F (5'-cttaaaggaggagctgttggcagtgcttgcctgctgaaaatacctcatcaaactCCTGTTGACAA-TTAATCATCGGCA-3') and GalK-G50-R (5'-cctcagcctttgaaggacatttcatgactcatgtaggagagctaccagTCAGCACTGTCCTGCTCCTT-3'); this PCR product generated from pGalK includes 50bp of homologous sequence upstream and downstream to the Orf50 locus. The PCR product was then introduced into the SW102 cells through electroporation and those cells expressing recombinants were selected through the use of minimal media with galactose. The ORF50/GalK recombinant BAC mutants (MHV68.Δ50galK) were confirmed through analyses using multiple restriction endonucleases.

To generate the G50DblKo virus two separate 25µl PCR reactions were performed on MHV68 WT BAC using phusion polymerase (New England Biolabs) with 30 cycles using the following cycling conditions: 94° for 30 seconds, 58° for 30 seconds, 72° for 1 minute. The primers used for reaction one amplification were forward primer Orf50F65040_65089 (5'-cttaaaggaggagctgttggcagtgcttgcctgctgaaaatacctcatcaaact-3') with reverse primer Orf50DpKo100RHindIII (5'-aatggactccagctgAAGCTTtagtcatagaacataccatga-3') and the primers used for reaction two amplification were reverse primer Orf50R66641_66690 (5'-cctcagcctttgaaggacatttcatgac-tcatgtaggaggagctaccag-3') with forward primer Orf50DpKo100FHindIII (5'-gtatgttctatgactAAGCTTcag-ctggagtccattattct-3') to generate

overlapping PCR products to be used in round two amplification, of note each internal primer contained a HindIII restriction enzyme site to be used for diagnostic purposes. Two microliters of each round one amplification was then used as template for a round 2 reaction using the external forward primer from reaction one Orf50F65040_65089 and the reverse external primer from reaction two Orf50R66641_66690. The resulting product containing a 50bp deletion within the distal promoter region of the Orf50 locus was gel purified and used as template for a second overlapping PCR reaction using the same conditions as the first PCR reaction only this time targeting a deletion within the proximal promoter region. The primers used for reaction one amplification were forward primer Orf50F65040_65089 (5'-cttaaaggaggagctgttggcagtgttgcgtaaaaatacctcatcaact-3') with reverse primer Orf50PpKORHindIII (5'- gaacagtatgagaaaAAGCTTcagggaaattttgttatgtgc-3) and the primers used for reaction two amplification were reverse primer Orf50R66641_66690 (5'-cctcagcctttgaaggacatttcatgactcatgtaggaggagctaccag-3') with forward primer Orf50PpKoFHindIII (5'- ccctggaatcatagaAAGCTTtttctcatactgttcctttt-3'). Like before 2 μ of each round one amplification was used as template for a round 2 reaction using the same external primers as before Orf50F65040_65089 and Orf50R66641_66690. The resulting PCR product was gel purified and now contained a 50bp deletion within the Orf50 distal promoter region, a 70bp deletion within the Orf50 proximal promoter region, and 50bp homology to the region directly external to the MHV68. Δ 50galK Orf50galK region. A WT Orf50 PCR product containing the 50bp homology arms was also generated in order to create an Orf50 marker rescue of the MHV68. Δ 50galK parent BAC to ensure no spontaneous mutations had arose. This mutant or WT PCR product was electroporated into SW102/MHV68. Δ 50galK and after recombination was selected on minimal media plates containing glycerol and 2-deoxy-D-galactose. The colonies were then screened by colony PCR using primers ORF50E0F (5'-

cacaaccagcacatgttcaaacat-3') and ORF50E0R (5'- ctgtgtctcactgaaaac-actc-3'). Colonies were then further verified by restriction digest using the *HindIII* diagnostic sites, as well as confirmation by PCR of the ORF50 region and DNA sequencing of the PCR product (Macrogen Sequencing). The integrity of the non-mutated BAC was confirmed through further restriction endonuclease digestion using *PstI* and *EcoRI*. Restriction endonuclease digests were then subjected to Southern blotting analyses using a PCR-generated fragment spanning the entire Orf50 region as the probe.

Production of virus. Both the G50DbIKo and G50DbIKo.MR viruses were generated from YFP BAC (42). In order to ensure proper viral growth of the G50DbIKo virus a protocol was developed in which the virus would be passaged and tittered in the absence of Type 1 interferons. Both mutant and marker rescue BACs were transfected using LT-1 transfection reagent (Mirus) into Vero-Cre cells. When cells reached 70% CPE, cells and supernants were collected and freeze/thaw lysed three times. The resulting stock was used to infect new Vero-Cre cells to ensure the excision of the BAC. At 70% CPE cells and supernants were once again collected, lysed, and used to infect large quantities of Vero-Cre cells to scale up viral stocks. Viral titers were determined as described below.

Tissue culture. Mouse Embryonic Fibroblasts (MEFs), NIH 3T12, Raw264.7, and Vero-Cre cells were maintained in Dulbecco's modified Eagle's medium (DMEM) supplemented with 10% fetal calf serum, 2mM L-glutamine, 100 U of streptomycin per ml and 100 U of penicillin per ml (cMEM). Vero-Cre cells used for virus generation were passaged with the addition of 300µg of hygromycin B/ml. Cells were maintain at 37°C in a tissue culture incubator with 5%

CO2. MEFs were obtained from C57BL/6 mouse embryos and IFN α / β R $^{-/-}$ MEFs were obtained from 129S2/SvPas.IFN- α / β R $^{-/-}$ mice as previously described (261).

Growth curves, plaque assays and viral titers. Growth curves were performed using Vero-cre, 3T12, IFN α / β R $^{-/-}$ MEFs, or C57BL/6 MEF cells plated in six well plates at a concentration of 1.75×10^5 cells per well 24 hours prior to infection. Cellular concentration after 24 hours was determined and viral stocks were diluted to a 200 μ l volume in cMEM at MOIs of .01, .1, and 10. These inoculums were added to the cellular monolayer and plates were rocked every 15 minutes at 37°C for one hour. After one hour fresh cMEM at a volume of 2ml was added back to each well. Wells were collected at indicated time points and frozen at -80°C until plaque assays were performed to determine titers. Growth curves with the addition of mouse recombinant IFN α (Miltenyi Biotec) were performed in a similar manner, but IFN α was added to the plated cells at a concentration of 10,000 IU/ml one hour before infection. IFN α was subsequently added at a concentration of 5,000IU/ml every 24 hours for the duration of the infection. Plaque assays were performed by plating Vero-cre cells in six well plates at a concentration of 1.75×10^5 cells per well 24 hours prior to infection. Viral stocks or growth curve stocks at the indicated timepoint were freeze thawed 3 times and a 10 fold serial dilution was generated, 200 μ l of each dilution was added to the Vero-cre monolayer and plates were rocked every 15 minutes at 37°C for one hour. After one hour cells were overlaid with 2% FBS complete medium containing 20 g/liter methylcellulose (Sigma). Plaques were visualized 14 days postinoculation by staining with neutral red (Sigma) at a concentration of 6% overnight.

RACE analysis. 100mm plates were seeded with Raw 264.7, Vero-cre or IFN α / β R $^{-/-}$ MEF cells in cMEM and 24 hours later infected with WT-YFP or G50DblKo virus at an MOI of 5. Total RNA was isolated from these cells 24 or 48 hours postinfection using Trizol reagent (Invitrogen). 5 μ g of RNA was DNase 1 treated (Invitrogen) and subjected to 5' RACE performed using the GeneRacer system (Invitrogen). RACE ready cDNA was generated using superscript III (Invitrogen) reverse transcription using random primers as per manufacturer instruction. Race ready cDNA was used to look for additional 5' transcripts through the use of nested PCR utilizing Phusion High Fidelity Taq (NEB) and Platinum Taq (Invitrogen). Nested PCR was performed using the 5' universal forward primer (round 1), the 5' universal forward primer (round 2), and various reverse primers located in the Orf50 region; E2R1 (5'-attcgaacagactgcaggccagaggtga-3'), E2R2 (5'-cgaacatggggcagtcagaaacagc-3'), E1R (5'-ttcaattctcatggtcacatct-3'), E0R (5'-tttgaacatgtgctgggtgtg-3'). The following cycling conditions for Phusion Taq were used where 1 μ l of cDNA was used in a 50 μ l PCR reaction, 98 $^{\circ}$ C for 30 seconds, and 30 cycles of denaturing at 98 $^{\circ}$ C for 10 seconds, annealing at 60 $^{\circ}$ C for 30 seconds, and extension at 72 $^{\circ}$ C for 1 minutes, followed by a final extension of 72 $^{\circ}$ C for 10 minutes. Round 2 nested amplification was performed using 2 μ l of round 1 product in a 50 μ l reaction using the same cycling conditions. The following cycling conditions for Platinum Taq were used where 1 μ l of cDNA was used in a 50 μ l PCR reaction, 95 $^{\circ}$ C for 5 minutes, and 30 cycles of denaturing at 94 $^{\circ}$ C for 30 seconds, annealing at 60 $^{\circ}$ C for 30 seconds and annealing at 72 $^{\circ}$ C for 1 minute and 30 seconds, with a final extension of 72 $^{\circ}$ C for 7 minutes. Round 2 nested amplification was performed using 2 μ l of round 1 product in a 50 μ l reaction using the same PCR conditions. PCR products were visualized through running on a 1% ethidium bromide gel and excised bands were purified using a geneclean II kit (MP Bio). Purified PCR products from

Phusion PCR were ligated into a pCR-Blunt II TOPO vector (Invitrogen), and purified PCR products from Platinum Taq PCR were ligated into either a pCR4-TOPO vector (Invitrogen) or a pGEMT-Easy vector (Promega) and analyzed by DNA sequencing (Macrogen USA).

Cell transfections and luciferase assays. Transfection of Vero-Cre and RAW 264.7 cells was done in 6 well plates, where 1 day prior to transfection cells were plated at 2×10^5 cells per well in cMEM. Transfections were prepared using 2.5 μ g of reported plasmid and 5ng of pHR-LUC *Renilla* luciferase vector as a transfection control. Transfections were performed using LT-1 transfection reagent (Mirus) according to manufacturer's instructions. pGL4.13[Luc] was used as a positive control, pGL4.10[luc] was used as a negative control, and the green fluorescent protein pMaxGFP was used to determine transfection efficiency. For assays treated with IFN α , 5,000IU/ml was added 24 hours post transfection, and all cells were collected 48 hours post transfection and lysed. All dual luciferase assays were performed using the Dual Luciferase kit (Promega) according to manufactures instructions. Single luciferase assays were performed using lab made luciferase agent (1.5 mM HEPES, pH 8, 80 μ M MgSO $_4$, 0.4 mM DTT, 2 μ M EDTA, 10.6 μ M ATP, 5.4 μ M Coenzyme A, and 9.4 μ M beetle Luciferin) where 10 μ l of cell lysate was added to 50 μ l of luciferase agent. Both single and dual luciferase assays were read using a TD-20/20 luminometer (Turner Biosystems). All transfections were repeated in triplicate and presented as a fold over empty pGL4.10 vector ratio.

Reporter plasmids and cloning. DNA from the Orf50 region was amplified from the MHV68 WT BAC and cloned into a luciferase reporter construct. Phusion Taq (NEB) was used with the following cycling parameters for all amplifications, 95°C for 5 minutes, 30 cycles of denaturing

at 94°C for 30 seconds, annealing at 58°C for 30 seconds, and extension at 72°C for 30 seconds, followed by a final 72°C extension for 10 minutes. Overlapping PCR was used with the following primers to generate E0 luciferase promoter constructs with 50bp deletions. Round 1 PCR used forward primer E0-250F (5'-gatcggctagcttaacctatatggagat-3') with the following reverse primers; del 65822-65872R (5'-catgtctcagccaacagctcgacacttcgagtagc-3'), del 65772-65822R (5'-agaataatggactccagctgagctcatagaacatac-3'), and del 65722-65772R (5'-gcacgtattgctgaaaagga atgatcaggaattct-3'), reverse primer E0ATGR (5'-gatcgaagcttgtgctgggttggaag-3') was used with the following forward primers; del 65822-65872F (5'-ggtactcgaagtgtcagctgttgctgagacatg-3'), del 65772-65822F (5'-gtatgttctatgactcagctggagtagcattattct-3'), and del 65722-65772F (5'-agaat tctgatcattccttttcagcaatacgtgc-3'). After Round 1 PCR, 2µl of PCR products from del 65822-65872, del 65772-65822, del 65722-65772 was used as template for a round 2 PCR reaction following the same cycling conditions as round 1 with forward primer E0-250F and reverse primer E0ATGR. These second round PCR products were gel purified and cloned into pCR-Blunt (Invitrogen) for vector shuttling and sequence confirmation. The pCR-Blunt plasmid was then cut with HindIII and NheI to excise the E0 fragments, and the luciferase reporter construct pGL4.10[luc2] (Promega) was also digested with HindIII and NheI. The digested E0 products and pGL4.10[luc2] vector were then gel purified, resuspended in TE, and ligated together using T4 DNA Ligase (NEB) overnight at 16°C. Ligations were transformed into Top 10 chemically competent cell and colonies were screened for the presence of correctly oriented E0 pGL4.10[luc2] vectors through restriction digest and DNA sequencing. Clones containing correct E0 deletion and expression were cultured and plasmid DNA was isolated using an Endofree Maxi kit (Qiagen). The process of generating Orf50 N3 and N4/N5 promoter luciferase

constructs followed a similar method as above with only a single PCR amplification required to generate 1000bp long PCR fragments. The primers used for this single PCR reaction were as follows, the reverse primer N4_N5RBgl2 (5'- cgatagatctaagccgtggcagcaggt-3') was used with the forward primer N4_N5F1000NheI (5'- agtcgctagcaatcgccggggggttaa-3'), The reverse primer N3RBgl2 (5'- cgatagatctagcctggggcatagttctt-3') was used with the forward primer N3FNheI (5'- agtcgctagctcaggatgcagttaagca-3'). These products were gel purified, shuttled through pCR-blunt, digested with NheI and BglII then ligated into pGL4.10[luc2]. The generation of the Proximal Promoter expression constructs followed the same protocol as described above. Forward primer ProxPromF (5'-gatcgctagctctttataggtaccagggaa-3') was used with reverse primer ProxPromR (5'- tagcagatctggtcacatctgacagagaaa-3') to generate the 410bp Proximal Promoter luciferase construct. Overlapping PCR using Forward Primer ProxPromDelF (5'- ccctggaatcatagatttctcatactgttctctttt-3') with primer ProxPromR and Reverse Primer ProxPromDelR (5'- gaacagtatgagaaatctatgattccaggaattt-3') with primer ProxPromF was used to generate the Proximal Promoter 70bp Deletion construct. Digestion, ligation, and purification also followed the same protocol as described above.

Limiting dilution-PCR and limiting dilution-reactivation assays. Limiting dilution PCR to determine the frequency of viral genomes and a limiting dilution CPE assay to determine the number of cells reactivating from latency were performed as previously described (261, 262). Briefly, to determine the frequency of viral genomes splenocytes or PECs were serially diluted in 96 well plates and subjected to protease K digest. After digest cells were used in a two round nested PCR using primers found in the G50 region. PCR products were resolved on a 2% agarose gel and analyzed. To determine frequency of infected cells reactivating from latency,

splenocytes or PECs were counted and diluted in cMEM. Cells were then plated as serial two-fold dilutions onto a MEF or IFN α / β R $^{-/-}$ MEF monolayer in 96 well plates. Also in parallel mechanically disrupted cells were plated as a serial two-fold dilution to detect any preformed infectious virus. At 21 days postplating, each well was assessed for cytopathic effect (CPE) and scored as a percentage. For both LD-PCR and LD-Reactivation poisson distribution was used to determine frequencies.

Mice, infections, and tissue preparation. Female C57Bl/6 mice (The Jackson Laboratory) and 129S2/SvPas.IFN- α / β R $^{-/-}$ mice 6 to 8 weeks of age were maintained at Emory University. Mice were sterile housed and maintained in accordance with Emory University School of Medicine (Atlanta, GA), as well as all federal guidelines. C57Bl/6 or 129S2/SvPas.IFN- α / β R $^{-/-}$ mice were infected intranasally with 1,000 PFU of WT-YFP, G50DbIKo or G50DbIKo .MR virus in 20 μ l cMEM following isofluorane anesthetization. 129S2/SvPas.IFN- α / β R $^{-/-}$ mice were weighed at the time of infection and weight was monitored daily, mice were sacrificed if they lost 20% of their original bodyweight. C57Bl/6 mice were also infected intraperitoneal with 1,000 PFU of WT-YFP, G50DbIKo or G50DbIKo.MR virus in 200 μ l cMEM. Both routes of infection C57Bl/6 mice were sacrificed at day 18 post-infection, or 7 days post-infection for lung titers. Surviving 129S2/SvPas.IFN- α / β R $^{-/-}$ mice were sacrificed at day 28 post-infection. Mice were sacrificed by isofluorane and cervical dislocation. PECs were collected by peritoneal lavage using 10ml cMEM, spleens were harvested and splenocytes prepared by manual homogenization, while lungs were harvest and prepared by mechanical bead disruption using 1.0mm silca beads. Splenocytes were treated with Tris-ammonium chloride to eliminate red blood cells. All cells prepared were counted using a cellometer auto T4 (Nexcelom) and immediately used for lung

titer, reactivation or genome analysis. Cells not used immediately were stored in cMEM-10% dimethyl sulfoxide at -80°C.

Immunoblotting. Infections were carried out as described previously for growth curves. At 24, 48, and 72 hours post-infection cells were harvested, washed with 1x PBS buffer, and then resuspended in 40µl of lysis buffer containing 150mM NaCl, 50mM Tris-HCl, 1mM EDTA and 0.1 % TritonX-100 supplemented with 1mM NaF, 1mM Na₃VO₄ and EDTA-free protease inhibitor tablet (Roche). Protein quantifications were carried out using a DC protein assay (Bio-Rad). For all blots 30µg of protein was mixed with 6X SDS loading buffer, boiled for 5 minutes at 100°C and resolved by SDS-PAGE. SDS PAGE gels were transferred to a nitrocellulose membrane using a semi-dry apparatus (Bio-Rad). After transfer membranes were blocked in 5% milk in TBS-Tween for one hour at room temperature. After one hour membranes were washed three times with TBS-Tween and the primary antibody rabbit anti-MHV68 RTA (58) diluted 1:1000 in blocking buffer was added and left overnight rocking at 4°C. Following overnight incubation the primary antibody was removed and the membrane washed three times with TBS-Tween. The membrane was then incubated with the secondary antibody donkey anti-rabbit (Jackson immunoresearch) diluted 1:2000 in blocking buffer for one hour at room temperature. This was followed with three additional washes with TBS-Tween. The blot was then developed using Supersignal West Pico Chemiluminescent substrate (Pierce). Membranes were stripped using Restore PLUS Western Blot Stripping Buffer (Thermo Scientific). Membranes were then subjected to the same protocol using the primary mouse monoclonal β-Actin (Sigma) at 1:5000 and the secondary antibody donkey anti-mouse (Jackson immunoresearch) at 1:5000. Membranes also followed the same protocol to blot for v-cyclin, where primary rabbit

monoclonal antibody v-cyclin was used at 1:2000 overnight, and the secondary antibody donkey anti-rabbit was used at 1:2000 (Jackson immunoresearch) for 1 hour at 4°C.

2.IV. RESULTS

Characterization of the Orf50 Distal Promoter Activity in vitro.

We previously reported the generation and characterization of a gene 50 proximal promoter knockout virus (G50pKO), which led to the identification of an additional promoter upstream of the proximal promoter - now referred to as the distal promoter (81). The additional distal promoter drives the expression of a new exon (E0), and the core promoter region corresponds to the first 250bps upstream of the E0 transcriptional start site. To further characterize the activity of this newly defined promoter region we generated serial 50bp deletions ($\Delta 65672-65722$; $\Delta 65722-65772$; $\Delta 65772-65822$; $\Delta 65822-65872$) in the core 250bp distal promoter region (Fig 2). These serial 50bp deletion fragments were cloned into the pGL4.10 luciferase reporter vector, and the resulting reporter plasmids transfected into RAW 264.7 cells. It was previously reported that the gene 50 distal promoter was most active in RAW 264.7 cells with the addition of LPS (81).

Luciferase assays confirmed the previous finding that the 250bp distal promoter region drives significant gene expression, ~30-fold over empty vector in the RAW 264.7 cells with the addition of LPS (Fig 2). Notably, deletion of the sequences from bp 65,672-65,722 resulted in a substantial increase in promoter activity over empty vector (~4.6-fold above that observed with the full length 250bp promoter construct), indicating the presence of negative cis-elements in this region. Similarly, deletion of the sequences from bp 65,822-65,872 also resulted in a strong enhancement of activity (~40-fold above that observed with the full length 250bp promoter construct). This would indicate that both of these regions play an important role in limiting gene 50 transcription. Conversely, deletion of the sequences from bp 65,772-65,822 resulted in nearly

complete silencing of distal promoter activity (ca.16-fold below that observed with the full length 250bp promoter construct) – arguing that essential positive cis-elements map to this region. As such, we chose to delete the latter region in the context of the viral genome to ablate distal gene 50 promoter activity.

Generation of a recombinant MHV68 lacking both the proximal and distal gene 50 promoters.

With the identification of a second promoter driving RTA expression, we set out to generate a gene 50 functionally null virus through the deletion of both the distal and proximal promoters. We targeted the promoter regions as previous attempts to propagate gene 50 null viruses harboring mutations within the coding sequence were confounded by the generation of wild type revertant viruses upon growth on complementing cell lines (i.e., recombination of wild type gene 50 sequences into the viral genome) (190). Since the gene 50 null mutants grow slowly on complementing cell lines, any wild type revertant virus quickly overtakes growth of the gene 50 null virus and ends up dominating the viral stock generated. In a previous attempt to overcome this problem we deleted a 183bp region of the proximal gene 50 promoter (the only known gene 50 promoter at the time), and it was the analysis of this mutant virus that led to the identification of the distal gene 50 promoter (81). Notably, the deletion introduced into the viral genome to generate the proximal promoter mutant virus (G50pKO) also deleted the splice acceptor site utilized by the distal gene 50 promoter driven gene 50 transcript. To circumvent this issue, we redesigned the proximal promoter deletion to introduce a 70bp deletion (corresponding to the region immediately upstream of the exon 1 transcript at coordinates bp 66,412-66,482) leaving the splice acceptor site intact (Fig. 3A). This new gene 50 proximal

promoter knockout virus (G50PpKO) was used as the backbone for the generation of the G50DbIKo virus.

To disrupt the distal gene 50 promoter we targeted the 50bp region from bp 65,772-65,822 which was determined to be essential for promoter activity in the in vitro analyses carried out in the RAW 264.7 cell line (Fig. 2). To confirm the generation of the G50DbIKo virus, we sequenced the areas of interest to ensure that the desired deletions were present in the viral genome (data not shown). To further confirm that the virus was intact and that the deletions were inserted into the gene 50 locus, as well as the absence of spontaneous rearrangements and insertions in the viral genome, we digested the mutant BAC with the restriction endonuclease *Hind* III, *Pst*I and *Eco*RI. Notably, in the process of generating the desired deletions we introduced diagnostic *Hind* III sites (Fig. 3B, 3C). *Hind* III digestion of the G50DbIKo mutant yielded the 3 expected digestion fragments (590bp, 874bp, and 1,059bp), while *Hind* III digestion of wild type virus and the marker rescue BAC DNAs resulted in the expected 2,643bp product. To further assess the presence of the deletions in the gene 50 locus, we performed a Southern blot of the *Hind* III digested BAC DNAs (Fig. 3C). We probed the blot with a 1,651bp probe corresponding to genome coordinates from bp 65,040-66,690 - which hybridized to all three fragments generated. Notably, the band intensities varied and were dependent on the extent that the probe overlapped with the fragments generated. Importantly, the wild type sized fragment was absent from the G50DbIKo and G50PpKO viral genomes, eliminating the possibility of a genome duplication of the gene 50 locus or recombination of the targeting sequences into another region of the viral genome. The final confirmation that the mutant generated was specific to the area of interest was the generation and confirmation of the G50DbIKo.MR and G50PpKO.MR viruses, in which the Orf50 GalK region was replaced with

the WT Orf50 region. These marker rescue viruses were all analyzed by sequencing, restriction enzyme digest, and Southern blotting, and all three methods confirmed reversion back to WT virus. To ensure the phenotypes observed with the G50pDblKo virus were in fact the result of the desired mutations, this process was conducted four independent times resulting in the isolation of four independently generated mutant clones. These clones are used throughout the experiments interchangeably, and each experiment was conducted using at least two if not all the clones. The use of multiple independent clones, in conjunction with the G50pDblKo.MR virus, makes it very unlikely that the observed phenotypes were the result of spontaneous mutations arising elsewhere within the genome.

Replication of the MHV68 G50DblKo mutant, but not wild type MHV68, is inhibited by type I interferons.

To generate the G50DblKo virus the mutated BAC was first transfected into Vero cells expressing Cre-recombinase (Vero-Cre) (167) to excise the BAC from the MHV68-BAC. The removal of the BAC sequence is necessary since virus containing BAC sequences is significantly attenuated *in vivo* (2). Upon successful removal of the BAC in Vero-Cre cells, viral stocks are generated by growth on murine NIH 3T12 cells (167). Surprisingly, Vero-Cre cells transfected with the G50DblKo BAC DNA supported growth of this mutant – indicating that the proximal and distal gene 50 promoters are not required for RTA expression. However, upon low MOI infection NIH 3T12 fibroblasts with the resulting viral stock generated from growth in Vero-Cre cells, we failed to observe any replication of the G50DblKo mutant. To further investigate this phenomenon, multi-step growth curves were performed on both NIH 3T12 and Vero-Cre cells (Fig. 4). Consistent with the initial analyses, the G50DblKo mutant was able to grow in Vero-

Cre cells exhibiting only a mild replication defect (Fig. 4B) – indicating that both the proximal and distal gene 50 promoters are dispensable for RTA expression in these cells. However, we failed to observe any growth of the G50DbIKo mutant on NIH 3T12 fibroblasts (ca. 4-5 log defect in viral titers between marker rescue virus and G50DbIKo mutant at late times post-infection) (Fig. 4A).

Since a major difference between Vero cells and NIH 3T12 fibroblasts is that Vero cells lack the ability to generate type 1 interferons, we assessed whether a type I IFN response can block replication of the G50DbIKo mutant virus. We infected mouse embryo fibroblasts (MEFs) generated from C57BL/6 mice with the G50DbIKo virus and once again we failed to see efficient replication (Fig. 5A). The G50DbIKo virus exhibited nearly a 4 log defect in viral titers at late times post-infection. To determine whether type I interferons were responsible for this large defect, we infected MEFs generated from 129S2/SvPas. $IFN-\alpha/\beta R^{-/-}$ mice. Similar to the results obtained in Vero cells, the inability of the MEFs from mice lacking the $IFN\alpha/\beta$ receptor to respond to a type I IFN response rescued the replication defect seen in the C57BL/6 MEFs (Fig. 5B). Notably, in the 129S2/SvPas. $IFN-\alpha/\beta R^{-/-}$ MEFs the G50DbIKo virus replication was indistinguishable from wild type virus (Fig. 5B). To directly examine the impact of type I IFNs on replication of the G50DbIKo mutant, we compared virus replication in Vero cells in the absence and presence of $IFN\alpha$. Vero-Cre cells were pretreated with $IFN-\alpha$, and then every 24 hours post-infection. Cells that were not treated with $IFN-\alpha$, as seen before, showed normal growth and kinetics of the G50DbIKo virus similar to WT and G50DbIKo.MR viruses (Fig. 5C). However, adding $IFN\alpha$ severely inhibited replication of the G50DbIKo mutant (Fig. 5D).

The latter analyses revealed an impact of type I interferons on in vitro replication of MHV68 [although it has previously been shown that acute viral titers in the lungs of $IFN\alpha/\beta R^{-/-}$

mice is significant higher than in wild type mice and that the absence of a type I IFN response renders mice highly susceptible to lethal MHV68 infection (6, 10, 59)]. These analyses also reveal that, despite replication of the G50DbIKo virus being attenuated in the presence of a type I IFN response, there appears to be little or no replication defect in comparison to wild type virus when a type I interferon response is absent – either due to the lack of the IFN α / β R or the absence of type I IFN expression. In addition, these analyses demonstrate that despite the deletion of the known gene 50 promoters, the G50DbIKo mutant is replication competent under some experimental conditions – suggesting that there are alternative mechanisms for expression of the essential immediate-early RTA.

Notably, upon higher MOI infections, the observed growth defect of the G50DbIKo can be partially rescued (Fig. 6A). This suggests that increasing the MOI may alter the kinetics of expression of a viral gene product(s) involved in blocking the action of type I IFNs. However, even under conditions where the G50DbIKo mutant does not exhibit a growth defect, we have observed that it exhibits a small plaque phenotype (Fig. 6B). As noted above, the growth characteristics and small plaque phenotype of the G50DbIKo mutant were observed with 4 independently derived BAC clones, making it unlikely that any of the observed phenotypes are the result of secondary mutations in the viral genome.

Identification of three additional gene 50 transcripts driven by 2 promoters mapping upstream of the distal gene 50 promoter.

We have previously shown that transcription of MHV68 gene 50 is driven by two distinct promoters: the proximal promoter encoding a short 288bp exon, E1, which splices to the large 1800bp exon, E2; and the distal promoter which encodes a short 181bp exon, E0, which

splices to E1, which in turn splices to E2 (81, 149, 255) (see Fig. 1). We further showed that this organization of gene 50 transcription was conserved in both EBV and KSHV (81). The unexpected ability of the G50DbIKo mutant to replicate under some experimental conditions, indicated that there must exist alternative mechanisms for driving gene 50 transcription since RTA is known to be absolutely required for virus replication (this has been shown for EBV, KSHV and MHV68) (60, 87, 190, 259, 272). To determine if this hypothesis was indeed correct, we performed 5' RACE analysis of RNA from Vero-Cre, RAW 264.7 and IFN- α/β R^{-/-} MEFs, infected with either wild-type MHV68 or the G50DbIKo mutant. From this analysis we were able to detect three previously unidentified gene 50 transcripts which initiated from 2 distinct upstream transcription initiation sites (Fig. 7).

The three additional transcripts were identified in all three cell types examined, and also were identified in both wild-type MHV68 as well as G50DbIKo virus infected cells. It is important to note that the 5' RACE analyses conducted using the G50pDbIKo virus failed to detect the presence of any E1-E2 or E0-E1-E2 transcripts - further confirming that the G50pDbIKo is indeed a true knockout of the proximal and distal gene 50 promoters. The first new exon, which we have termed N3, is a 330bp extension of the previously characterized E0 exon. This new N3 exon is 511bp long and maps to coordinates bp 65,579 to 66,090 in the MHV68 genome. The 3' end of this exon is identical to the 3' end of the E0 exon. Like E0, this newly identified N3 exon splices to the E1 exon leading to removal of a 419bp intron, which in turn splices to the E2 exon removing an 865bp intron (Fig. 7). The second new exon, which we have termed N4, is a 743bp extension of the E0 exon. The N4 exon map to bp 65,166-66,090 in the MHV68 genome and is 924bp long (Fig. 7). The 3' end of this exon is also identical to the 3' end of the E0 and splices to the E1 exon and then to E2 exon. The final alternatively spliced

transcripts contains a new exon, which we have termed N5, which is 216bp long and maps to bp 65,142-65,358 in the MHV68 genome (Fig. 7). This new exon mainly consists of the 5' end of the newly identified N4 exon, with a 24bp extension indicating that the N4 and N5 exons share a common promoter region. However unlike N4 which is an extension of E0, the N5 exon exhibits a completely unique splicing event in which the 3' end at bp 65,358 splices to E1 directly eliminating a large 1151bp intron. Like the other known exons, the E1 exon then splices to the E2 exon.

It is important to note that none of the newly identified exons have been observed to splice directly to the E2 exon, but rather all of them splice to the E1 exon – which contains the RTA translation initiation codon. Thus, to date, there is no evidence for alternative RTA translation initiation sites. This, however, does not exclude the possibility of unique splicing events from the newly identified transcripts to a novel position within the E2 exon, or elsewhere within the viral genome. It should be noted that there are several short ATG-initiated open reading frames encoded within the newly identified exons – which may play an important role (i.e., encoding novel viral gene products and/or interfering with RTA translation) (Fig. 7).

Neither the N3 promoter nor the N4/N5 promoter exhibit sensitivity to IFN α , but RTA levels from the G50DblKo mutant are diminished in the presence of a type I IFN response at low MOI.

The identification of alternative gene 50 transcripts provides a clear mechanism by which the G50DblKo virus is apparently able to generate sufficient levels of RTA to drive virus replication – at least in the absence of a type I IFN response. However, it does not address the issue of why replication of the G50DblKo mutant is suppressed by type I IFNs. To begin to

address this issue, we cloned 1000bp fragments immediately upstream of the 5' end of the N3 and N4/N5 transcripts into the pGL4.10 luciferase reporter vector (Promega Biotech) and the resulting reporter constructs were transfected into Vero-Cre cells. While the N3 promoter resulted in expression ~4 fold over empty vector, the N4/N5 promoter resulted in slightly higher levels of luciferase expression (~13 fold over empty vector) (Fig. 8). This data demonstrates that the region immediately upstream of the newly identified gene 50 transcripts exhibit modest promoter activity. To determine if the type I IFN sensitive replication of the G50DbIKo mutant virus reflects type I IFN-mediated suppression of gene 50 transcription from the G50DbIKo mutant, we examined N3 and N4/N5 promoter activity in the presence of IFN α treatment (Fig. 8). Since Vero cells fail to produce IFN α , but retain the ability to respond to exogenously added IFN α (see Fig. 5D), IFN α was added to the transfected Vero cells and promoter activity assessed (Fig. 8). Similar luciferase assays of previous identified Orf50 transfected promoters have shown them to be sensitive to IFN γ (79). However, our analysis showed no evidence of IFN α suppression of reporter gene activity, suggesting that IFN α inhibition of G50DbIKo replication acts downstream of gene 50 transcription.

Since it appeared that the newly identified gene 50 promoters are not sensitive to IFN α , we examined the levels of RTA protein expression in wild-type MHV68 and G50DbIKo mutant infected cells. To assess RTA levels following infection, immunoblots were probed at several time points following low MOI infection (Fig. 9). Consistent with the observed replication defect of the G50DbIKo mutant virus in either NIH 3T12 fibroblasts or C57Bl/6 MEFs, RTA levels were lower at all time points assessed (Fig. 9, panels A & B). However, equivalent levels of RTA were detected in 129S2/SvPas.IFN- α / β R^{-/-} MEFs infected with either wild type MHV68 or the G50DbIKo mutant virus. It is also notable that RTA was readily detectable by 24 hours

post-infection of either C57Bl/6 MEFs or 129S2/SvPas.IFN- α/β R^{-/-} MEFs, but not NIH 3T12 fibroblasts (Fig. 9, compare panels B and C to panel A). We have previously noted that MEFs are more sensitive to MHV68 infection as determined by a limiting dilution CPE analysis which can detect between 0.1 and 0.2 pfu of virus titered on NIH 3T12 fibroblasts (128), and this likely accounts for the earlier detection of RTA expression (i.e., effectively a higher MOI infection).

When looking at RTA levels from growth curves in which there is a partial rescue of the G50pDblKo growth defect (Fig. 6A) the early kinetics and expression of RTA appear to be at similar or slightly higher levels than WT infection (Fig. 6B). RTA was detectable at significant levels 8 hours post-infection in the G50pDblKo virus, while RTA was detectable at 12 hours post-infection in WT virus infected fibroblasts. However, the levels of RTA begin to wane by 24 hours post-infection with the G50pDblKo mutant, while WT RTA continues to increase. This may help explain the partial rescue in the growth phenotype at high MOI. Notably, the induction of v-cyclin expression parallels that of RTA expression for both WT and the G50pDblKo infections. These results demonstrate that despite an increased sensitivity to type 1 interferons, as well as a partial growth defect at high MOI, the G50pDblKo virus is able to generate functional RTA capable of driving transcription as well as launching expression of downstream viral targets such as v-cyclin.

The G50DblKo mutant establishes latency in the spleen and in PECs, but is severely impaired for virus reactivation.

To assess infection in mice with the G50DblKo mutant, we initially infected C57BL/6 mice intranasally with 1,000 PFU of either the G50DblKo virus, WT MHV68, or the G50DblKo.MR virus. We then assessed vial latency at day 18 post-infection, the peak of

infection in the spleen, and determined both the frequency of splenocytes harboring viral genome and the frequency of splenocytes able to reactivate from latency. Splenocyte reactivation was determined by the previously described limiting dilution CPE assay (261) modified by plating splenocytes on IFN- α / β R^{-/-} MEF monolayers to ensure the ability to detect any reactivated G50DbIKo mutant virus. The reactivation analyses revealed the nearly complete absence of detectable reactivation of the G50DbIKo virus from splenocytes (Fig. 10A). In contrast, splenocytes harvested from wild-type virus infected animals reactivated at a frequency of 1 in 7,035 cells, while the frequency of reactivation from the G50DbIKo.MR virus was 1 in 9,549 cells (Fig. 10A and Table 1). No preformed infectious virus was detected in the harvested splenocyte samples, as measured by mechanical disruption of the cells as previously described (261) (data not shown).

To determine if this failure to reactivate from splenocytes observed with the G50DbIKo mutant virus was the result of a failure to establish latency, limiting dilution PCR was performed to determine the frequency of splenocytes harboring viral genomes (261). We observed that the frequency of splenocytes harboring latent virus was roughly equivalent in the wild-type virus and the G50DbIKo.MR virus at 1 in 223 and 1 in 305 cells, respectively, while the G50DbIKo mutant virus was present in splenocytes at a frequency of ca. 1 in 1,941 cells (Fig. 10B and Table 1). While the frequency of viral genome positive splenocytes in the G50DbIKo virus infected animals was around 8.5- fold lower than wild-type virus infected animals, these analyses demonstrate that this mutant virus is able to get to the spleen and establish latency. Thus, the lack of detectable reactivation of the G50DbIKo mutant reflects a significant defect in virus reactivation from B cells – the dominant latently infected cell population in the spleen (41, 42)

We extended these analyses to address whether the inability of the G50DbIKo mutant virus to reactivate from splenocytes was dependent on either route of inoculation, and to assess latency and reactivation from PECs. To do this we assessed virus reactivation from splenocytes and PECs following intraperitoneal inoculation. C57BL/6 mice were infected by intraperitoneal inoculation with 1,000 PFU of G50DbIKo, wild-type, or G50DbIKo.MR virus, and splenocytes and PECs harvested 18 days post-infection. We first examined the ability of the virus to reactivate from splenocytes, as described above. As observed following intranasal inoculation, the G50DbIKo mutant exhibited a large defect in reactivation – although a low level, but significant level of virus reactivation was detectable (estimated by extrapolation that the G50DbIKo mutant reactivates at a frequency of 1 in 422,863 splenocytes) (Table 1). In these analyses, wild-type virus reactivated at a frequency of 1 in 36,107 splenocytes, while the G50DbIKo.MR virus reactivated at a frequency of 1 in 65,962 splenocytes (Table 1). Notably, the frequency of splenocytes reactivating virus at day 18 following intraperitoneal inoculation was 5 to 7-fold lower than observed at the same time point following intra-nasal inoculation. This likely reflects faster kinetics of establishment and contraction of splenic latency following intraperitoneal inoculation. This effect, coupled with the observed low level reactivation of the G50DbIKo mutant, provides evidence that the route of inoculation does have an impact on reactivation of this mutant virus – which could be linked to better establishment of B cell latency (see discussion below). We then assessed whether the observed reactivation defects correlated with a defect in the establishment of latency. Notably, the 8.5-fold defect in establishment of latency in splenocytes observed following intranasal inoculation was largely rescued following intraperitoneal inoculation (Table 1). The frequency of viral genome positive cells in the

splenocytes following intraperitoneal inoculation was 1 in 388 cells for wild-type MHV68, 1 in 1,047 cells for the G50DbIKo.MR virus, and 1 in 627 cells for the G50DbIKo mutant (Table 1).

While nearly all virus reactivation from splenocytes arises from latently infected B cells (144, 262), macrophages represent the major latently infected cell type in PECs. Thus, to address whether the observed defect in G50DbIKo reactivation from splenocytes reflects a B cell-specific defect, we determined the frequency of PECs reactivating virus. In contrast to the previous observation that the G50pKO virus retained the ability to reactivate from PECs (81), the G50DbIKo exhibited no detectable reactivation from PECs (Fig. 10C and Table 1). As expected, both wild-type MHV68 and the G50DbIKo.MR virus reactivated from PECs at a frequency of 1 in 17,782 cells and 1 in 14,417 cells, respectively (Fig. 10C and Table 1). These results indicate that despite the ability to drive viral replication, the absence of both the proximal and distal gene 50 promoters results in a substantial impairment in the ability of MHV68 to reactivate from infected cells *in vivo*. Despite rescue of establishment of latency in splenocytes following intraperitoneal inoculation, an ca. 6-fold defect in the establishment of latency in PECs was observed (the frequency of viral genome positive PECs in wild-type infected animals was 1 in 401 cells, in G50DbIKo.MR infected animals it was 1 in 562 cells, and in G50DbIKo it was ca. 1 in 2,137 cells) (Fig. 10D and Table 1). Despite the modest impairment of the G50DbIKo mutant in the establishment of latency in PECs, it is clear that this mutant is significantly impaired in reactivation from latency from both splenic B cells and peritoneal macrophages.

The G50DbIKo phenotype in vivo is partially rescued in mice lacking the IFN α / β receptor.

Since we have shown that the G50DbIKo mutant virus retains the ability to grow with normal kinetics and to high titer in cells that lack a type I IFN response (Figs. 4B and 5B), we

assessed whether the absence of a type I IFN response *in vivo* would rescue the G50DbIKo replication and reactivation defects. Thus, we infected 129S2/SvPas.IFN- α / β R^{-/-} mice with 1,000 PFU of either the G50DbIKo mutant or wild-type MHV68 via intranasal inoculation. It has previously been shown that MHV68 infection of mice lacking the IFN α / β receptor results in the majority mice succumbing during the acute phase of infection (6, 10, 59, 186). Surprisingly, while the G50DbIKo mutant replicates to high titers in the lungs of IFN α / β R^{-/-} mice (Fig. 11C), all infected mice survived (Fig. 11A). However, as expected only 3 of 19 mice infected with 1,000 PFU wild-type MHV68 WT virus survived past 2 weeks post-infection (Fig. 11A). Parallel analyses in C57Bl/6 mice confirmed the severe replication defect observed with the G50DbIKo mutant (virus replication in the lungs was below the limit of detection in all infected mice). Notably, acute replication of the G50DbIKo mutant in the lungs of IFN α / β R^{-/-} mice was rescued to near wild-type MHV68 levels (Fig. 11C). To further address the absence of lethality in IFN α / β R^{-/-} mice with the G50DbIKo mutant, we extended these studies using higher inoculating doses. We did not observe any lethality, even when mice were infected with ca. 400-fold higher dose of the G50DbIKo mutant (5 of 5 mice infected survived for greater than 4 weeks post-infection) (Fig. 11D). Thus, while acute virus replication of the G50DbIKo mutant in the lungs following intranasal inoculation was largely rescued by loss of a type I IFN response, MHV68-associated lethality was not observed – indicating a requirement for the gene 50 proximal and/or distal promoters for RTA expression in some anatomical site during the acute phase of virus infection.

Having shown that the severe defect in acute replication of the G50DbIKo mutant observed in C57Bl/6 mice was largely rescued in mice lacking the ability to respond to type I IFNs, we assessed establishment of latency and virus reactivation in IFN α / β R^{-/-} mice. Spleens

were harvested at day 28 from IFN α / β R $^{-/-}$ mice intranasally infected with 1,000 PFU of either wild-type or G50DbIKo virus. It is important to note that the latency and reactivation analyses for wild-type virus infected IFN α / β R $^{-/-}$ mice was carried out using the subset of infected animals that survived acute virus replication (see Fig. 10A). Like the rescue of acute virus replication in the lungs, the frequency of viral genome positive splenocytes went from an ca. 8-fold defect in I.N. infected C57BL/6 mice (Fig. 10B) to an almost identical frequency of virus infected splenocytes in IFN α / β R $^{-/-}$ mice (1 in 131 cells for wild-type MHV68, and 1 in 133 for the G50DbIKo mutant) (Fig. 12A and Table 1). More importantly, the defect in virus reactivation observed in C57Bl/6 mice was completely rescued in IFN α / β R $^{-/-}$ mice (1 in 77,624 splenocytes in WT infected mice compared to 1 in 52,420 splenocytes in G50DbIKo virus infected mice) (Fig 12B and Table 1). The latter result argues in favor of a model in which the sole defect in G50DbIKo virus reactivation from C57Bl/6 splenocytes is the inability to overcome type I IFN suppression of virus replication.

One possible explanation for the ability of the G50pDbIKo virus to replicate in the absence of type 1 interferons would be an increased expression of E1-E2 transcripts. This would make the G50pDbIKo virus not a true double promoter knockout virus as E1-E2 transcripts would be responsible for the ability of the virus to replicate. However, this does not appear to be the case because: (i) as shown in figure 6, RTA expression from the G50pDbIKo in normal fibroblasts is not impaired; and (ii) analysis of 5' RACE products generated from Vero cells, as well as IFN α / β R $^{-/-}$ MEFs, using the G50pDbIKo virus failed to detect any proximal promoter (E1-E2) or distal promoter (E0-E1-E2) initiated transcripts. However, to more directly assess potential residual proximal promoter activity in the absence of a type I IFN response, we cloned both the proximal promoter and the proximal promoter deletion mutant into the pGL4.10Luc

reporter plasmid. These reporter constructs were transfected into Vero cells, in the presence and absence of IFN α treatment. Importantly, the proximal promoter does not appear to be sensitive to the presence of IFN α (Fig. 13) - which is consistent with the results shown in Figure 5D where pretreatment with IFN α has no effect on WT MHV68 growth. Furthermore, the proximal promoter deletion mutant exhibited significant lower promoter activity – both in the presence and absence of added IFN α . Thus, taken together these results argue against proximal promoter-driven RTA expression accounting for the rescue of G50pDblKo virus replication in the absence of type I IFN.

2.V. DISCUSSION

Here we demonstrate that MHV68 gene 50 transcription is more complex than previously reported (81, 149, 255). Based on the current analyses, MHV68 RTA expression can be driven from four distinct promoters, and these promoters drive expression of 5 different spliced gene 50 transcripts. The identification of multiple promoters driving expression of a single gene is not a novel concept - there are many human and viral genes whose expression has been shown to be regulated by multiple promoters (52, 124, 126, 161, 185). For example, EBV has been shown to use differential splicing and from 2 distinct promoters in the generation of the transcripts encoding the six EBNA gene products (20, 210, 231, 232, 269). The use of multiple promoters is often the result of a complex lifecycle and/or, particularly in the case of viruses, the infection of multiple cell types. We have shown that alternatively initiated gene 50 transcripts is conserved in MHV68, KSHV and EBV infected cells – having previously reported the detection of both proximal and distal promoter-initiated gene 50 transcripts (81). In addition, it has been previously shown by others that HVS RTA expression is driven from distinctly initiated transcript expressed at different times in the viral replication cycle (266). Here we identify 2 additional gene 50 transcription initiation sites - gene 50 transcripts arising from these promoters could be detected in MHV68 infection of a macrophage cell line (RAW 264.7), a non-human primate epithelial cell line (Vero), and IFN α / β R $^{-/-}$ mouse embryonic fibroblasts, indicating that these promoters appear to be widely active during virus replication and not restricted to a particular cell type. However, we have not carried out a detailed analysis of the abundance of specific gene 50 transcript species as a function of cell type or time post-infection and it is certainly possible that their activities *in vivo* are more restricted. Thus, the current analyses do not rule out the possibility that the identified gene 50 promoters behave differently depending on

cell type infected, or address the contribution that each promoter plays in different cell types during the course of infection.

The utility of MHV68 infection of mice is that it provides a tractable small animal model to identify basic aspects of gammaherpesvirus pathogenesis that may be relevant to the human viruses EBV and KSHV. As such, we have begun to explore whether the complex gene 50 transcription observed during MHV68 replication is conserved in the human viruses. Notably, our preliminary characterization of gene 50 transcription during KSHV reactivation from latently infected B cells has identified multiple distinct gene 50 transcription initiation sites, as well as alternative splicing that is very similar to that observed in MHV68 infected cells (data not shown). Further analyses are necessary to fully characterize these novel gene 50 transcripts expressed during KSHV reactivation from B cells, as well as characterize BRLF1 transcription during EBV infection.

The data presented here is among a limited number of studies (271) showing that type I interferons play an important role in suppressing MHV68 replication in tissue culture. This is strikingly different than WT MHV68 in which *in vitro* growth is not affected by the presence of type I interferons. However, it is important to emphasize that *in vivo* type I interferons play a critical role in controlling acute MHV68 replication as mice lacking the IFN α/β receptor are highly susceptible to lethal MHV68 infection (10, 59). In addition, it has previously been shown that type 1 interferons play a role in controlling viral reactivation from latency (10, 155).

The levels of RTA protein were greatly reduced in G50DbIKo infected cells in the presence of a type I IFN response (Fig. 9A,B), and abrogating the ability to respond to type I IFNs by disrupting the IFN α/β R rescued wild-types levels of RTA expression from the G50DbIKo mutant virus (Fig. 9C). Since RTA is the first immediate-early gene expressed

during gammaherpesvirus infection, it directly and indirectly begins the lytic replication cascade by turning on a variety of downstream genes (37, 39, 54, 150, 157, 200, 228). Many of these downstream genes are responsible for an anti-type 1 interferon response, such as Orf45, M2, and Orf54 (132, 143, 147, 220, 291, 292). Importantly, the ability of MHV68 to overcome the type I IFN response appears to be not only essential, but also immediate. Growth curves where IFN α was added prior to infection and during infection (Fig. 5D) demonstrate that the virus is able to overcome a type I IFN induced anti-viral cell environment; wild-type MHV68, even at low MOI, is unaffected by IFN α treatment. We hypothesize then that this may involve three distinct mechanisms. First, the virion contains a viral protein(s) able to suppress the type I IFN response. MHV68 proteins associated with the virion have been identified, and this includes the Orf45 encoded protein which has already been implicated in regulating the type I IFN response (22). Second, RTA may itself be involved in mediating an anti-type I IFN response – but this would likely require that sufficient levels of RTA be expressed in an appropriate time frame post-infection to be effective. Third, RTA expression and function may be insensitive to type 1 interferon effects, and thus is able to initiate downstream gene signaling despite the presence of an anti-viral cellular state. Future studies will need to address these possibilities.

It is notably that replication of the G50pDblKo is partially rescued at high MOI infection. However, replication following high MOI infection is still severely impaired (as shown in Fig. 6, titers never rise significantly above the input levels). Furthermore, this likely reflects the difference between a single cycle of replication vs. multiple rounds of replication required following low MOI infection. Indeed, following high MOI infection initial RTA levels following infection with the G50pDblKo virus are higher than WT virus infected fibroblasts, but these levels decrease over time (Fig. 6B hours 16, 20, 24). This indicates that RTA expression is

deregulated in G50pDblKo cells and this likely impacts the tightly regulated lytic cascade ultimately leading to diminished virus production and the observed small plaque phenotype (Fig. 6C).

Overall these studies further reveal the complex nature of gammaherpesviruses replication. The identification of 3 additional Orf50 transcripts was surprising, but likely illustrates how the virus has evolved to carefully control expression of the essential lytic switch gene. Though beyond the scope of this study, future work will investigate the function of these alternative gene 50 promoters and transcripts, as well as their presence/absence in other gammaherpesviruses. It is clear that in the absence of type 1 interferons the newly identified gene 50 transcripts are able to drive viral replication nearly as efficiently as wild type MHV68. This suggests that these promoters may play a cell type specific and/or time dependent role in the viral lifecycle. Indeed, independent studies have recently revealed that the N4/N5 promoter is responsive to IL4 treatment in macrophages, which has been shown to trigger MHV68 reactivation from latently infected macrophages (Reese et al., unpublished data). Another possibility is that upstream initiated gene 50 transcription may, under some conditions, serve to suppress RTA expression by interfering with transcription from the more proximal gene 50 promoters. Transcriptional interference has been shown before for some EBV transcripts (188, 221, 269, 270). In addition, the role of the short ATG-initiated open reading frames in the 5' untranslated regions of upstream initiated gene 50 transcripts remains to be investigated.

In summary, the analysis of the G50DblKo mutant extends our understanding of RTA expression, and has revealed a hitherto unappreciated complexity of gene 50 transcription. It is notable that until the analysis of the G50DblKo mutant, little or no impact of type I interferons on wild type MHV68 replication was observed. This was in stark contrast to the analysis of

MHV68 replication during the acute stages of infection in IFN α / β R $^{-/-}$ mice, where substantially higher levels of virus replication are observed in the lungs of type I interferon unresponsive mice compared to wild type mice following i.n. virus inoculation (e.g., see Fig. 11) (59). Based on the observations with the G50DbIKo mutant replication *in vitro*, it is perhaps reasonable to speculate that during acute virus replication there may be a role for type I IFN-sensitive gene 50 transcription. Future studies will address whether any of the newly identified gene 50 transcripts play such a role during acute virus replication *in vivo*.

2.VI. FIGURE LEGENDS

Figure 1. Genomic Alignment of Orf50/BRLF1/Rta region from MHV68, EBV, KSHV, and HVS gammaherpesviruses illustrating the conserved organization of gene 50 transcription. Schematic diagram of the Orf50 region with Exon 2, Exon 1, and recently discovered Exon 0 shown. The anti-sense coding regions Orf48/BRRF2, and Orf49/BRRF1 are shown to demonstrate the conserved organizational context. Boxes drawn around Exon 1 and Exon 0 show their relative position within the genome. The nucleotide positions of exon 0 (E0), exon 1 (E1), and exon 2 (E2) are given.

Figure 2. Promoter deletions within the MHV68 E0 250bp promoter region. Reporter constructs were generated within the context of the 250bp promoter through overlapping PCR. The 50bp E0 promoter mutants were cloned into the pGL4.10[luc] luciferase report construct. RAW 264.7 cells were cotransfected with pGL4.10[luc] luciferase report constructs containing 50bp deletions as illustrated and pHR-Luc (*Renilla* luciferase). RAW 264.7 cells were stimulated with LPS (5µg/ml) 24 hours after transfection and 48 hours after transfection luciferase assays were performed. Data is presented as the fold difference in the ratio of firefly: *Renilla* luciferase verse the pGL4.10[luc] empty vector control. The data were compiled from 3 independent transfections, each done in triplicate. Standard error of the mean is shown.

Figure 3. Generation of MHV68 G50DbIKo and G50DbIKo.MR viruses. (A) Schematic diagram of alternatively initiated gene 50 transcripts. The locations of the known proximal and distal gene 50 promoters are shown. The two hashed areas depict the regions deleted within the mutant G50DbIKo virus; a 50bp deletion extending from bp 65,772-65,822 in the distal promoter region

and a 70bp deletion extending from bp 66,412-66,482 in the proximal promoter region. There are two *HindIII* sites in the WT genome located at bp 64,898 and 67,541; the G50DblKo virus has two additional *HindIII* sites introduced within the deletions, located at bp 65,797 and 66,447. The splicing of E1 to E2 driven by the proximal promoter and the splicing of E0 to E1 to E2 driven by the distal promoter is shown. (B) *HindIII* restriction endonuclease digests of G50DblKo, G50PpKo, G50DblKo.MR, G50PpKo,G50GalK, and WT-YFP BAC. The diagnostic restriction fragments are depicted (●). (C) Southern blot of the *HindIII* digest shown in panel B using a probe specific for the Orf50 region. Three unique digestion fragments are shown for the G50DblKo virus, WT and MR rescue virus are shown to be the same, and the galK parent fails to hybridize the Orf50 probe due to the Orf50 region replacement with the GalK cassette.

Figure 4. G50DblKo virus replicates *in vitro* in Vero-Cre cells, but fails to replicate in NIH 3T12 fibroblasts. (A) Multistep growth curve of NIH 3T12 cells infected with an MOI of 0.1. Cells were infected with G50DblKo, G50DblKo.MR, and WT-YFP virus and collected for viral titer analysis at the indicated times post-infection. (B) Multistep growth curve of Vero-Cre cells infected at an MOI of 0.1. Cells were also infected with G50DblKo, G50DblKo. MR, and WT-YFP virus and collected for viral titer analysis at the indicated times post-infection.

Figure 5. G50DblKo virus fails to replicate *in vitro* when IFN α is present. (A) Multistep growth curve of C57BL/6 mouse embryonic fibroblasts (MEFs) infected with G50DblKo or WT-YFP virus at an MOI of .01. (B) Multistep growth curve of 129S2/SvPas.IFN- α / β R^{-/-} mouse embryonic fibroblasts (IFN α / β R^{-/-} MEFs) infected with G50DblKo or WT-YFP virus at an MOI of 0.01. (C) Multistep growth curve of Vero-cre cells infected with G50DblKo, G50DblKo.MR,

or WT-YFP virus at an MOI of 0.1. (D) Multistep growth curve of Vero-cre cells, treated with IFN α (10,000IU/ml) at time of infection and every 24 hours thereafter, infected with G50DblKo, G50DblKo.MR, or WT-YFP virus at an MOI of 0.1. All cells were collected at times indicated and repeated at least in triplicate.

Figure 6. Single-step growth analyses of the G50pDblKo mutant, and analysis of the kinetics of RTA expression. (A) Single-step growth curve of G50pDblKo or WT-YFP virus in NIH 3T12 fibroblast infected at an MOI of 10. (B) Western Blot staining for RTA, v-cyclin, and β -actin expression from same cells used in the single-step growth curve shown in A. (C) Representative sample of the small plaque phenotype exhibited under all experimental conditions when using different G50pDblKo clones.

Figure 7. RACE analyses reveal three additional G50 exons upstream of E0. RACE analyses were performed using cDNA generated from WT-YFP and G50DblKo infected Vero-Cre, Raw 264.7, and IFN α / β R $^{-/-}$ MEFs at 24 and 48 hours postinfection. 5' RACE analysis using reverse primers located in E2, E1, and E0 were used in conjunction with the universal 5' RACE forward primer. All three experiments identified three additional exons upstream of E0. Exon N3 representing a 330bp extension of E0, Exon N4 representing a 743bp extension of E0, and N5 representing a small novel 216bp exon. All three new exons follow canonical splicing in which they splice to E1 which in turn splices to E2. Green arrows denote short ATG-initiated open reading frames that lie upstream of the RTA coding sequences which are indicated in blue. The locations of the major open reading frames antisense to gene 50 are also shown. Red arrows

denote primers used in the 5' RACE analyses; the positions of the primers used were as follows: E2-1, bp68095-68066; E2-2, bp68051-68027; E1, 66530-66509; and E0, 65930-65909.

Figure 8. Promoter activity in the region immediately 5' to MHV68 N3, N4, and N5 exons. Vero-Cells were transfected with pGL4.10[luc] luciferase report constructs containing either 1000bp upstream of N3 or 1000bp upstream of the N4/N5 exon. Vero-cells were stimulated with IFN α (10,000IU/ml) 24 hours after transfection and 48 hours after transfection luciferase assays were performed. Data is presented as the fold difference of firefly luciferase activity verse the pGL4.10[luc] empty vector control. The data represented in triplicate at least three independent transfections.

Figure 9. Immunoblot analyses of RTA protein expression levels in WT and G50DblKo infected NIH 3T12 fibroblasts, C57BL/6 MEFs, and 129S2/SvPas.IFN- α / β R^{-/-} MEFs. (A) NIH 3T12 cells were infected with wild-type MHV68 or the G50DblKo mutant at an MOI of 0.1 and cells harvested at 24, 48, and 72 hours post-infection. Cells were lysed and 30ug of protein was used for the immunoblot analyses to assess RTA expression levels. MEFs prepared from either C57BL/6 (panel B) or 129S2/SvPas.IFN- α / β R^{-/-} (panel C) were infected at an MOI of 0.1 and cells were harvested at 24, 48, and 72 hours post-infection. As in panel A, cells were then lysed and 30ug of protein used in a immunoblot analysis to detect RTA expression levels. All immunoblots were stripped and then reprobed for β -actin levels to ensure equal protein loading.

Figure 10. G50DblKo virus exhibits a severe reactivation defect and a moderate latency defect *in vivo*. Female C57BL/6 mice were infected with 1000PFU I.N. (A and B) or 1000 PFU I.P (C,

D). Splenocytes and PECs were harvested 18 days postinfection and assessed for the establishment of latency and reactivation from latency by limiting dilution CPE and PCR assays. (A) Splenocytes from I.N. infections were plated in serial dilutions onto an IFN α / β R $^{-/-}$ MEF monolayer and 21 days post plating wells were individually scored for CPE. The percentage of these wells was used to calculate the frequency of virally reactivating cells. (B) Splenocytes from I.N. infections were plated in serial dilutions and subjected to nested PCR to detect gene 50 copies. The percentage of genome-positive cells in each dilution was used to calculate the frequency of latency. (C) PECs from i.p. infections were plated in serial dilutions onto an IFN α / β R $^{-/-}$ MEF monolayer and 21 days post plating wells were individually scored for CPE. The percentage of these wells was used to calculate the frequency of virally reactivating cells. (D) PECs from i.p. infections were plated in serial dilutions and subjected to nested PCR to detect gene 50 copies. The percentage of genome-positive cells in each dilution was used to calculate the frequency of latency. For all reactivation assays (A and C), mechanically disrupted cells were plated in parallel for each virus shown to control for preformed infectious virus, all mechanically disrupted cells were negative for reactivation (data not shown). Data are representative of at least two independent experiments consisting of 5 mice per group. Error bars were calculated using the standard error of the mean.

Figure 11. Infection of 129S2/SvPas.IFN- α / β R $^{-/-}$ mice with G50DbIKo virus does not result in lethality as seen with WT virus despite the presence of high viral titers in the lungs. (A). Kaplan Meier curve depicting 129S2/SvPas.IFN- α / β R $^{-/-}$ mice survival when challenged with 1,000 PFU I.N. of WT or G50DbIKo virus. (B). Lung titers at day 7 from C57BL/6 mice infected with 1,000PFU I.N. of G50DbIKo or G50DbIKo.MR virus. (C) Lung titers at day 7 from

129S2/SvPas.IFN- α / β R^{-/-} mice infected with 1000PFU I.N. of G50DbIKo or G50DbIKo.MR virus. (D) Kaplan Meier curve depicting 129S2/SvPas.IFN- α / β R^{-/-} mice survival when challenged with 440,000 PFU I.N G50DbIKo virus compared to mice survival when challenged with 1,000PFU G50DbIKo.MR virus.

Figure 12. G50DbIKo virus establishes latency and reactivates to similar levels as WT Virus when used to infect 129S2/SvPas.IFN- α / β R^{-/-} mice *in vivo*. Female 129S2/SvPas.IFN- α / β R^{-/-} mice were infected with 1,000 PFU of G50DbIKo Virus, WT Virus, or G50DbIKo.MR Virus by intranasal injection. Day 28 postinfection surviving mice (N=20 G50DbIKo, N= 3 WT/G50DbIKo.MR) were harvested for splenocytes and assessed for establishment of latency and reactivation from latency. (A). As in figure 10A splenocytes were serially diluted and used in a CPE assay to look for frequency of viral reactivating cells. (B) As in figure 10B splenocytes were serially diluted and used in a nested PCR assay to look for frequency of viral genome positive cells.

Figure 13. Promoter activity in the region immediately 5' to the MHV68 proximal promoter and proximal promoter deletion. Vero cells were transfected with pGL4.10[luc] luciferase reporter constructs containing either 410bp upstream of exon 1 or 340bp upstream of exon 1 containing the 70bp deletion as shown in Figure 3a. Vero cells were stimulated with IFN α (10,000IU/ml) 24 hours after transfection and 48 hours after transfection luciferase assays were performed. Data is presented as the fold difference of firefly luciferase activity verse the pGL4.10[luc] empty vector control. The data represents in triplicate at least three independent transfections.

2.VII. FIGURES AND TABLES

1. Genomic Alignment of Orf50/BRLF1/Rta region from MHV68, EBV, KSHV, and HVS gammaherpesviruses illustrating the conserved organization of gene 50 transcription
2. Promoter deletions within the MHV68 E0 250bp promoter region
3. Generation of MHV68 G50DbIKo and G50DbIKo.MR viruses
4. G50DbIKo virus replicates *in vitro* in Vero-Cre cells, but fails to replicate in NIH 3T12 fibroblasts
5. G50DbIKo virus fails to replicate *in vitro* when IFN α is present
6. Single-step growth analyses of the G50pDbIKo mutant, and analysis of the kinetics of RTA expression
7. RACE analyses reveal three additional G50 exons upstream of E0
8. Promoter activity in the region immediately 5' to MHV68 N3, N4, and N5 exons
9. Immunoblot analyses of RTA protein expression levels in WT and G50DbIKo infected NIH 3T12 fibroblasts, C57BL/6 MEFs, and 129S2/SvPas.IFN- α/β R^{-/-} MEFs
10. G50DbIKo virus exhibits a severe reactivation defect and a moderate latency defect *in vivo*
11. Infection of 129S2/SvPas.IFN- α/β R^{-/-} mice with G50DbIKo virus does not result in lethality as seen with WT virus despite the presence of high viral titers in the lungs
12. G50DbIKo virus establishes latency and reactivates to similar levels as WT Virus when used to infect 129S2/SvPas.IFN- α/β R^{-/-} mice *in vivo*
13. Promoter activity in the region immediately 5' to the MHV68 proximal promoter and proximal promoter deletion

Table 1. Summary of virus latency and reactivation

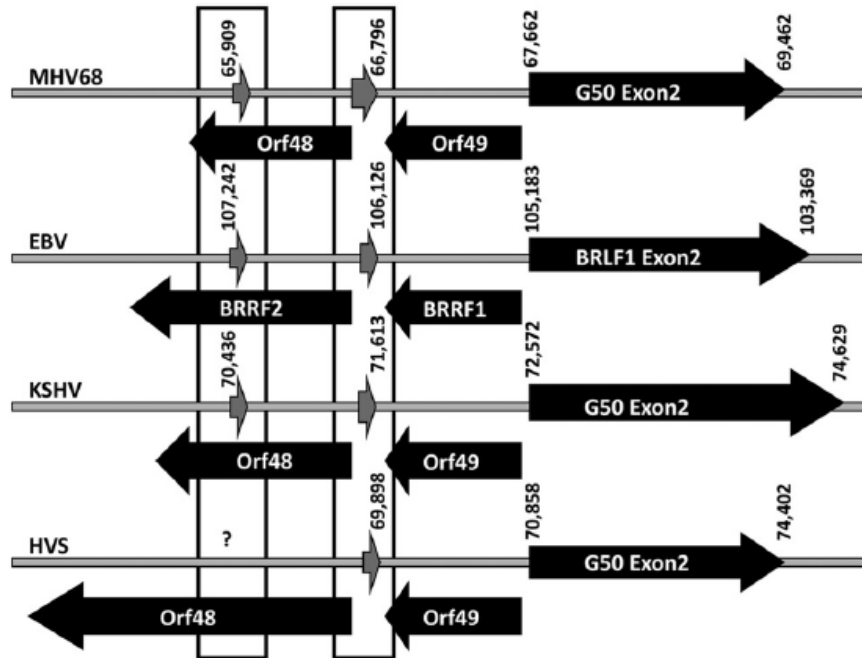


Figure 1

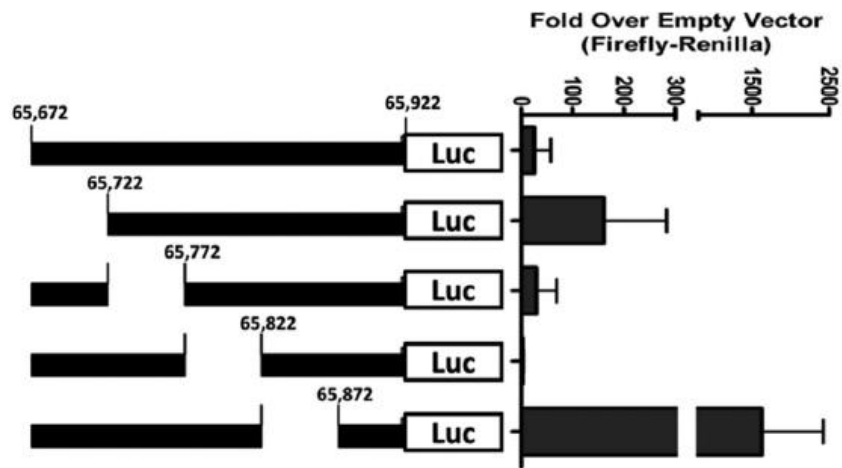


Figure 2

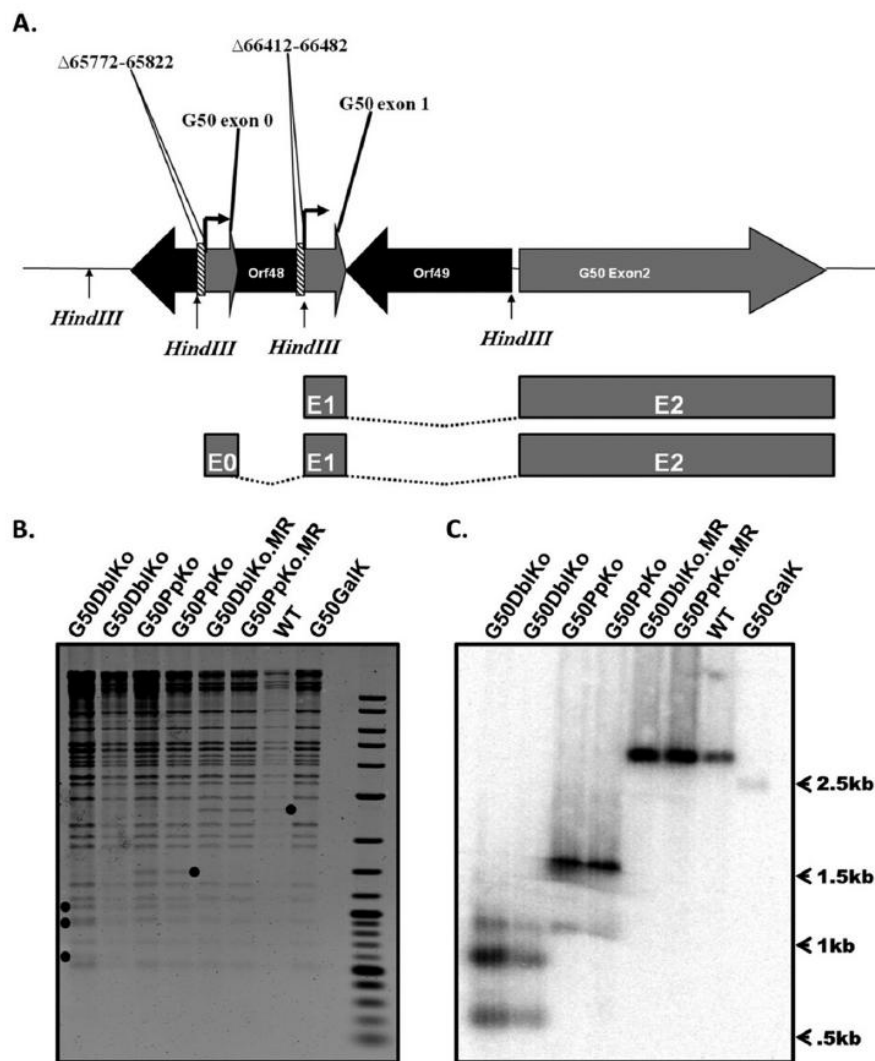


Figure 3

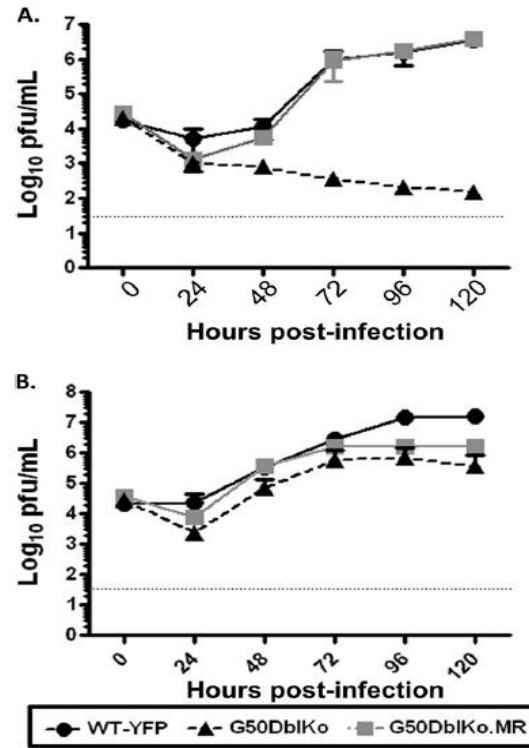


Figure 4

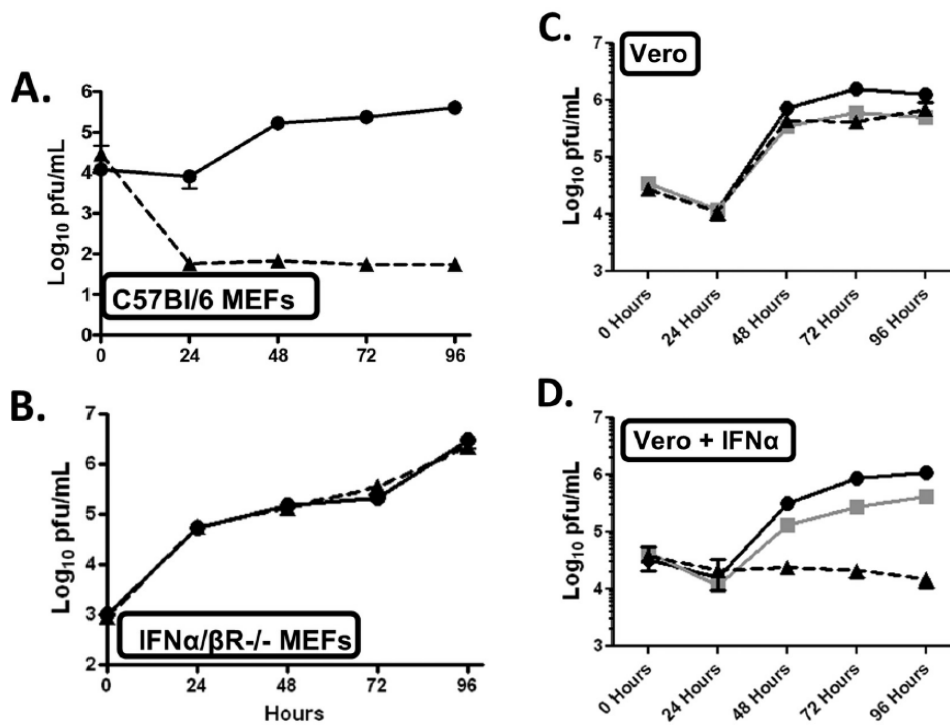


Figure 5

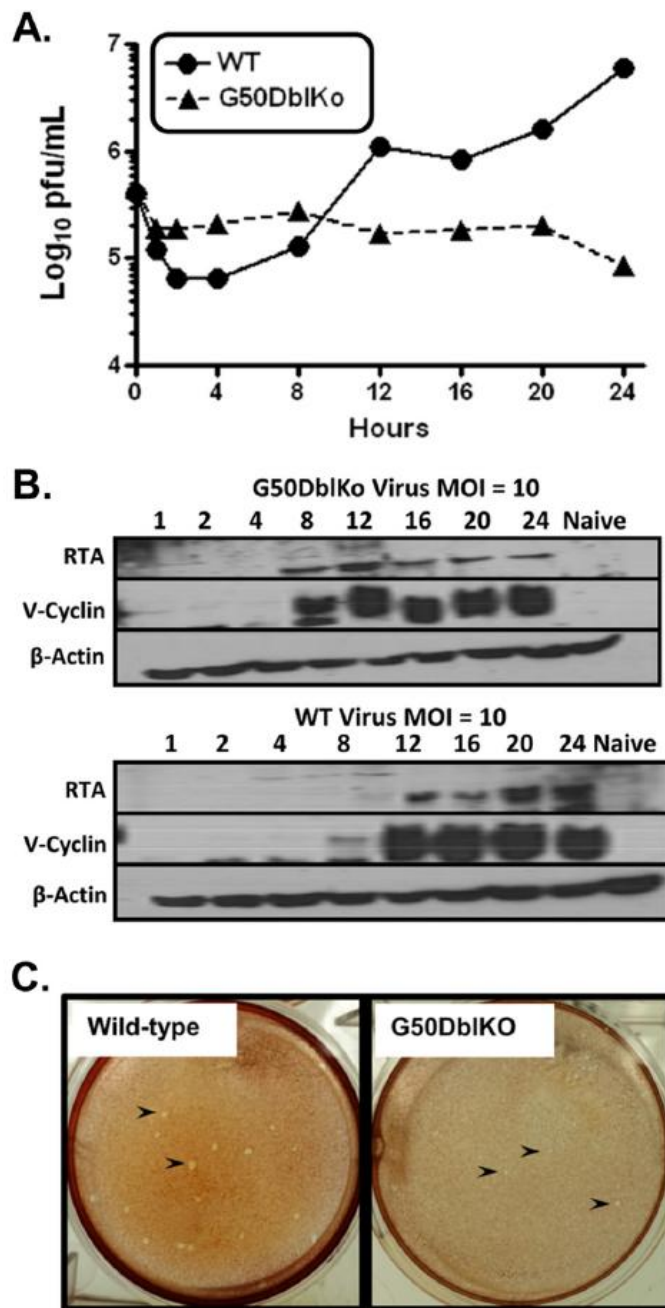


Figure 6

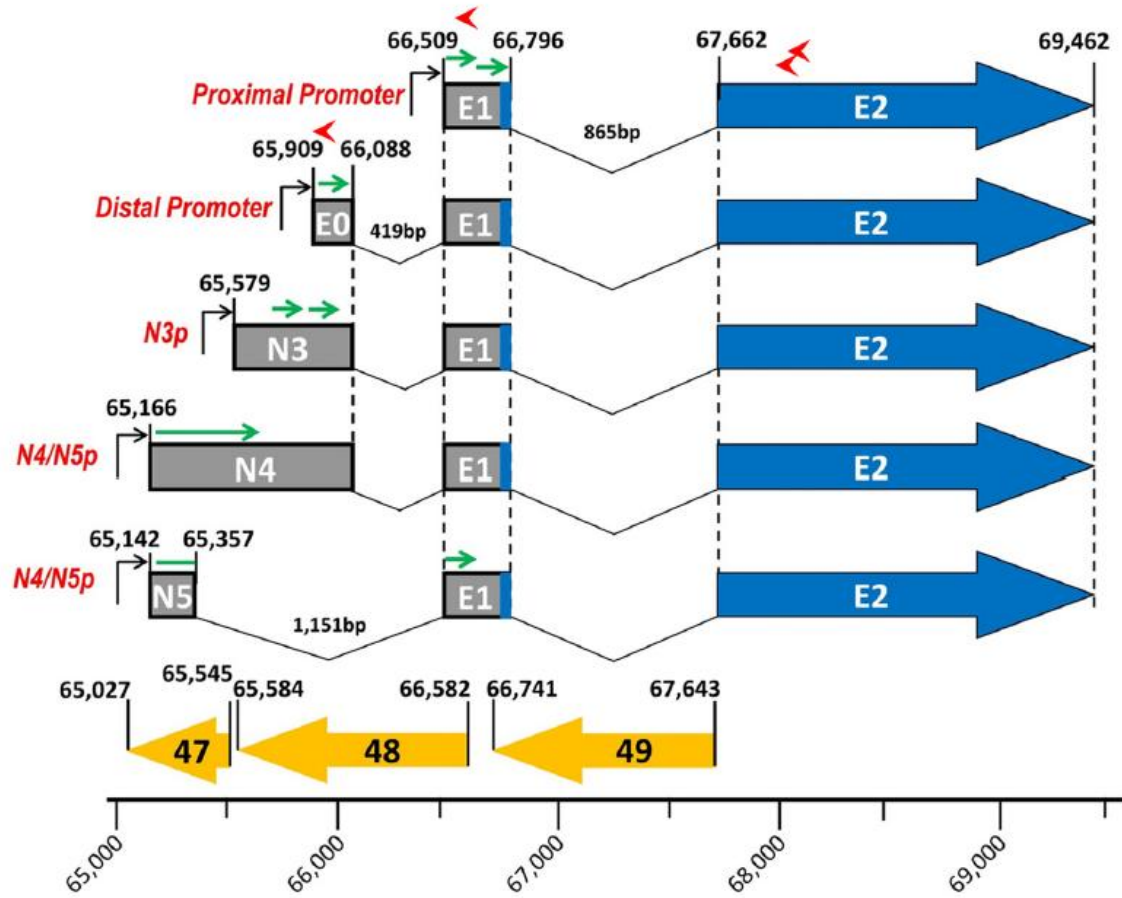


Figure 7

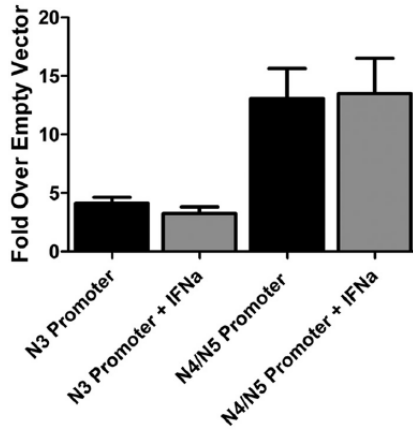


Figure 8

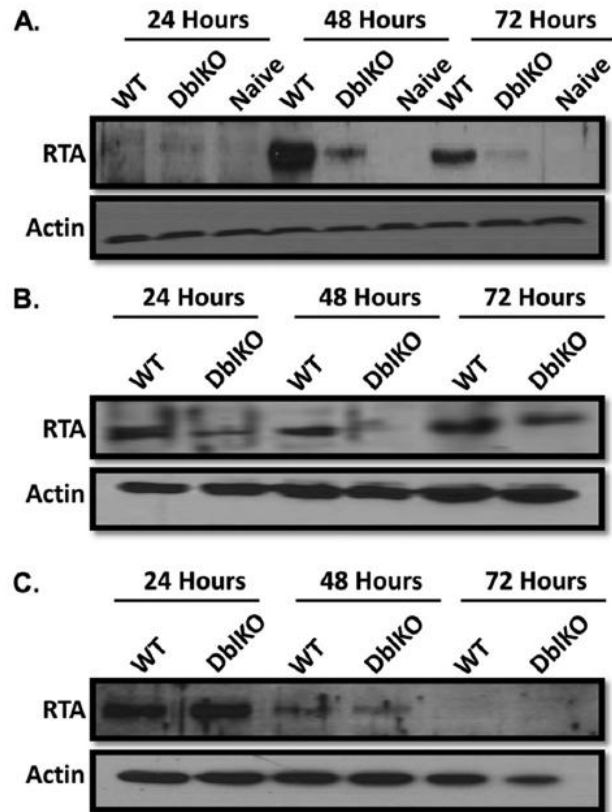


Figure 9

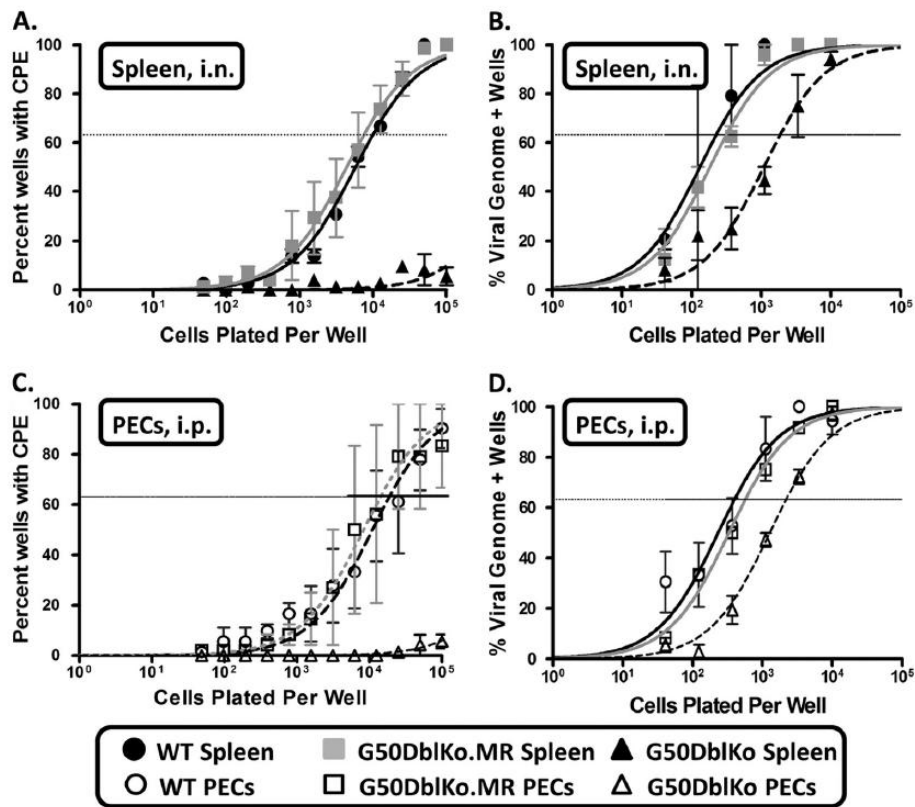


Figure 10

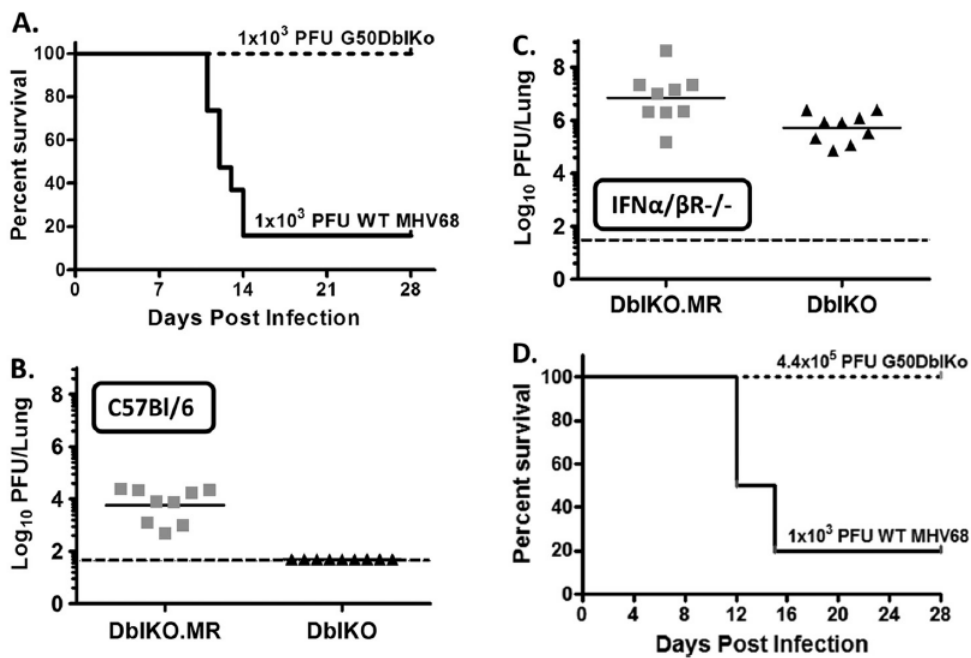


Figure 11

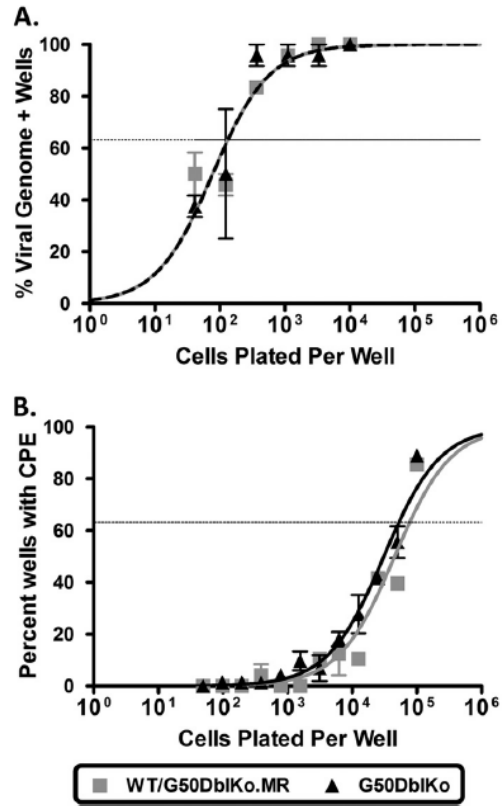


Figure 12

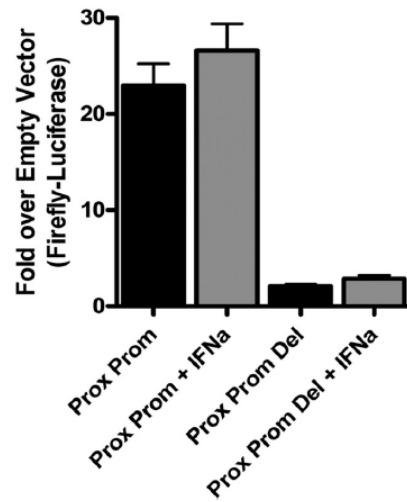


Figure 13

Mouse	Route	Day	Virus	Splenocytes		PECs	
				Reactivation	Latency	Reactivation	Latency
C57BL/6	i.n.	18	WT	1 in 7,035	1 in 223	ND ^a	ND
			MR	1 in 9,549	1 in 305	ND	ND
			DblKo	Undetectable	1 in 1,941	ND	ND
	i.p.		WT	1 in 36,107	1 in 388	1 in 17,782	1 in 401
			MR	1 in 65,962	1 in 1,047	1 in 14,417	1 in 562
			DblKo	1 in 422,863	1 in 627	Undetectable	1 in 2,137
IFN α BR ^{-/-}	i.n.	28	WT ^b	1 in 77,624	1 in 131	ND	ND
			DblKo	1 in 52,420	1 in 133	ND	ND

^a ND, not determined.

^b Latency and reactivation were determined by pooling splenocytes from the 3 IFN α BR^{-/-} mice that survived wild-type MHV68 infection.

Table 1

Chapter 3: Identification of novel KSHV Orf50 transcripts: discovery of new RTA isoforms with variable transactivation potential

3.I. Abstract

3.II. Introduction

3.III. Materials and Methods

3.IV. Results

3.V. Discussion

3.VI. Figure legends

3.VII. Figures

1. RACE analyses and primer walking reveal the existence of six G50 exons upstream of exon 2
2. Upstream exons extend the KSHV G50 open reading frame to form unique RTA isoforms.
3. Promoter deletions of the four G50 promoters identify minimal promoter length as well as activity in various cell types
4. Transactivation of Orf50 promoters by isoform 1 (E1-E2) and isoform 4 (N5-E2) RTA
5. Promoter truncation from 1000bp to 100bp within the KSHV E1, E0A/B, N3/4 and N5 promoters showing essential region required for E1-E2 isoform 1 RTA transactivation
6. KSHV Orf50 promoter region transactivation by XBP-1, transactivation by IL-4, and inhibition by IFN γ
7. Promoter activity of various KSHV Orfs transactivated by either E1-E2 isoform 1 RTA or N5-E2 isoform 4 RTA
8. KSHV b-ZIP and PAN promoter activity when transactivated by E1-E2 isoform 1 RTA or N5-E2 isoform 4 RTA in virus containing cells

*Material in this chapter will be submitted for publication and is currently under revision; version submitted here may be slightly modified.

Identification of novel KSHV Orf50 transcripts: discovery of new RTA isoforms with variable transactivation potential

Brian S. Wakeman,^a Yoshihiro Izumiya,^b and Samuel H. Speck^a

Emory Vaccine Center and Department of Microbiology & Immunology, Emory University
School of Medicine, Atlanta, Georgia, USA^a
Department of Dermatology, University of California Davis School of Medicine,
Davis, California, USA^b

*All figures were generated by Brian Wakeman

3.I ABSTRACT

Kaposi's sarcoma-associated herpesvirus (KSHV) is a gammaherpesvirus that has been associated with primary effusion lymphoma, multicentric Castleman's disease, as well as its namesake Kaposi's sarcoma. As a gammaherpesvirus KSHV is able to acutely replicate, enter latency, and reactivate from this latent state. A key protein involved in both acute replication and reactivation from latency is the replication and transcriptional activator (RTA) encoded by the gene Orf50. RTA is a known transactivator of multiple viral genes allowing for it to control the switch between acute replication and latency. Here we report the identification of six total Orf50 transcripts that are generated from four distinct promoters. These newly identified promoters are shown to be transcriptionally active in 293T (embryonic kidney), Vero (African-green monkey kidney epithelial cells), 3T12 (mouse fibroblast), and Raw 264.7 (mouse macrophage) cell lines. We go on to show that these new promoters are also upregulated by x-box binding protein 1 (XBP1), and that only the E1-E2 promoter is upregulated by IL-4. We also show that all four promoters can be transcriptionally repressed by IFN γ . The six transcripts generated from the four promoters encode four different isoforms of the RTA protein varying slightly in 5' sequence. Here we report that all four Orf50 promoters are transcriptionally upregulated by both isoform 1 and isoform 4 RTA protein. Finally, we demonstrate that isoform 1 and isoform 4 transcriptionally activate a variety of viral promoters to various levels and that the pattern of transactivation is dependent on which isoform is expressed.

3.II. INTRODUCTION

Herpesviruses are large double-stranded DNA viruses that encode a variety of proteins required for acute replication and maintenance within a host during latency. Latency is the hallmark of herpesvirus infection and results in a life-long infection that can't be cleared. This lifelong infection is marked by sporadic viral reactivation resulting in viral replication and reseeding of the latency reservoir. One important member of the herpesvirus family is the gammaherpesvirus Kaposi's sarcoma-associated herpesvirus (KSHV). This gammaherpesvirus is associated with the development of Kaposi's sarcoma, multicentric Castleman's disease and primary effusion lymphoma (PEL). Though seroprevalence of KSHV is not as dramatic as that of its gammaherpesvirus relative Epstein-Barr virus (EBV), dependent on geographical location approximately between five to twenty percent of individuals are latently infected by KSHV by adulthood (120, 139, 206, 211). While KSHV associated malignancies are rare, especially in immunocompetent individuals, people who are immunocompromised through secondary infection such as HIV and immunosuppressive drug therapies run a higher risk of KSHV associated complications (29-31, 36, 180, 183).

One of the most highly conserved genes amongst gammaherpesviruses is the Orf50 gene encoding the RTA protein, which is critical for gammaherpesvirus replication and reactivation from latency (190, 272, 276). Reactivation from latency to lytic replication requires a cascade of gene expression, immediate-early, early, and late, which leads to viral DNA replication and the assembly and release of newly formed infectious virions (240). The RTA protein is essential to this cascade of gene expression and is a very strong transactivator of downstream viral genes. RTA is powerful enough to initiate the entire reactivation from latency process when ectopically expressed with cells harboring latent virus, indicating at the strong transactivation potential RTA

possesses (80, 152, 205, 239). The transactivation potential of RTA has been demonstrated for a variety of downstream targets in both KSHV and the mouse homolog virus murine herpesvirus 68 (MHV68). For example RTA has been shown to transactivate Orf57, K12, PAN, and K8 genes (25, 35, 189). A comprehensive screening of RTA transactivation potential has been conducted and showed many genes to be targets of at least some upregulation by RTA (62). Additionally RTA has shown the ability to target human genes for regulation as well, for example RTA has been shown to bind and upregulate the IL-6 promoter (53, 208).

With the magnitude of effects that RTA expression shows on the viral life cycle as well as its ability to transactivate many different viral and cellular genes, RTA is highly regulated by a variety of mechanisms. Recently MHV68 was used as a model to demonstrate that the Orf50 region is much more complex than previously identified. It was first discovered that the Orf50 region contained not just one promoter driving an exon 1 to exon 2 splicing event, but that a second promoter called the distal promoter was able to drive an exon 0 to exon 1 to exon 2 splicing event resulting in a novel Orf50 transcript (81). It was further shown that this splicing event occurs in not just MHV68 but the two human gammaherpesviruses EBV and KSHV as well (82). More recently work based off of this finding was published to show that in MHV68 even more Orf50 transcripts are generated. In this work it is shown that MHV68 encodes three additional transcripts, exon N3, exon N4, and exon N5, driven from two more unique promoters (256). It is further demonstrated in this work that the previously known transcripts E1-E2 and E0-E1-E2 are dispensable for replication *in vitro*, but only in the absence of a type I interferon response (161).

Here we demonstrate that the expression of RTA in KSHV can also be driven from multiple previously unknown promoters upstream of the distal promoter. We demonstrate that

Orf50 transcription is generated from six different transcripts driven by four different promoters. Unique from MHV68, these six different KSHV Orf50 transcripts independently splice to exon 2 resulting in the generation of four different RTA isoforms which vary slightly in amino acid composition at the 5' end. We further characterize the four promoters demonstrating that they are transcriptionally active in various cell lines. Furthermore the promoters are demonstrated to be upregulated by XBP-1 expression and inhibited by the presence of IFN γ . We also show that all four promoters can be self-regulated by expression of RTA, and that both isoform 1 and isoform 4 RTA have the ability to upregulate all four promoters. Finally, we demonstrate that isoform 1 and isoform 4 RTA have the ability to transactivate a variety of viral genes. Importantly, the transactivation potential of the two isoforms varies, indicating a different role for the various promoters and the Orf50 transcripts they generate.

3.III. MATERIALS AND METHODS

Cell Culture. 293T (Human embryonic kidney), Vero-Cre (African green-monkey kidney epithelial), NIH 3T12 (BALB/C murine fibroblasts), RAW 264.7 (murine macrophages), and 293T Δ 50BAC cells (293T cells containing stably transfected BAC missing the Orf50 region (276)) were maintained in Dulbecco's modified Eagles medium (DMEM) supplemented with 10% fetal calf serum, 100U penicillin per ml, 100U streptomycin per ml, and 2mM L-glutamine (cMEM). BCBL-1 (PEL KSHV⁺EBV) cells were maintained in Roswell Park Memorial Institute medium (RPMI) supplemented with 10% fetal calf serum, 100U penicillin per ml, 100U streptomycin per ml, and 2mM L-glutamine (cRPMI). All cells were maintained at 37°C in a tissue culture incubator containing 5% CO₂.

RNA and DNA extraction. DNA extraction was conducted using the basic preparation of genomic DNA from mammalian tissue protocol. Cells suspensions were centrifuged for 5min at 500 x g at 4°C and supernatant discarded. Cells were then resuspended in 1 volume digestion buffer (100mM NaCl, 10mM Tris-Cl pH 8, 25mM EDTA pH 8, .5% SDS, and 0.1mg/ml proteinase K) for 12 to 18 hours while shaking at 50°C. After incubation samples were extracted using an equal volume of chloroform while centrifuging for 10min at 1,700 x g. After centrifugation the aqueous top layer was transferred to a new tube and a ½ volume of 7.5M ammonium acetate and 2 volumes (of original top layer amount) of 100% ethanol were added. This precipitate is centrifuged at 1,700 x g for 2 additional minutes. Pelleted DNA is rinsed with 70% ethanol, spun at 1,700 x g for 2 minutes and supernatant removed. DNA is resuspended at 1 mg/ml in TE buffer. Final DNA solution is stored at 4°C. RNA extraction was performed using

TRIZol reagent (Invitrogen) or Pure link RNA mini Kit (Invitrogen). Briefly cells were pelleted at 2,000 x g for 10min at 4°C. Supernatant was removed and either 1ml of TRIZol was added or cell pellets were stored at -80°C. If TRIZol was added, 300µl of chloroform was also added and cells were vortexed for 30 second and incubate for 10 min at room temperature. Cells were then centrifuged at 12,000 x g for 20min at 4°C. The top aqueous layer was removed and 1ml of isopropanol was added. Cells were shaken and incubated for 10min at room temperature before being subjected to a 12,000 x g centrifugation for 10min at 4°C. The supernatant was removed and cells washed with 1ml 75% ethanol and incubated for 10min at room temperature. Finally cells were centrifuged at 12,000 x g for 5min at 4°C, supernatant removed, and RNA resuspended in appropriate volume of buffer TE. For Pure link RNA mini Kit extraction -80°C frozen cell pellets were resuspended in lysis buffer, passaged through a 21-gauge needle 10 times, and subjected to column purification and washing. All RNA was used immediately or stored in 75% ethanol at -80°C.

RACE analysis and primer walking. BCBL-1 cells were plated at 2×10^5 cells per a ml and 24 hours later were treated with 25ng/ml of 12-O-tetradecanoylphorbol-13-acetate (TPA). Total RNA from BCBL-1 cells was collected at 24, 48, and 72 hours post-TPA treatment as described. One microgram of RNA was treated with DNase I (Invitrogen) and subjected to 5' rapid amplification of cDNA ends (RACE) performed using the GeneRacer system (Invitrogen). RACE-ready cDNA was generated using Superscript III (Invitrogen) reverse transcription using random primers as per the kit's instructions. RACE-ready cDNA was used to look for additional 5' transcripts through the use of nested PCR utilizing Platinum Taq (Invitrogen). Nested PCR was performed using the 5' universal forward RACE primer bound to the 5' RACE tag, either

universal primer 1 for round 1 or universal primer 2 for round 2 nested PCR and various reverse primers located in the Orf50 region: E2KSHVR1 (5'-cctccgattgcagacgagtc-3'), E2KSHVR2 (5'-aacatgtaatgtctgtaaacaga-3'), E2KSHVR3 (5'-tgcacacatctccaccactct-3'), E2KSHVR4 (5'-cgccgagaggccgacgaagct-3'), E1KSHVR1 (5'-tggctgcctggacagtattc-3'), E1KSHVR2 (5'-ccttgccgagtaaggttgac-3'). For 5' primer walking a universal reverse primer located in exon 2 (E2KSHVR4) was used in conjunction with a series of forward primers listed in the table below. The following cycling conditions were used for all PCR reactions, 1µl of cDNA in a 50µl PCR mixture at 95°C for 2 min, 30 cycles of denaturing at 94°C for 30s, annealing at 58°C for 30s, and extension at 70°C for 2 min; and a final extension at 70°C for 10 min. Round 2 nested amplification was performed with 2µl of the round 1 PCR reaction product and cycling conditions remained the same. PCR products were visualized through running on a 1% ethidium bromide gel, and excised bands were purified using GeneClean II kit (MP bio). Purified PCR products were ligated into pGEM-T easy vector system (Promega), transformed into E.coli, purified using DNA miniprep kit (Qiagen), and analyzed by DNA sequencing (Macrogen USA).

Primer Name	Forward Primer Sequence	Primer Name	Forward Primer Sequence
N3-N4-1F	5'-cggcaaatagcgcaaagatc-3'	KSHV-N14F	5'-aatggccttgccccacagg-3'
N3-N4-2F	5'-gcaacatggtaaggcgacgtat-3'	KSHV-N15F	5'-agaggccagcggagatggatgc-3'
N4-N5-1F	5'-gcagcttggtatacagacccc-3'	KSHV-N16F	5'-caaatagtcgttgctaggtta-3'
N4-N5-2F	5'-cctcagattaaaccattcacg-3'	KSHV-N17F	5'-taciaagcacacgagttattgc-3'
KSHV-N7F	5'-ctccggctgctgcttttagccc-3'	KSHV-N18F	5'-gtgtgtgctagacgaggtcctc-3'
KSHV-N8F	5'-tgcaacctgcgtccatgttga-3'	KSHV-N19F	5'-ccagcatagccgcgcggcctgc-3'
KSHV-N9F	5'-ccggtcgtccaccctgactg-3'	KSHV-N20F	5'-catattcagattcggcgtcga-3'
KSHV-N10F	5'-gaaatgatgagaggctcagaaa-3'	KSHV-N21F	5'-gcaggggaaaatccgtatcct-3'
KSHV-N11F	5'-gttagcctaagtccgaatct-3'	KSHV-N22F	5'-aacttgtgtccaggtact-3'
KSHV-N12F	5'-gcagcagtgggaccaccacatc-3'	KSHV-N23F	5'-gttcacgtccgagagttggaa-3'
KSHV-N13F	5'-accgtgggaaggagtactgaa-3'	KSHV-N24F	5'-ttctggcccacgtccatgagcc-3'

Cloning and reporter plasmid generation. DNA from BCBL-1 cells was extracted as previously described. BCLB-1 DNA was used as a template for the cloning out of the promoter

constructs in which the promoters were then cloned into a luciferase reporter construct. Phusion Taq (NEB) was used with the following cycling parameters for all promoter amplifications: 95°C for 2 min, 30 cycles of denaturing at 94°C for 30s, annealing at 58°C for 30s, and extension at 72°C for 30s; and a final extension at 70°C for 10 min. Standard single round PCR was used to generate the following constructs using the primers listed. KSHVE1pRBgl2 (5'- actgAGATCT tgcattgccaccagctac-3') reverse primer was used with KSHVE1pF1000Nhe1 (5'- actgGCTAGC cggtttctctaattgcatca-3'), KSHVE1pF500Nhe1 (5'- actgGCTAGCaccacaggcctgttccagt-3'), KSHVE1pF250Nhe1 (5'- actgGCTAGCaatacgtcggcttggacga-3'), and KSHVE1pF100Nhe1 (5'- actgGCTAGCccataggaccagctacagc-3') forward primers to generate Exon 1 promoter constructs of 1000bp, 500bp, 250bp, and 100bp length. KSHVE0aBRBgl2 (5'- actgAGATCTcttgcttggcccgg atacgagc-3) reverse primer was used with KSHVE0aBF1000Nhe1 (5'- actgGCTAGCctgctgctttt agcccaggt-3'), KSHVE0aBF500Nhe1 (5'- actgGCTAGCcttggtcggctccccag-3'), KSHVE0aBF250Nhe1 (5'- actgGCTAGCctgcacacgtctggctgaga-3'), and KSHVE0aBF100Nhe1 (5'- actgGCTAGCtgtccatacgggcccgtgtgc-3') forward primers to generate Exon 0 promoter constructs of 1000bp, 500bp, 250bp, and 100bp length. KSHVN3N4RBgl2 (5'- actgAGATCT aagggggctccctggggagc-3') reverse primer was used with KSHVN3N4F1000Nhe1 (5'-actgGCTAGCaacacaccctggcgagccca-3'), KSHVN3N4F500Nhe1 (5'- actgGCTAGCtaacagaacctgtccggttc-3'), KSHVN3N4F250Nhe1 (5'- actgGCTAGCtcgcagcttggctatacaga-3'), and KSHVN3N4F100Nhe1 (5' actgGCTAGCggtggtccacaggacggcaa-3') forward primers to generate Exon N3/N4 promoter constructs of 1000bp, 500bp, 250bp, and 100bp length. Finally, KSHVN5RBgl2 (5'- actgAGATCTgccatgaaccggacaggttc-3') reverse primer was used with KSHVN5F1000Nhe1 (5'- actgGCTAGCgcgaggcgtcctcaattg-3'), KSHVN5F500Nhe1 (5'- actgGCTAGCcaggaccctgg gaagga-3'), KSHVN5F250Nhe1 (5'- actgGCTAGCctgtctgagcagcagagca-3'), and KSHVN5-

F100NheI (5'- actgGCTAGCcatgttgaactattttccc-3') to generate Exon 5 promoter constructs of 1000bp, 500bp, 250bp, and 100bp length. Additionally the following primer pairs were used to generate promoter constructs of Orf50 viral targets as previously described (62). The PAN promoter using forward primer PanPromNhe1F (5'-cgtaGCTAGCtggaggtgccaagttcgcaaca-3') and the reverse primer PanPromBgl2R (5'-gcatAGATCTtgggcagtcccagtgctaaact-3'); the K12 promoter using forward primer K12PromNhe1F (5'-cgtaGCTAGCgcgtaaaccctgctgctaaac-3') and the reverse primer K12PromBgl1R (5'-cgtaAGATCTtaaataccaagatccgctcctc-3'); the Orf59 promoter using the forward primer Orf59PromNhe1F (5'-cgtaGCTAGCgtgccttgccaacgattacatt-3') and the reverse primer Orf59PromBgl2R (5'-gcatAGATCTttgcgccgtagacgcacagag-3'); the Orf57 promoter using the forward primer Orf57PromNhe1F (5'-cgtaGCTAGCcaagaccattagctatctgccg3') and the reverse primer Orf57PromBgl2R (5'- gctaAGATCTgtctatcattgcttgaccatg-3'); and finally the K-bZIP promoter using forward primer KBzipPromNhe1F (5'-cgtaGCTAGCggtgcaaagtggagttaaccta-3') and the reverse primer KBzipPromBgl2R (5'-gctaAGATCTttggcagggttacacgtttaca-3'). All of these PCR products were gel purified and cut using NheI (NEB) and BglII (NEB) restriction enzymes, additionally the luciferase reporter construct pGL4.10[luc2] (Promega) was also digested with NheI and BglII. The digested products and the vector were gel purified again, resuspended in TE buffer, and ligated together for 1 hour using T4 DNA ligase (NEB) at room temperature. Ligation products were transformed into Top 10 chemically competent cells, and the colonies were screened for the presence of correct promoter orientation within the pGL4.10[luc2] vector through DNA sequencing. Clones containing the correct insert and orientation were cultured to high levels and plasmid DNA was isolated using an Endofree Maxikit (Qiagen). The process of generating expression constructs followed a similar protocol as the generation of the reporter constructs. BCBL-1 RNA was extracted as previously described

and treated with DNase I (Invitrogen), 1µg of RNA was used to generate cDNA using superscriptIII (Invitrogen). This cDNA was used as a template for the generation of E1-E2, E2ATG and N5-E2 expression constructs. These constructs were generated using the same reverse primer KSHVE2Xho1R (5'- gcatCTCGAGgtctcgggaagtaattacgcc-3') while E1-E2 used the forward primer KSHVE1Not1F (5'-cgtaGCGGCCGCatggcgcaagatgacaaggg-3'), E2ATG used the forward primer KSHVE2AtgNot1F (5'-cgtaGCGGCCGCatgaaagaatgtccaagct-3'), and finally N5-E2 used the forward primer KSHVN5Not1F (5'-cgtaGCGGCCGCatgcctgaattg cgcaacat-3'). Platinum Taq (Invitrogen) using the following cycling parameters was used: 95°C for 2 min, 40 cycles of denaturing at 94°C for 30s, annealing at 64°C for 30s, and extension at 72°C for 3min; and a final extension at 72°C for 10 min. PCR products were gel purified, cut using NotI and XhoI while at the same time also cutting the expression vector pCMV-Tag2b (Stratagene). These restriction digested products were gel purified, ligated, and DNA was generated as described above. The expression vector XBP-1 pCMB-Tag2b was generated as described previously in our lab (156).

Luciferase Assay and transfections. Transfection of 293T, Vero, 3T12, and Raw 264.7 cells was done in 6-well plates. One day prior to transfection cells were plated at 2×10^5 cells, or for Raw 264.7 cells 1×10^6 cells in cMEM. Transfection mixtures were prepared using either 2.5µg of report plasmid for single transfection or 1.5µg report plasmid and 1µg expression plasmid for dual transfections. Transfection were done using LT-1 transfection reagent (Mirus) according to the manufactures instructions. Briefly, 250µl of DMEM was used for each transfection well and the appropriate amount of DNA added, 7.5µl LT-1 per a well was added to the media and mixed briefly, the solution incubate at room temperature for 30mins, and then was added dropwise to

cells. pGL4.13[luc] was used as a positive control. For assay mixtures using external stimulus, 10ng/ml of IL-4, 10ng/ml IFN γ , and 25ng/ml TPA was used. Luciferase assays were performed by lysing cells and using 10 μ l of lysate in 50 μ l luciferase agent (1.5mM HEPES [pH 8], 80 μ M MgSO₄, 0.4 mM dithiothreitol [DTT], 2 μ M EDTA, 10.6 μ m ATP, 5.4 μ M co-enzyme A, and 9.4 μ M beetle luciferin). Luciferase assays were read using a TD-20/20 luminometer (Turner Biosystems). All transfections were repeated in triplicate, and results are presented either as fold over empty pGL4.10[luc] vector, or fold over vector + empty pCMV-Tag2b vector.

3.IV.RESULTS

Identification of additional KSHV Orf50 transcripts. The Orf50 region of gammaherpesviruses is highly conserved amongst all gammaherpesvirus family members. We have previously shown that transcription of KSHV Orf50 is driven by two distinct promoters: the proximal promoter, encoding a short 102bp exon, E1, which splices to the large 2,057bp exon, E2; and the distal promoter, which encodes two short exons, 234bp exon E0A, and 292bp exon E0B, which splices to the large 2,057bp exon, E2 (81). It was further shown that this organization of the Orf50 region and the use of two distinct promoters was conserved in the KSHV human gammaherpesvirus relative EBV as well as the murine model MHV68 (81). Recently we discovered the existence of additional promoters encoding novel transcripts upstream of the known proximal and distal promoters in MHV68 (256). In addition to the proximal and distal promoters is the existence of two other promoters driving the transcription of 3 unique transcripts. There is the N3 promoter, encoding a 508 exon, N3, which splice to the short 287bp exon E1, which in turn splices to the large 1,800bp exon, E2. There is also the N4/N5 promoter which encodes two different transcripts. First it encodes the very large 922bp exon, N4 which splices to the E1 exon which then splices to the E2 exon. The N4/N5 promoter also encodes a short 215bp exon, N5 which also splices to the E1 exon which then splices to the E2 exon. So far in MHV68 transcripts that do not splice through the small E1 exon have not been discovered; meaning all transcripts, despite being driven by different promoters, share the same ATG located in the E1 region encoding only a singular isoform of RTA (256).

With the identification of newly discovered Orf50 transcripts in the murine virus MHV68, we have expanded these studies to the human virus KSHV to determine if these

additional transcripts are conserved amongst gammaherpesviruses. To test this conservation hypothesis we performed 5' RACE analysis of RNA from BCBL-1 cells treated with TPA. From this analysis, we were able to detect three previously unidentified gene 50 transcripts which initiated from two unique upstream promoters (Fig. 1). We expanded these studies to primer walking in which a reverse primer was anchored in the E2 exon region and forward primers were used to walk up the 5' direction of the gene 50 Orf. Primer walking confirmed the existence of three additional transcripts that we had previously identified through RACE. It is important to note that previously identified transcripts were also detected in our analysis. We now have a better global picture of the KSHV Orf50 transcription region. The first exon is exon 1 (E1) encoded from the proximal promoter which encodes a 102bp exon, which splices out a 958bp intron, while splicing to the 2,057bp exon 2 (E2) (Fig. 1). The splicing of E1 to E2 results in the extension of the E2 open reading frame, as there is an in frame ATG located 15bp from the 3' end of E1 which encodes an additional six amino acids and forms isoform 1 RTA (Fig. 2A). The next exons are exons E0A and E0B which are encoded from and share the distal promoter. E0A is a short 234bp exon which splices out a 1,901bp intron while splicing to E2. E0B is slightly larger 292bp exon which splices out a 1,834bp intron while splicing to E2 (Fig. 1). While being driven from the same promoter, the different splicing generated by E0A and E0B results in different extensions of the E2 open reading frame. E0A extends the open reading frame by six unique amino acids generating isoform 2 RTA, while E0B extends the open reading frame by ten unique amino acids generating isoform 3 RTA (Fig. 2B). The next identified transcript is encoded by the N3/N4 promoter and this drives the transcription of an 857bp exon, N3, which splices out a 1,747bp intron while splicing to E2 (Fig. 1). This transcript does not result in the extension of the E2 open reading frame and does not result in the generation of the RTA protein

and may be considered an abortive transcript. Also being expressed from the N3/N4 promoter is a very large 1,646bp exon, N4, which shares splicing homology with the E1 exon, in which the N4 exon is just an 1,544bp extension of the E1 exon (Fig 1). Since this N4 exon shares splicing with E1, it extends the open reading frame of E2 in a similar manner, resulting in the generation of isoform 1 RTA (Fig. 2A). The last transcript identified is driven from the N5 promoter and results in a 351bp exon, N5, which splices out a very large 2,728bp exon, while splicing to E2 (Fig. 1). The N5 exon contains an ATG that extends the E2 open reading frame by seven amino acids and results in isoform 4 RTA (Fig. 2C). To date there is no evidence that splicing occurs between these exons in a similar manner to what is seen in MHV68 which results in transcripts splicing through the E1 exon. It is unlikely for this to occur as the E1 exon in KSHV does not contain a splice acceptor site.

Characterization of the proximal, distal, N3/N4, and N5 promoters *in vitro*. With the identification of two previously unidentified promoters, as well as the lack in characterization of the KSHV distal promoter we attempted to characterize the activity of these promoter regions. For all four promoters, E1, E0, N3/N4, and N5, 1000bp, 500bp, 250bp, and 100bp promoter fragments were cloned into the pGL4.10 luciferase reporter vector. To first determine the minimal promoter region we transfected the reporter vectors into the easily transfectable cell line 293T cells. Luciferase assays confirmed that promoter activity was seen in all four Orf50 promoters (Fig. 3A). These assays show that the E1 promoter in 293T cells is the most active in the 250bp fragment and that this activity is ~275.75 fold over that with empty vector. It is additionally seen that the E0 promoter in 293T cells is ~33.25 fold over that with empty vector and most active with the 500bp promoter fragment. Also most active with the 500bp promoter

fragment is the N3/N4 promoter with ~101.5 fold activity over empty vector as well as the N5 promoter 500bp fragment with ~54.25 fold activity over empty vector. While 293T cells are easily transfectable we wanted to determine the promoter activity of the Orf50 promoters in various cell types. All four different promoters, with constructs showing the greatest minimal promoter activity, were transfected into Vero, 3T12, and Raw 264.7 cells. The E1 promoter showed the greatest activity in the Vero and Raw 264.7 cells with ~5.7 fold and ~137.65 fold activity over empty vector (Fig. 3B). Interestingly the E1 promoter did not show the greatest activity in 3T12 cells with ~12.45 fold expression compared to the N3/N4 promoter which showed ~55.5 fold change over empty vector (Fig. 3B/D). This is potentially interesting because the N3/N4 promoter generates the N4 transcript which encodes the same RTA isoform 1 as the E1 promoter. The N3/N4 promoter also showed good activity in Raw 264.7 cells with ~42.6 fold increase, as well as Vero cells with ~4.2 fold increase (Fig. 3D). The N5 promoter showed modest activity in all three cell lines when compared to the E1 or N3/N4 promoter with ~2.2 fold increase in Vero, ~11.72 in 3T12 and ~31.67 in Raw 264.7 cells (Fig. 3E). The least active promoter was the E0 promoter which is interesting because it drives transcripts that encode for two unique RTA isoforms 2 and 3. The E0 promoter showed no promoter activity in Vero cells, while only showing ~3.05 fold and ~2.5 fold increase in 3T12 and Raw 264.7 cells (Fig. 3C). This indicates that these transcripts may be very rare or that the activation of this promoter requires a specific cellular environment or cellular stimulation.

KSHV isoform 1 RTA and isoform 4 RTA are able to transactivate all four Orf50 promoters. While promoter activity was observed for all four promoters in a variety of cell lines, it is well known that KSHV Orf50 is able to transactivate its self to increase RTA

production (54, 55, 200). We decided to test to see if the newly identified Orf50 promoters were able to be upregulated by RTA itself. We also wanted to see if it was possible for the new isoform of RTA, isoform 4, which varies slightly in the N-terminal end of amino acid structure retains the ability to upregulate Orf50 promoters. To test these hypothesis we transfected 293T cells with the 1000bp Orf50 promoter constructs along with either an empty vector control, or the E1-E2 isoform 1 RTA, the N5-E2 isoform 4 RTA, or a negative control E2ATG RTA in which the entire extended open reading frame of the N-terminal end is missing, expressed from the constitutively active CMV promoter driven pCMV-Tag2B expression vector. The first thing observed is that the E2ATG RTA negative control has no effect on the expression of the Orf50 promoters in comparison to the empty vector control, while both isoform 1 and isoform 4 RTA expression leads to a large increase in promoter activity (Fig. 4A-D). The E1 promoter was shown to be upregulated ~28 fold by isoform 1 RTA and ~19.6 fold by isoform 4 RTA (Fig. 4A). The N3/N4 promoter was shown to be upregulated ~7.1 fold by isoform 1 RTA and ~4.73 fold by isoform 4 RTA (Fig. 4C). The N5 promoter was shown to be upregulated ~66.4 fold by isoform 1 RTA and ~38.8 by isoform 4 RTA (Fig 4D). This is interesting in that the N5 promoter shows greater increase by the isoform 1 RTA encoded by the E1 transcript over the isoform 4 RTA encoded by its self. Finally, the E0 promoter, which has minimal promoter activity in all cell lines tested, was shown to be ~195 fold increased with isoform 1 RTA and ~82.5 fold increased with isoform 4 RTA (Fig. 4B). This fold increase seen in E0 promoter by both isoform 1 and 4 RTA was the greatest fold increase observed indicating that the E0 promoter is highly responsive to upregulation by RTA self. It is also important to note that despite the ability of isoform 4 RTA to transactivate all of the promoters, in no instance was the transactivation potential greater than that of isoform 1.

We next attempted to determine if RTA transactivation of the Orf50 promoters was sequence dependent. RTA response elements are well known binding sites of RTA, but in KSHV multiple sequences have been shown and no consensus sequences has been determined. To test if there is minimal promoter needed for RTA transactivation we utilized the Orf50 promoter truncations described previously. We transfected 293T cells, this time with the various truncated Orf50 promoters, along with the expression vectors for isoform 1 RTA, as it was the most potent transactivator. For the E1 promoter the results show that RTA has the greatest upregulation with the 250bp promoter fragment (Fig. 5A). The 1000bp and 500bp fragments show reduced upregulation in comparison to the 250bp fragment indicating that these upstream sites may contain areas of promoter repression. For the E0 promoter region the best upregulation occurred with the 1000bp fragment which maintained ~313.3 fold increase, this increase however was cut in half to ~181.3 fold when the 500bp fragment was used (Fig. 5B). After this the fold change dropped significantly indicating that the RTA responsive elements are located somewhere between 500 and 1000 base pairs within the E0 promoter. The N3/N4 promoter showed a similar pattern as observed with the E0 promoter in which the 1000bp fragment gave the greatest fold increase, while the 500bp fragment also generated a significant fold increase, with the 250bp and 100bp failing to be upregulated by RTA (Fig. 5C). Finally, the N5 promoter did not display a true RTA pattern of transactivation. While the 1000bp fragment did show the greatest fold increase, the 500bp and 100bp fragment also showed potential with only the 250bp fragment failing to be upregulated by RTA (Fig. 5D). This pattern would suggest, at least for the N5 promoter, the promoter fold increase in activity by RTA binding is much more complicated.

The Orf50 promoters are upregulated and downregulated by various cellular factors other than RTA. While we have shown that all of the Orf50 promoters have the ability to be upregulated by RTA itself, it is well known that Orf50 promoters respond to various external stimuli. One known factor for upregulating the KSHV Orf50 proximal promoter is the plasma cell specific x-box binding protein 1 (XBP-1), which has been shown to stimulate both the KSHV and MHV68 proximal E1 promoter (156, 268, 285). To test to see if the newly identified promoters are also XBP-1 sensitive, we transfected 1000bp promoter luciferase constructs into 293T cells along with a constitutively active XBP-1 pCMV-Tag2B expression construct. As expected the E1 proximal promoter was increased ~7.55 fold over that of empty vector control, indicating that XBP-1 has the ability to upregulate the promoter (Fig. 6A). Additionally we were able to show that despite having low basal promoter activity, the E0 promoter was upregulated ~5.5 fold in the presence of XBP-1. The N5 promoter was able to show mild upregulation of activity with a ~2.9 fold increase. Interestingly the N3/N4 promoter was not transactivated by the XBP-1 transcription factor (Fig. 6A).

Another way that Orf50 is important in the viral life cycle is its ability to sense external stimulus, such as when the cell is exposed to cytokines. For this reason the previously known Orf50 promoter has been shown to respond to particular cytokines, one being IFN γ as a strong repressor of promoter activity (79, 235). To determine if the new Orf50 promoters are sensitive to IFN γ we transfected the various Orf50 promoter constructs in Raw 264.7 cells and treated them for 48 hours with 10ng/ml of IFN γ and compared promoter levels between treated and untreated cells. The first thing we observed is that all of the Orf50 promoters are sensitive to IFN γ treatment and result in approximately a two to three fold decrease across the board (Fig. 6B). Specifically the E1 promoter went from ~222.1 fold increase over empty vector to only ~75

fold increase over empty vector when treated with IFN γ . Additionally the N3/N4 promoter went from a ~77 fold increase to ~33.2 fold increase, and the N5 promoter went from a ~47 fold increase to ~22 fold increase (Fig. 6B). While the E0 promoter has extremely low basal activity in Raw 264.7 cells at ~3 fold induction, even this was reduced by treatment of cells with IFN γ to no induction at all.

Another cytokine that has recently been shown to be important for induction of Orf50 promoters is the cytokine IL-4, which was shown to upregulate the newly identified N4/N5 promoter in MHV68 (202). The induction of the N4/N5 promoter by IL-4 as a result of helminth co-infection leading to reactivation from latency represents a new pathway in which gammaherpesviruses may take advantage of an immunocompromised host. For this reason we tested to see if any of the newly identified KSHV Orf50 promoters were also upregulated by IL-4. We compared IL-4 treated to untreated cells transfected with our Orf50 promoter constructs. From this experiment we only saw induction of the E1 proximal promoter and no change in promoter activity in any of the newly identified E0, N3/4 and N5 promoters (Fig 6B). The E1 proximal promoter went from ~222.1 fold induction to a ~398.5 fold induction. The only other promoter that showed any sign of an effect with IL-4 treatment was the N5 promoter that went from a ~47 fold induction to a ~57 fold induction representing a minimal increase.

N5 transcript isoform 4 RTA has the ability to transactivate different viral promoters at varying levels in comparison to the known E1 transcript isoform 1 RTA. One of the most critical functions of the RTA protein is to act as a transactivator of downstream viral genes. The previously identified E1-E2 transcript results in the extension of the E2 open reading frame and this N-terminal extension is critical for the transactivation potential of RTA. This isoform 1 RTA

has been shown to transactivate many viral promoters (62). With the transactivation potential of isoform 1 known we wondered if the newly identified transcripts that encode different RTA isoforms that differ in their 5' end (Fig. 2) are capable of transactivating previously identified RTA targets. Using five viral promoters, K12, Orf57, Orf59, PAN, and k-bZIP, that are highly induced by E1-E2 isoform 1 RTA we looked to see if isoform 4 has the potential to also transactivate these promoters. Surprisingly isoform 4 N5-E2 RTA has a much different transactivation profile than the E1-E2 isoform 1 RTA previously characterized. Isoform 4 is able to transactivate some promoters to a higher level than isoform 1, some promoters to the same level as isoform 1, and finally unable to transactivate promoters that isoform 1 induces to a high level (Fig. 7A-E). The first promoter looked at for its ability to be transactivated by RTA was the K12 promoter which is induced ~17.2 fold with the previously identified isoform 1 RTA, this is in comparison to the new isoform 4 RTA which can induce this promoter to ~32.2 fold increase over empty vector control (Fig.7A). This is a 15 fold increase in promoter activity when K12 is in the presence of isoform 4 RTA in comparison to isoform 1. The next two promoters we looked at were the Orf57 and the Orf59 promoters which are induced to very high levels ~171 fold and ~275.4 in the presence of RTA isoform 1 (Fig. 7B/C). This fold increase is in comparison to RTA isoform 4 in which there is an increase of ~67.5 and ~122.4 respectively. This indicates that though RTA isoform 4 can induce the Orf57 and Orf59 promoter, it does not induce them to as high of level as seen with isoform 1 RTA. The PAN promoter is similar to the Orf57 and Orf59 promoter in that isoform 4 RTA can induce high levels of promoter induction ~65 fold increase and this is closer to isoform 1 RTA induction which is seen at ~98.1 fold increase (Fig. 7D). The last promoter that was measured for its ability to be induced by isoform 4 RTA was the K-bZIP promoter, which has a ~196.8 fold increase in promoter activity in the presence of isoform 1

(Fig. 7E). This large increase was non-existent in the presence of isoform 4 RTA where the promoter was induced only 26.4 fold over empty vector, indicating that isoform 4 RTA fails to induce the K-bZIP promoter.

While induction by isoform 4 and isoform 1 RTA is important alone, RTA also has the ability to interact with downstream targets and may require additional viral proteins to successfully initiate promoter induction. To test whether the inability of isoform 4 RTA to induce the K-bZIP promoter was caused by the lack of additional viral proteins we repeated the induction experiments using the 293T Δ 50BAC cell line in which the KSHV BAC lacking the Orf50 region is stably transfected into 293T cells. These cells, treated with TPA would allow for the production of additional viral products. Additionally the use of a BAC lacking the Orf50 region was essential as both isoforms of RTA have been shown to upregulate each other's promoters (Fig. 4A/D) and we wanted expression of RTA to be restricted to a single isoform. It is clear from this experiment that neither isoform 4 nor isoform 1 require additional viral gene products as both the TPA induced and uninduced promoter fold change induction was similar (Fig. 8). Furthermore, isoform 4 RTA was still unable to transactivate the K-bZIP promoter in the presence of additional viral proteins. Thus, taken together with the previous experiments discussed, these results argue that the RTA isoforms generated from different transcripts encoded by various Orf50 promoters result in different viral gene expression profiles.

3.VI. DISCUSSION

Here demonstrate that KSHV gene 50 transcription is more complex than previously described, and that it follows a pattern similar to recent observation we have made in MHV68 (81, 256). Based on this current analyses, KSHV RTA expression can be driven from four distinct promoters that drive the transcription of six different spliced gene 50 transcripts. Unique to KSHV Orf50 is that these six different splice gene 50 transcripts represent the encoding of four unique RTA protein isoforms. The identification of multiple KSHV promoters driving expression of a single gene is not novel to the KSHV Orf50 gene, as there are many genes described that behave in this manner (23, 126, 130, 275). Even within the gammaherpesvirus family genes other than Orf50 are encoded by multiple promoters resulting in differential splicing, EBV uses this process to encode six EBNA gene products (20, 210, 231, 232, 270). The use of multiple promoters to control such a critical factor in the gammaherpesvirus lifecycle points to the complex nature involved in control of acute replication, latency, and reactivation. Multiple promoters would give the virus the ability to respond to external stimuli and sense the environment in which the host cell is currently experiencing.

To address the role of the multiple Orf50 promoters we attempted to characterize the Orf50 transcripts in different cell lines. While it appears that all of the promoters have basal activity in the majority of cell lines tested, many of the promoters were more or less active depending on the cell type transfected (Fig. 3). The E1 proximal promoter appeared to be the most active in the Raw 264.7 cells, a macrophage cell line, as well as the most active in the Vero cells, a monkey kidney epithelial cell line. The N3/N4 promoter appeared to be the most active in 3T12 cells, a murine fibroblast cell line. It is interesting that the two promoters with the most basal activity in the three cell lines actually encode the same RTA isoform 1. This may indicate

that the preferred isoform of RTA is isoform 1 and that isoform 2, 3, and 4 are required for more subtle regulation. It was also interesting that the distal promoter E0 was the least active in all of the cell types tested. In fact the distal promoter had almost undetectable levels of basal activity in Vero and Raw 264.7 cells. The fact that this promoter has almost no activity in the cell lines tested is even more interesting because this single promoter results in the encoding of 2 of the 4 known RTA isoform, isoform 2 and isoform 3. Tight regulation of isoform 2 and 3 may indicate a unique effect these RTA isoforms play within the viral lifecycle in comparison to the other more constitutively active promoters.

While basal activity of promoters tells one side of the story, the reason for multiple promoters most likely is the ability to respond to the cellular environment. It is well characterized that gammaherpesviruses respond to many outside stimulus, one being $\text{IFN}\gamma$, as well as internal cellular transcription factors such as XBP-1 (156, 177, 178, 201, 235, 237, 268, 285). To determine if the newly identified promoters respond to these two well known regulators we tested them in the presence of XBP-1 as well as $\text{IFN}\gamma$. All of the promoters showed sensitivity to $\text{IFN}\gamma$ which is in line with current thinking of $\text{IFN}\gamma$ being a potent repressor of gammaherpesvirus infection and reactivation from latency (Fig. 6B). Additionally, three of the four promoters were upregulated by the expression of the transcription factor XBP-1 (Fig. 6A). While the E1 proximal promoter was induced the greatest, also interesting was the N3/N4 promoter which failed to be upregulated by the presence of XBP-1. One hypothesis is that despite the fact that the N3/N4 promoter encodes isoform 1 RTA the transcriptional length of the N4 exon wastes precious time during the critical step of viral replication during plasma cell differentiation. Another hypothesis is that because the N3/N4 promoter encodes the N3 non-coding transcript, this transcript may run transcriptional interference on normal RTA

transcription which is unwanted in the presence of XBP-1. The idea of transcriptional interference has been seen before in EBV, and could potentially be a role for this non-coding N3 transcript (188, 221, 269, 270). Another more recent example of the Orf50 gene specifically responding to outside stimulus is work done showing the effect of a helminth co-infection on viral reactivation. The cytokine IL-4 which is produced in large quantities during co-infection was able to overcome IFN γ viral repression and actually specifically upregulates one of the newly identified MHV68 Orf50 promoters N4/5 (202). While IL-4 was found to only upregulate the single Orf50 N4/N5 promoter in MHV68, it also only upregulated a single promoter in KSHV, the E1 proximal promoter (Fig. 6B). This upregulation of a single promoter represents a way of reactivating from latency that can be tightly controlled under the specific cellular environment of IL-4 induction through co-infection.

One of the most important functions of RTA is the ability to initiate a downstream gene cascade of transcription. The protein does this by binding to various viral promoters and inducing gene transcription (25, 62, 154, 189). While this ability to act as a transcriptional activator has only been observed with isoform 1 RTA, it begs the question can the newly identified RTA isoforms work in a similar manner to generate a cascade of gene transcription. While the majority of the RTA protein is homologous between all of the isoforms, the N-terminal end varies between the four in a few amino acid structures (Fig. 2). This N-terminal end is the DNA binding domain and is critical for the ability of RTA to act as a transcription factor (205, 272). It then begs the question if different isoforms vary at the N-terminal end, does this change the transactivation potential between isoforms. It is important to note that none of the changes to the amino acid structure between isoforms is even remotely homologous as demonstrated in Figure 2. The first thing we demonstrated was that both isoform 1 and isoform 4

can act as self regulators of RTA transcription. Both isoforms 1 and 4 were able to transactivate all of the new Orf50 promoters. It was also observed that isoform 4 works with less efficiency than isoform 1. Additionally both isoforms failed to induce very high expression of the N3/4 promoter, which once again could be due to the nature of the non-coding N3 transcript as well as the redundant nature of N4 encoding isoform 1. One surprising observation was that despite having extremely low basal levels in all cell lines tested (Fig. 3B), the E0 promoter had the highest induction observed for both isoforms of RTA (Fig. 4B). This indicates that despite not responding well to many stimuli, the E0 promoter and the generation of isoform 2 and 3 RTA is highly induced by the other forms of RTA. This may indicate that isoforms 2 and 3 RTA are what we could consider “late” gene RTA’s in which they require the activation and transcription of the other two forms of RTA to become active themselves. The effects isoforms 2 and 3 have on the cellular environment are still being investigated but represent a potential novel finding in which not only is there a cascade of viral gene expression from immediate-early, early, to late but also a cascade of RTA expression that differentially regulates the viral lifecycle.

To test the ability of isoform 1 and isoform 4 to act on downstream targets we tested its ability to transactivate a variety of viral promoters that have been shown to be upregulated by conventional isoform 1 RTA (62). The results seen when using isoform 4 RTA compared to the traditional isoform 1 are compelling. We observed the ability of isoform 4 RTA to upregulate the K12 promoter to a higher degree than previously observed with isoform 1 (Fig.7A). K12 is the transcript most abundantly generated during KSHV latency and therefore its greater upregulation may point towards the ability of isoform 4 RTA to impact the switch to viral latency (140, 215). We also observed isoform 4 has the ability to upregulate Orf57, Orf59, and the PAN promoter similarly to isoform 1 but not to as strong of levels (Fig. 7). In opposite regards to K12 which is

upregulated to a greater degree, isoform 4 failed to upregulate the K-bZIP promoter to very high levels (Fig. 7E). This is interesting because K-bZIP is known to associate with isoform 1 RTA to aid in the upregulation of several viral promoters (62, 109). This may indicate that the inability of isoform 4 RTA to upregulate certain promoters to a similar extent as that observed with isoform 1 RTA may be because of secondary transcription factors such as K-bZIP that are not present with isoform 4 RTA. Since previously isoform 1 RTA has been shown to act directly as well as through host transcription factors such as RBP-Jk, SP1, and Oct-1, the failure of isoform 4 to transactivate to a similar level may be a failure to associate with these factors (28, 39, 258, 265). We did attempt to address the failure of isoform 4 to transactivate K-bZIP through the use of a BAC containing cell line, but this too failed to induce K-bZIP to high levels when using isoform 4 even with TPA treatment of the cells (Fig. 8). This differential gene expression may indicate that isoform 4 plays a much different role than isoform 1 and that the ability of the promoters to sense different environmental clues is key to the gammaherpesvirus lifecycle. One can imagine that each promoter senses different signals, and that the activation of each promoter generates different isoforms of RTA. While the critical viral replication potential of RTA may be maintained for all isoforms, it is possible that each isoform acts in a different downstream manner such as isoform 4 failing to upregulate a critical early gene like K-bZIP but does upregulate to a higher level the latency associated K12 transcript. Additionally isoforms 2 and 3 are highly upregulated by the other two forms of RTA which may indicate they are necessary but at a later viral stage and these two isoforms, while not part of this study, are in critical need of further exploration.

In summary, our findings extend our understanding of the complex Orf50 region of the KSHV genome. We were able to identify 3 previously unknown transcripts, 2 previously

unknown promoters, and begin studies to investigate new RTA isoforms. The generation of new isoforms is critical in our understanding of the gammaherpesvirus lifecycle. This is especially true in light of the fact that the new RTA isoforms behave in a manner that differs from the previously well characterized isoform 1 RTA. With different transactivation abilities, and the ability of each isoform to possibly be generated at the same time, the complexity of the region becomes almost overwhelming. The new isoform RTAs greatly change the landscape of viral life cycle progression, as they may upregulate, downregulate, and act as interference in what has previously been described. Future studies will begin to address this complex dynamic in which the most critical gene for acute viral replication and reactivation from latency has now been shown to have multiple isoforms in which only one was previously known.

3.VI. FIGURE LEGENDS

Figure 1. RACE analyses and primer walking reveal the existence of six G50 exons upstream of exon 2. RACE and primer walking analyses were performed using cDNA generated from BCBL-1 PEL cells reactivated with TPA for 24, 48, and 72 hours. 5' RACE analysis using reverse primers located in E2 were used in conjunction with a universal 5' RACE forward primer. Primer walking was performed using a common reverse primer located in E2 and varying forward primers located upstream of known exons. These experiments identified the Orf50 region to contain six different transcripts, with four different promoters, which encode four unique RTA isoforms. All transcripts splice out large introns while splicing to the exon 2 region and extend the transcript by varying length, E1 a 102bp extension, E0A a 243bp extension, E0B a 292bp extension, N3 an 857bp extension, N4 an 1,646bp extension, and finally N5 a 351bp extension. Transcripts E1 and N4 encode the same RTA isoform using the same ATG initiation site, while E0A, E0B, and N5 all encode different RTA isoforms. The exon N3 does not extend the open reading frame.

Figure 2. Upstream exons extend the KSHV G50 open reading frame to form unique RTA isoforms. (A) Translation of the spliced E1-E2 and N4-E2 transcripts using an ATG located in light blue extends the E2 open reading frame by six amino acids. (B) Translation of the spliced E0A-E2 and E0B-E2 transcripts using an ATG located in the light blue extends the E2 open reading frame by six and ten amino acids respectively. (C) Translation of the spliced N5-E2 transcript using an ATG located in the light blue extends the E2 open reading frame by seven

amino acids. All extensions of the E2 open reading frame are within the same frame and only the very beginning of the E2 exon is shown translated.

Figure 3. Promoter deletions of the four G50 promoters identify minimal promoter length as well as activity in various cell types. (A) Reporter constructs were generated within the context of the E1, E0A/E0B, N3/4, and N5 promoters. Fragments in length of 1000bp, 500bp, 250bp, and 100bp of all four promoters were cloned into the pGL4.10[luc] luciferase reporter construct. 293T cells were transfected using these various promoter constructs and 48 hours after transfection luciferase assays were performed. (B). The 250bp E1 promoter construct described in (A) was used to transfect Vero, 3T12 and Raw 264.7 cells and luciferase assays were performed 48 hours post-transfection (C). The 500bp E0 promoter construct described in (A) was used to transfect Vero, 3T12, and Raw 264.7 cells and luciferase assays were performed 48 hours after transfection. (D) The 500bp N3/N5 promoter construct described in (A) was used to transfect Vero, 3T12, and Raw 264.7 cells in which 48hours post transfection luciferase assays were performed. (E) Transfection of Vero, 3T12, and Raw 246.7 cells was performed using the N5 1000bp construct described in (A). At 48 hours post transfection luciferase assays were performed. All data represents experiments performed in triplicate. Standard error of the means is shown.

Figure 4. Transactivation of Orf50 promoters by isoform 1 (E1-E2) and isoform 4 (N5-E2) RTA. The RTA E1-E2, E2ATG (control), and N5-E2 transcripts were cloned from BCBL-1 cDNA and ligated in pCMV-Tag2B expression vectors. These vectors or an empty pCMV-

Tag2B vector were transfected into 293T cells along with either full length 1000bp (A) Exon 1, (B) Exon0A/B, (C) Exon N3/N4 and (D) Exon N5 promoters constructs in pGL4.10[Luc]. After 48 hours these cells were read in a luciferase assay. Data is represented as promoter fold increase over empty vector transfection. Data is representative of three replicates and standard error of the means is shown.

Figure 5. Promoter truncation from 1000bp to 100bp within the KSHV E1, E0A/B, N3/4 and N5 promoters showing essential region required for E1-E2 isoform 1 RTA transactivation. Promoter constructs described in Figure 3 were transfected into 293T cells along with the E1-E2 pCMV-Tag2B or pCMV-Tag2B empty vector. (A) Exon 1, (B) Exon0A/B, (C) Exon N3/N4 and (D) Exon N5 promoter truncation were also transfected. After 48 hours luciferase assays were performed and the data is represented as promoter fold increase over empty vector transfection. Data is representative of three replicates and standard error of the means is shown.

Figure 6. KSHV Orf50 promoter region transactivation by XBP-1, transactivation by IL-4, and inhibition by IFN γ . (A) E1, E0A/B, N3/4, and N5 1000bp promoter constructs in pGL4.10[Luc] were cotransfected into Raw 264.7 cells with XBP-1s pCMV-Tag2B or pCMV-Tag2B empty vector. After 48 hours luciferase assays were performed and data is plotted as fold change over empty vector. (B). E1 250bp, E0A/B 500bp, N3/4 500bp, and N5 1000bp promoter constructs in pGL4.10[Luc] or pGL4.10[Luc] empty vector were transfected into Raw 264.7 cells. After 24 hours either 10ng/ml of IL-4 or 10ng/ml of IFN γ was added to the cells. At 48 hours luciferase

assays were performed and data is plotted as fold change over empty vector. Data is representative of three replicates and standard error of the means is shown.

Figure 7. Promoter activity of various KSHV Orfs transactivated by either E1-E2 isoform 1 RTA or N5-E2 isoform 4 RTA. (A). KSHV K12 promoter construct in pGL4.10[Luc] was transfected into 293T cells along with either E1-E2 pCMV-Tag2B, N5-E2 pCMV-Tag2B, E2-ATG pCMV-Tag2B (CTL), or pCMV-Tag2B empty vector. After 48 hours luciferase assays were performed and data is plotted as fold change over empty vector. The following panels were created using the same protocol except that (B) KSHV Orf57; (C) KSHV Orf59; (D) KSHV PAN; (E) KSHV b-ZIP promoters in pGL4.10[Luc] were used. All experiments were repeated in triplicate and standard error of the means is shown.

Figure 8. KSHV b-ZIP and PAN promoter activity when transactivated by E1-E2 isoform 1 RTA or N5-E2 isoform 4 RTA in virus containing cells. bZIP and PAN promoter constructs in pGL4.10[Luc] were transfected in 293TΔ50BAC cells along with either E1-E2 pCMV-Tag2B, N5-E2 pCMV-Tag2B, E2-ATG pCMV-Tag2B (CTL), or pCMV-Tag2B empty vector. After 24 hours 25ng/ml of TPA was used to induce viral gene production. At 48 hours cells were used in a luciferase assay which was plotted as fold change over empty vector. Experiments were repeated in triplicate and standard error of the means is plotted.

3.VII. FIGURES

1. RACE analyses and primer walking reveal the existence of six G50 exons upstream of exon 2
2. Upstream exons extend the KSHV G50 open reading frame to form unique RTA isoforms.
3. Promoter deletions of the four G50 promoters identify minimal promoter length as well as activity in various cell types
4. Transactivation of Orf50 promoters by isoform 1 (E1-E2) and isoform 4 (N5-E2) RTA
5. Promoter truncation from 1000bp to 100bp within the KSHV E1, E0A/B, N3/4 and N5 promoters showing essential region required for E1-E2 isoform 1 RTA transactivation
6. KSHV Orf50 promoter region transactivation by XBP-1, transactivation by IL-4, and inhibition by IFN γ
7. Promoter activity of various KSHV Orfs transactivated by either E1-E2 isoform 1 RTA or N5-E2 isoform 4 RTA
8. KSHV b-ZIP and PAN promoter activity when transactivated by E1-E2 isoform 1 RTA or N5-E2 isoform 4 RTA in virus containing cells

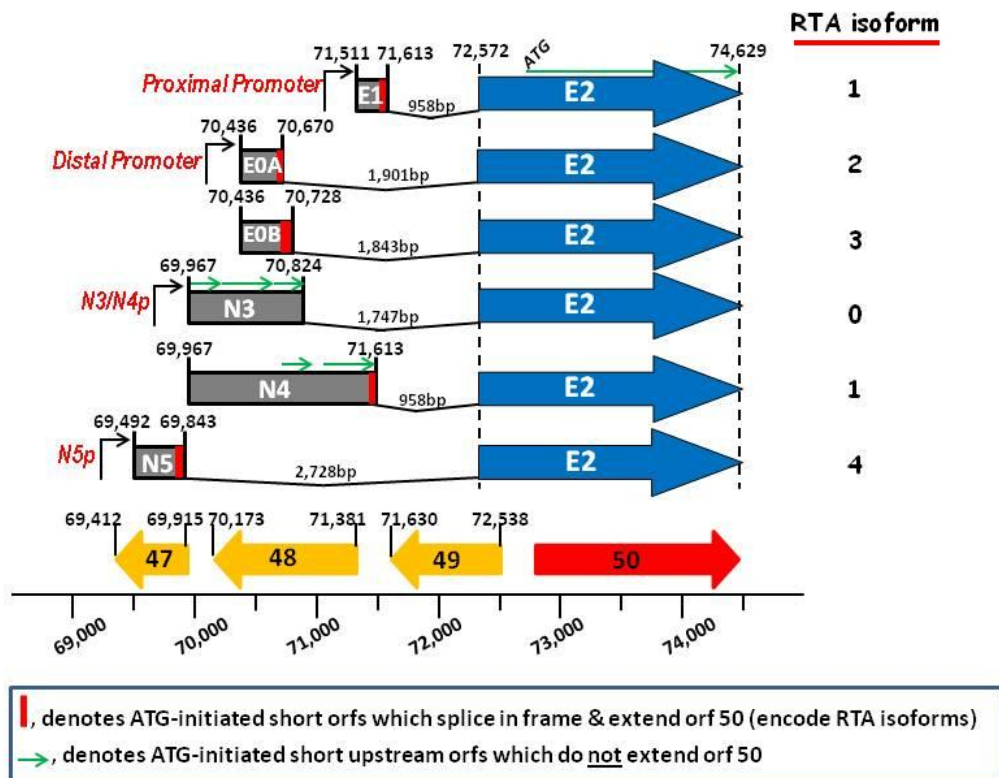
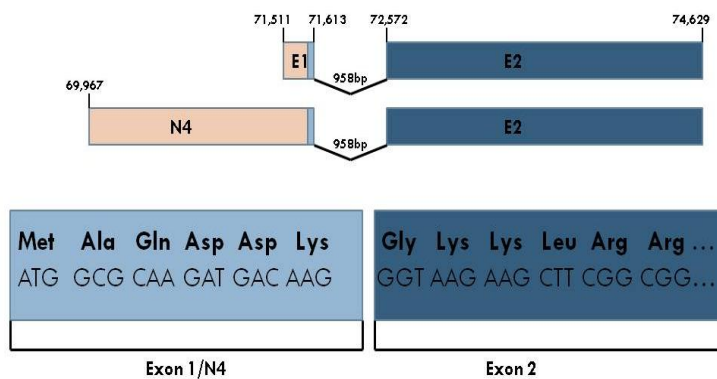
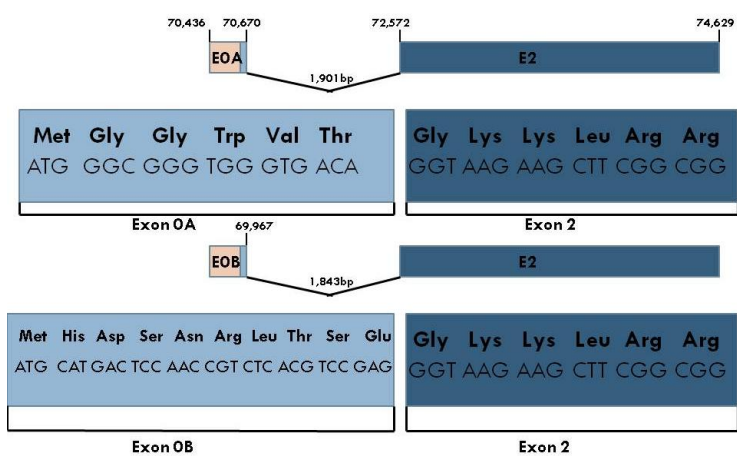


Figure 1

A.



B.



C.

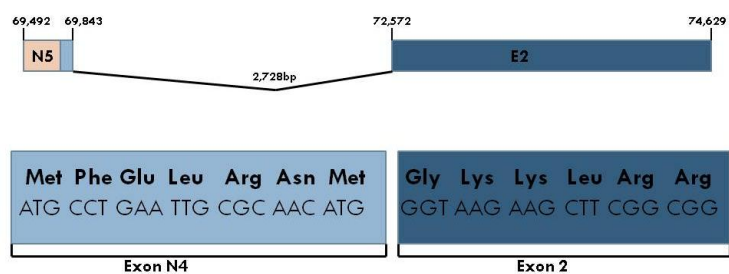


Figure 2

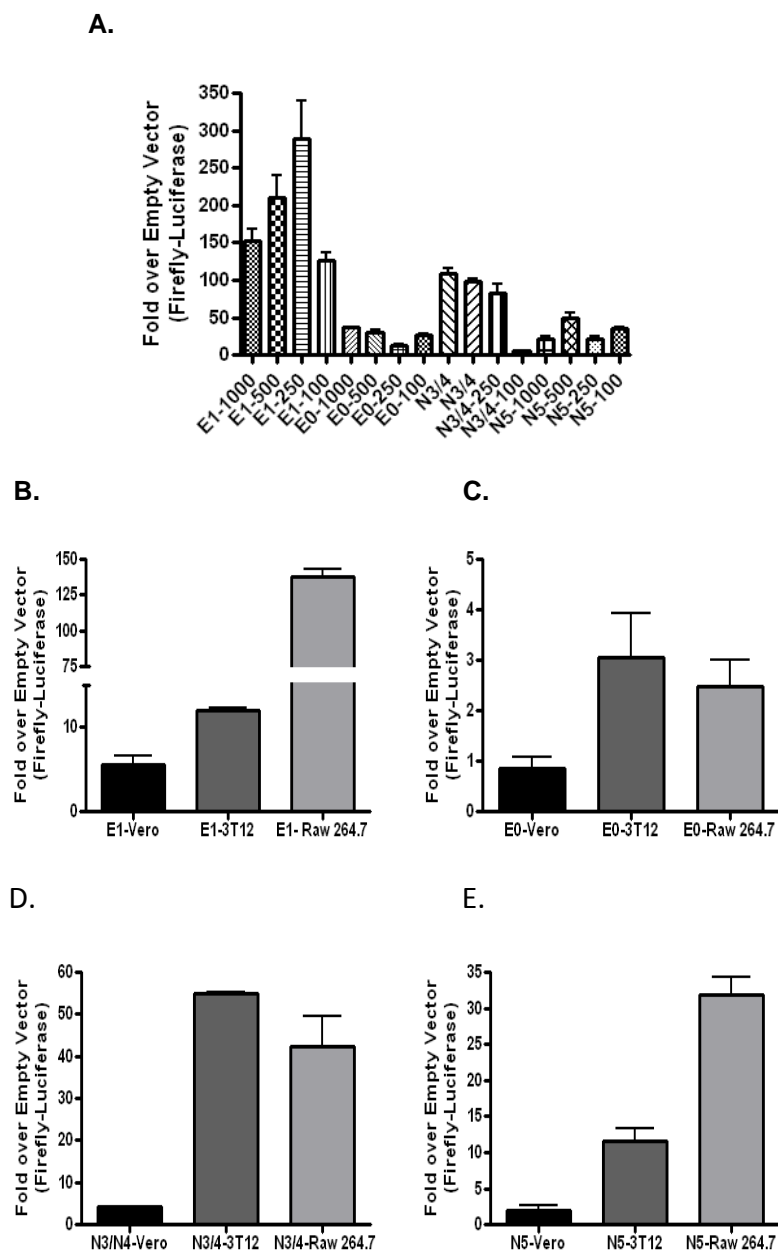


Figure 3

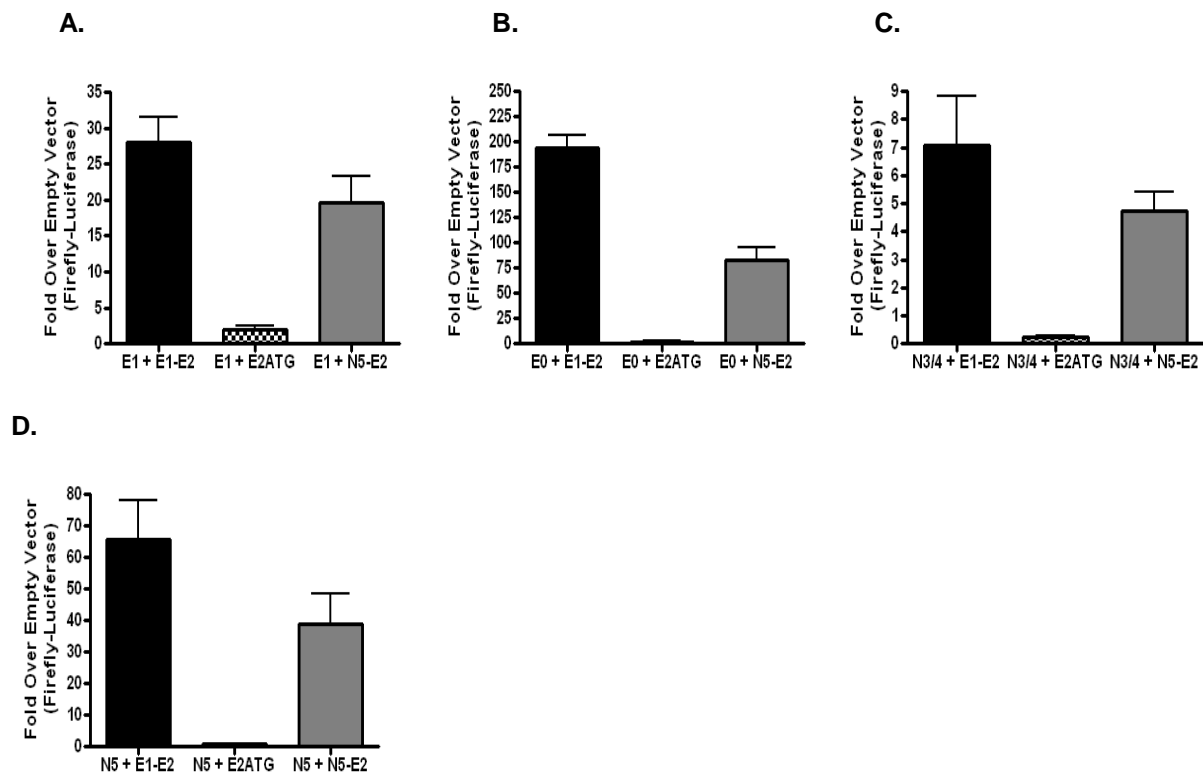


Figure 4

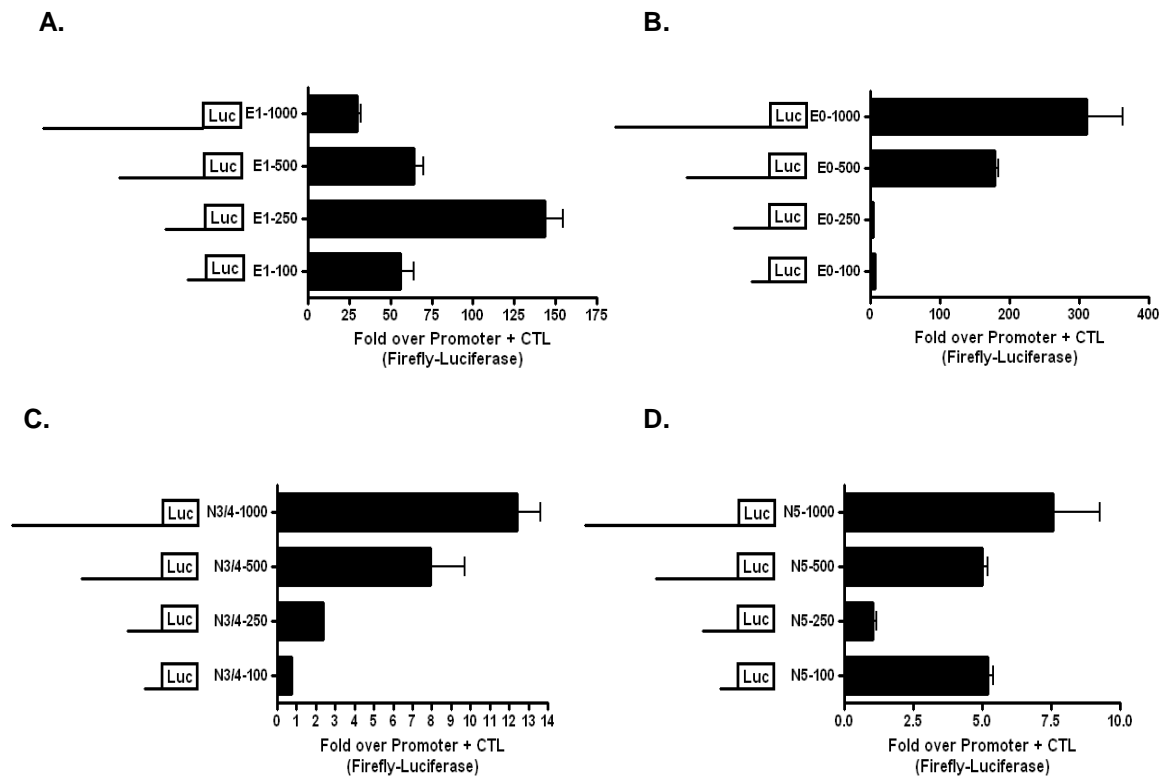


Figure 5

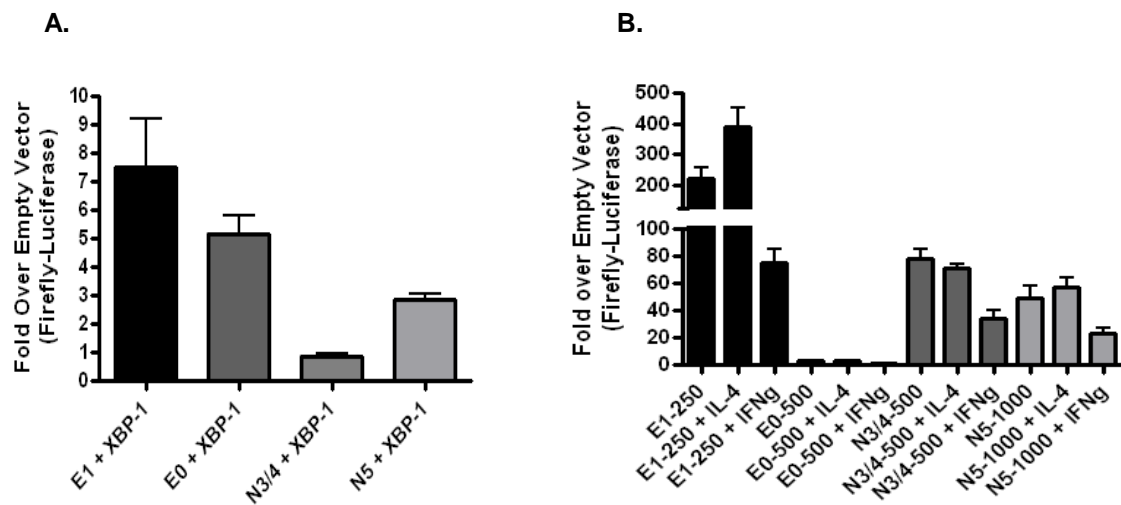


Figure 6

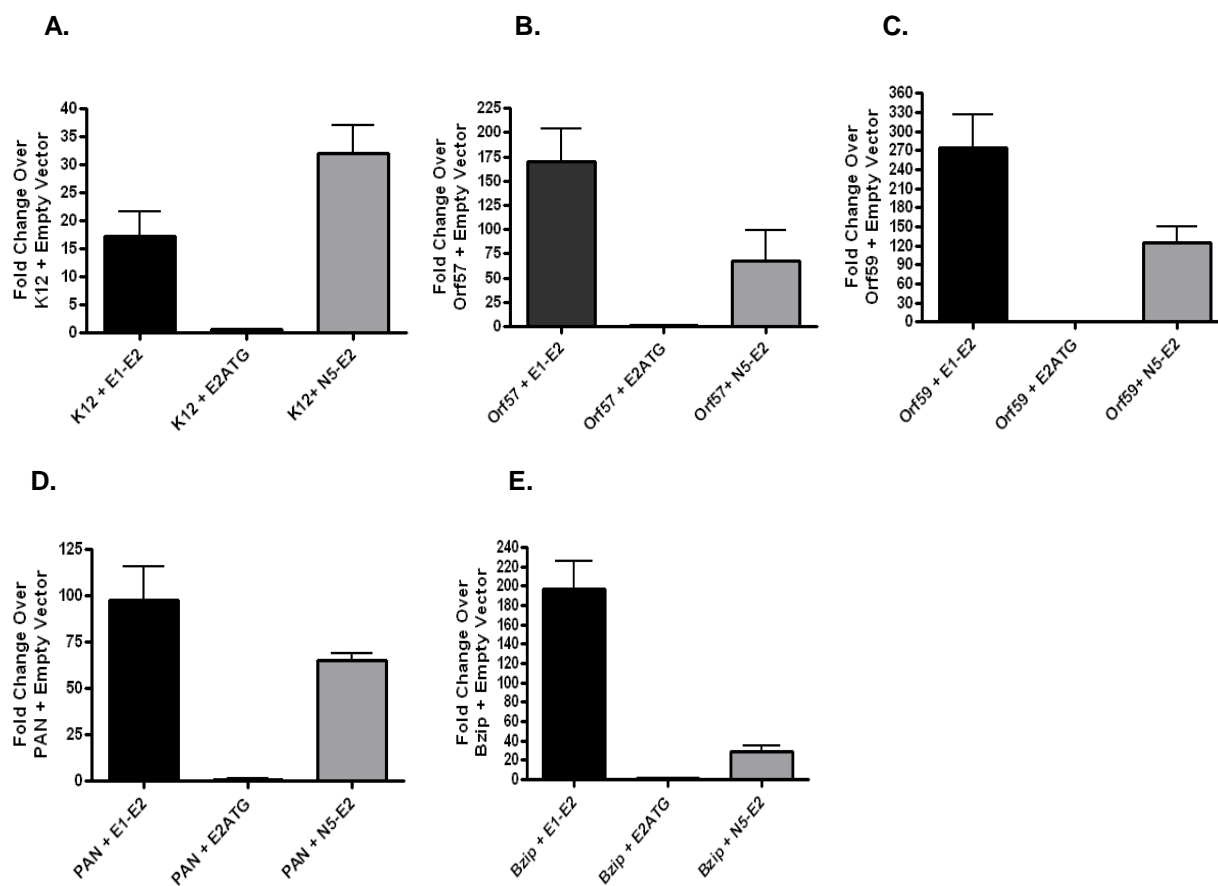


Figure 7

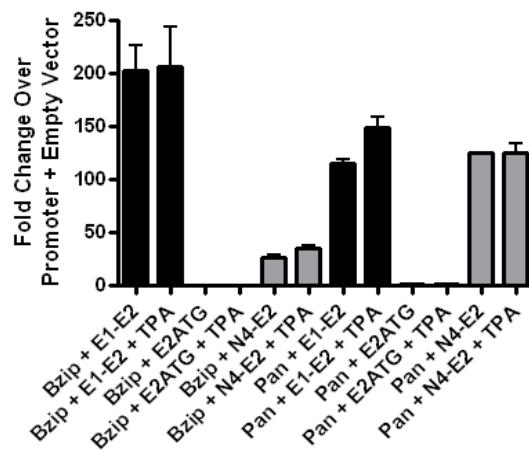


Figure 8

Chapter 4: CONCLUSIONS & FUTURE DIRECTIONS

Human gammaherpesviruses have been linked to a variety of human diseases; while these malignancies are rare in healthy hosts, they represent a problem in immunocompromised individuals. Unique to gammaherpesviruses is their wide spread infection rates in which large percentages of the world population harbor latent virus. This is a concern amongst transplant patients as organ transplantation requires suppression of the immune system to aid in graft survival. Additionally since a large percentage of the population is latently infected with human gammaherpesviruses, some individuals will be exposed to secondary infections that may result in gammaherpesvirus related illnesses. Finally, gammaherpesviruses represent a unique set of viral infections that remain with a host for life allowing for it to play a critical role in shaping the overall immune system. For these reasons gammaherpesviruses are a critical area of study.

Human viruses KSHV and EBV have a strict human tropism which severely restricts their study, as work is limited to narrow *in vitro* studies. The development of MHV68 as a model system has allowed for a wealth of knowledge to be gained on the normal life cycle and immune response to gammaherpesvirus infection. MHV68 represents a great model for infection as it shares strong homology with KSHV and EBV, behaves similarly during primary infection, and infects the small animal mouse. MHV68 has allowed for *in vivo* studies to be conducted to recapitulate KSHV and EBV driven *in vitro* experiments, additionally the study of MHV68 has allowed for new hypotheses about KSHV and EBV to be generated. In Chapter 2 of this study we successfully utilized the MHV68 model to manipulate the Orf50 region and assess the ability of a double promoter knockout virus to replicate. This allowed us to identify three additional Orf50 transcripts that had previously been unknown. Additionally these studies were able to

begin to assess why the lack of two of the five Orf50 transcripts resulted in sensitivity to type I interferons. We conclude this chapter by infecting *in vivo* which showed the rescue of the observed *in vitro* phenotypes in a model that lacks type I interferons.

The work in Chapter 2 set the foundation for the work discussed in Chapter 3 in which we used our recent knowledge of Orf50 transcripts in MHV68 to determine if these transcripts also show homology in the human virus KSHV. We were able to identify previously unknown Orf50 transcripts within KSHV, while these transcripts differed slightly from those of MHV68 their discovery can be credited through the use of the MHV68 model. As mentioned these transcripts differ, which is a concern in the use of the MHV68 model system as exact homology and life cycle is not completely shared. This however should not detract from the usefulness of MHV68 as a model, as the critical discovery of four RTA isoforms when previously there was believed to be only one in KSHV, would not have been possible without MHV68. It is our hope to expand the studies discussed in Chapter 2 and 3 through the use of the MHV68 where the complex regulatory aspect of multiple promoters can easily be manipulated through the MHV68 BAC system and phenotypes assessed *in vitro* and *in vivo*.

4.I. The MHV68 exon N3, exon N4, exon N5 and their promoters.

All previous work in which MHV68 was used as a model relied on the understanding that there was a single isoform of RTA generated. In MHV68, an ATG located within a short exon (Exon 1) spliced to a long downstream exon (Exon 2). This splicing extends the open reading frame of exon 2 resulting in the known RTA protein. More recently it was discovered that there was an additional exon (Exon 0), in which this exon splices to exon 1 which in turn splices to exon 2 forming an E0-E1-E2 transcript (81). Furthermore, this newly identified exon 0 was

found to be conserved within KSHV and EBV. In this study, little was explored as far as function of the distal promoter. It was seen that this promoter was able to drive Orf50 transcription and viral replication in the absence of the proximal promoter. Additionally, it was shown *in vivo* that this promoter retains the ability to establish latency but was only able to reactivate cells from PECs and not splenocytes (81). For this reason the generation of a G50DpKo (Orf50 distal promoter knockout virus) is necessary and has been completed within in our lab. Studies to elicit further understanding of this promoter are ongoing, though others have also begun work and have shown the distal promoter is highly sensitive to IFN γ (79)

With the original goal to generate an Orf50 null virus (a virus that lacks RTA protein expression) through the deletion of the promoter driving E1 transcription, we attempted once again to generate this Orf50 null virus through the deletion of both the proximal and now known distal promoters. The generation of a G50DbIKO virus resulted in the discovery of the three additional Orf50 transcripts and the two promoters which drive them. In addition now to the E1-E2 and E0-E1-E2 transcript there is the expression of an N3-E1-E2, N4-E1-E2 and a N5-E1-E2 transcript. While the N3 and N4 exon are extensions of the known E0 transcript, the N5 exon demonstrates unique splicing to the E1 exon. It was also interesting that all upstream transcripts identified splice through the E1 transcripts. The splicing through of the E1 transcript indicates that despite different transcripts they all encode for the same RTA isoform. As of now there are no known MHV68 transcripts that do not splice through the E1 exon. The lack of these transcripts however may simply be due to the low abundance of transcript generated by upstream promoters that are not the E1-E2 main Orf50 transcript. What is interesting is that an E0-E2 transcript would also extend the exon 2 open reading frame and code for a functional RTA

protein, though a different isoform than the currently generated E1-E2 form. Work is currently being conducted to determine if transcripts that encode different isoform RTA can be found.

While the organization of Orf50 seems complex there is precedent for this kind of multiple promoter driven transcription found within the gammaherpesvirus family. The non-human primate virus herpesvirus saimiri (HVS) uses dual promoters to drive RTA transcription (266). Additionally EBV lytic replication requires the immediate-early protein ZTA as well as the BRLF-1 RTA protein. This ZTA protein can be transcribed from a monocistronic transcript or from a polycistronic transcript that contains both ZTA and RTA coding regions which is the result of alternative splicing (34). This alternative splicing within the Orf50 region lays a foundation for the observations made in the MHV68 Orf50 region. While none of the newly discovered transcripts result in different isoforms of RTA, they are driven by various promoters. In the first part of our study, the generation of the G50DbIKo virus required analysis of the distal promoter and the identification of a region that when deleted results in promoter silencing. It was during this mapping that we also discovered an area related to promoter repression. Around 50bp upstream of the start of the E0 exon lies a region that when deleted results in a 1,500+ fold induction of the distal promoter. This indicates that under normal circumstances this region severely represses the ability of the Orf50 distal promoter to transcribe E0-E1-E2 transcripts. Currently it is unknown what transcription factors bind to this region, but studies are being conducted to determine the importance of this region. Utilizing the MHV68 BAC system we have also generated a G50DP $\Delta^{65872-65822}$ KO virus corresponding to this region of repression. Use of this virus *in vivo* is of interest as previous work shows that constitutively active RTA results in the inability to establish latency and a possible avenue for vaccine development (204).

While work to characterize the distal promoter is further along, the characterization of the newly discovered N3 and N4/N5 promoters is just beginning. While we have shown that these new promoters are not sensitive to type I interferon treatment beyond that little else is known. Despite this we have recently collaborated on work with the Virgin group in which the newly described N4/N5 promoter plays a critical role. It has now been demonstrated that MHV68 has the ability to reactivate from latency during co-infection with helminthes (202). It has been well established that gammaherpesvirus latent infection can either be beneficial or harmful during secondary infections including but limited to adenoviruses, bacteria, and influenza (11, 176, 218, 254). This study was the first to address the role that helminth infection has on the gammaherpesvirus lifecycle. Reactivation from latency was dependent on the expression of IL-4, and IL-13 cytokines, and it was found that the only MHV68 promoter that was responsive to IL-4 and IL-13 was the N4/N5 Orf50 promoter (Fig. 1A). Additionally the N4/N5 promoter was sensitive to IFN γ treatment, but this effect was overcome by the addition of IL-4 (Fig. 1B). Finally we were able to show that this N4/N5 Orf50 promoter induction by IL-4 was done in a STAT-6 dependent manner, as deletion of two of the four potential STAT transcriptional binding sites alleviate upregulation of the N4/N5 Orf50 promoter (Fig 1C). These important observations were only made possible through the discovery of the additional Orf50 promoters. Without the N4/N5 promoter, no direct role for IL-4 induction would have been observed since the previously known proximal promoter is unresponsive. This work demonstrates an important role for the N4/N5 promoter in the context of sensing the cellular environment. In one case the replication of virus is inhibited through the promoter's response to IFN γ , in another case the promoter responds to an IL-4 environment signifying the need to replicate and reactivate. It will

be important to study the new Orf50 promoters in the context of other cellular environments beyond IL-4 and IFN γ to determine if different promoters can respond to different stimuli.

With the recent observation in the importance of the N4/N5 promoter in response to IL-4 stimulus we have generated an N4/N5 promoter deletion to determine the importance the N4 and N5 transcripts play in the course of a normal infection. Complicating the generation of an N4/N5 promoter mutant is the anti-sense strand of DNA which encodes the Orf47 gene. Orf47 encodes glycoprotein L a non-essential viral structure protein (151, 174). Though this protein is non-essential it is found to be a major target for neutralization by monoclonal antibodies and is critical for the neutralization profile of MHV68 (75, 77, 78). For this reason we also generated an Orf47.Stop mutant which would not disrupt the N4 and N5 transcript. However we only have generated a crude G50N4/N5pKo in which the entire N5 exon was removed. While generating these two mutants we also hypothesized that splicing was important in the context of the Orf50 region and therefore we generated a G50E1SaKo in which the gene 50 exon 1 splice acceptor was mutated and a G50E0SdKo in which the gene 50 exon 0 splice donor was mutated. A preliminary study with these mutants has resulted in some complicated findings. We first observed that the Orf47.Stop, G50N4/N5pKo, and G50E0SdKo mutant were able to replicate in all cell types tested. This differs from the G50E1SaKo mutant in which the deletion of E1 splicing resulted in viral sensitivity to type I interferons (Fig 2A/B). Using the G50N4/N5pKo and the Orf47.Stop mutant *in vivo* results in a complicated phenotype in which the Orf47.stop mutant results in a hyper-reactivation and the G50N4/N5pKo virus results in a reactivation defect (Fig. 3). The fact that Orf47 results in a phenotype muddles the interpretation of the G50N4/N5pKo virus data, as this virus would also eliminate the Orf47 region. For this it is imperative that N4/N5 promoter data be generated in which minimal changes to this region can

be introduced in which Orf47 transcription remains intact. With the data we have generated so far it does point to their being a role for the N4/N5 transcripts in reactivation, which would confirm the findings observed in the co-infection model. In the future it would also be of interest to use the N4/N5 mutant in an *in vivo* co-infection model of study.

4.II. Type I interferon sensitivity

One of the most unique findings from work done in Chapter 2 was the role that Orf50 plays in sensitivity to type I interferons. With the generation of the G50DbIKo virus we were only able to show growth in the absence of the type I interferon response. Fortunately this observation was made through the process in which we scale up BAC derived virus. BAC containing virus is transfected into Vero-cre cells containing cre recombinase to excise the BAC, as BAC containing virus shows a significant phenotype *in vivo* (2). Luckily Vero cell lines are unique in they lack the ability to produce a type I interferon response, though they are able to respond properly. It was in our scale up procedure in which virus was used to infect large flasks of 3T12 fibroblast cells that it was observed that the mutant virus failed to replicate. With the only major difference between Vero and 3T12 cells being an interferon effect we were able to devise experiments to test this hypothesis.

We have been able to show that the new promoters driving Orf50 replication are not directly type I interferon sensitive but so far have been unable to determine the role the missing Orf50 transcripts play in type I interferon evasion. The RTA protein is made in abundance during initial infection and this immediate transcription would point to its involvement in type I interferon evasion. Many Orfs such as Orf45 and Orf64 have been found in the virion and help the virus to evade the initial type I interferon response (22, 84, 107, 292, 293). Though only

minimal work has been done, RTA itself has been shown to help suppress the type I interferon immune response through E3 ligase activity that targets IRF-7 for proteasome-mediated degradation (286). We are able to show in Chapter 2 that RTA is produced at a high level in the absence of the proximal and distal promoter, however the pattern of expression appears to be deregulated in which RTA appears earlier within the initial viral infection and begins to be degraded or shutdown earlier. It may be that a change in RTA kinetics results in the phenotype observed. RTA is well known to transactivate downstream genes and the upregulation of these genes may include potential Orfs that play a role in immune evasion. It would be of interest to examine virions that are generated between wild-type and the G50DbfKo virus to determine if the same viral proteins are found as well as found at the same level.

Initial work to classify the role RTA plays in the type I interferon evasion was to look for a direct novel role RTA may be playing. We were able to show that specific to the type I interferon response that the G50DbfKo virus was able to replicate in MEFs that lacked PKR/RNaseL (Fig. 4). Many viruses are known to target the PKR pathway of the type I interferon response. Specifically the alphaherpesvirus HSV is able to target eIF2 α phosphorylation using the viral gene ICP34.5 (51, 253, 273). By targeting the phosphorylation of eIF2 α , HSV is able to subvert the PKR response and its ability to inhibit cellular translation. While no gammaherpesvirus protein has been shown to target this pathway, RTA would be a likely candidate as its expression is immediate upon viral entry and the gene cascade requires the ability of cellular machinery to translate new proteins. To test this hypothesis we looked at eIF2 α phosphorylation levels between WT and G50DbfKo virus and observed a significant increase in eIF2 α phosphorylation in the G50DbfKo virus compared to WT (Fig. 5). This initial data is not conclusive that RTA specifically targets this pathway, however it does provide insight into one

mechanism in which the type I interferon evasion mechanism is disrupted in the G50DbIKo virus. Further work needs to be conducted to show that RTA is responsible for targeting eIF2 α phosphorylation. The easiest method would be to utilize an RTA inducible cell line system in which the direct effects RTA has on a cell can easily be quantified.

The G50DbIKo virus shows a unique phenotype that was previously unknown and further reveals a critical role type I interferons play during viral infection. Interestingly the G50DbIKo has high levels of virus in the lungs in the absence of type I interferons but is unable to induce mortality like the WT virus. Also despite a dose approximately five thousand times the lethal dose of WT, the G50DbIKo is unable to induce death. While the global effects the lack of type I interferons play during infection has been known for awhile, how has remained a mystery (131). Recently it has been shown that CD8⁺ T cells may play a role during the lack of type I interferons leading to the hyper-reactivation phenotype observed (111). The problem with these studies is they are complicated by the increased viral replication that takes place in the lungs when type I interferons are absent, and in this study treatment with cidofivir restored the CD8⁺ T cell functions in preventing viral reactivation. To determine a more direct role for type I interferons early during infection and late during infection we designed adoptive transfer experiments to address the role type I interferons play early in infection and the role they play late in infection. Gammaherpesviruses are unique in that they initially replicate in somatic cells such as lung epithelial cells, but long term latency and infection takes place in bone marrow derived B cells. Through bone marrow transfers, we were able to generate two chimeric mouse strains, one which lack type I interferon receptors on their somatic cells but retain type I interferon receptors on their immune cells. The other mice lack type I interferon receptors on their immune cells but retain type I interferon receptors on their somatic cells (Fig. 6A). Initial

infection of these mice reveals an interesting phenotype in which mice that lack type I interferon receptors only on their somatic cells succumb early to infection, as seen with global type I interferon knockout mice (Fig. 6B). Mice that only lack type I interferons on their immune cells are able to control initial infection, but begin to succumb to infection later on. Mice that lack type I interferons on their somatic cells that do survive have WT levels of reactivation observed, this most likely being because their latently infected B cells do respond to type I interferons (Fig. 6C). Opposite of this is the mice that have type I interferons receptors on their somatic cells but lack these receptors on their B cells. They most likely have low levels of initial infection in the lung like a WT infection however reactivation levels are elevated due to the inability of type I interferons to control reactivation from B cells. This pilot study raises some interesting questions and some unique features of gammaherpesvirus control. This study indicates that type I interferons are both important for control of initial infection in the lungs as well as important for control of reactivation from latently infected B cells later on during infection. Additional studies are underway to further investigate this phenomenon. Lung titers will need to be determined to show that the type I interferon responses on somatic cells is able to control viral replication to WT levels. Additionally it is important to determine changes in immune response over time and serum will be collected throughout additional experiments. Overall this initial study further reveals the complicated role the type I interferon response plays during the complex gammaherpesvirus infection.

4.III. The new KSHV transcripts and their promoters

In Chapter 2 we were able to identify 3 new Orf50 transcripts that had previously gone unnoticed. Since MHV68 is a model for the human gammaherpesviruses we extended these

studies in Chapter 3 to KSHV. In this chapter we were able to identify new KSHV transcripts as well, further solidifying MHV68 as a model of gammaherpesviruses. What was interesting in the identification of the new transcripts in KSHV was that their splicing differed from what was previously observed in MHV68. We were able to show that not only are there new transcripts but these new transcripts encode new RTA isoforms. So combining the generation of new isoforms with the transcription occurring from different promoters, the Orf50 region becomes a lot more complicated.

We were able to show that the four promoters are active in all of the cell types tested, however the distal promoter driving the transcription of E0A and E0B had very low to non-existent basal level of transcription. This was interesting because this promoter drives the formation of two of the four RTA isoforms. Furthermore the transcripts are highly upregulated by isoform 1 and isoform 4 which may point to a role later in viral replication. Another interesting promoter is the N3/4 promoter which shares the responsibility of transcribing both the N3 non-coding transcript and the N4 transcript which contains a long 5' UTR before encoding the isoform 1 RTA. The long N3 non-coding transcript may be used in a form of transcriptional interference which was previously discussed in regards to MHV68. In addition the sharing of the promoter may help regulate the generation of isoform 1 RTA, as this transcript may inhibit transcription of E1, but isoform 1 RTA could still be generated at a lower abundance from the N4 transcript. The abundance of transcripts is currently unknown and is a pressing need for better understanding. One can make the hypothesis that the E1-E2 transcript is most abundant while the E0A and E0B transcripts are the least abundant, but this hypothesis is driven from promoter assays and no actual transcriptional analyses. Complicating the understanding of

transcript abundance will be how these transcripts are generated in different cell types, with primary infection models of KSHV lacking in comparison to MHV68.

One of the most critical features of Orf50 is its ability to act as a viral transactivator of gene expression. With the identification of four isoforms of RTA this ability needs to be compared between all four isoform. In collaboration with the Izumiya group and based off of their viral promoter library (62), we have begun to screen the ability of isoform 4 to transactivate downstream viral genes. So far the results have been promising in that it appears that isoform 4 and isoform 1 differ in their ability to act as viral transactivators. This difference lies in the changes observed in the 6-10 amino acid of the N-terminal of the RTA protein. How this affects binding and protein folding has yet to be determined. Experiments to determine the role isoform 2 and 3 play are also underway. These transcripts are more difficult to work with because of their rare nature, at least in the cell lines we utilize. This difficulty will be overcome with simple cloning techniques and we expect to have constitutively active isoform 2 and 3 expression vectors generated shortly. In addition to the role these isoforms play on transactivation directly it is important to determine if any role exists in their ability to alter the function of other isoforms. Overall the discovery of these new promoters driving new RTA isoforms is a major discovery in the KSHV field. Almost all work previously utilizing isoform 1 RTA needs to be conducted now using isoform 2, 3, and 4 RTA, a monumental task.

4.IV. Summary

This work has identified new MHV68 Orf50 transcripts as well as new KSHV Orf50 transcripts. This discovery was generated through the use of a MHV68 G50DbIKo virus in which despite the lack of both the proximal and distal promoter was able to replicate. This replication of the G50DbIKo virus was complicated by the fact that the virus was highly sensitive to the type I interferon response and that replication was inhibited in the presence of type I interferons. Using this virus *in vivo* revealed that the virus fails to reactivate from latency and exhibits lower seeding of the latency reservoir. This phenotype was rescued through the use of type I interferon KO mice and shows a novel role for Orf50 in type I interferon evasion. Using the knowledge gained through the MHV68 model we expand the study to KSHV and showed the existence of new Orf50 transcripts in the human gammaherpesvirus as well. Uniquely KSHV not only has new Orf50 transcripts but these transcripts encode novel RTA protein isoforms which vary at the N-terminal transactivation domain. This variation in the N-terminal domain leads to changes in transactivation potential and provides clues to a novel role different RTA isoforms play in viral gene expression.

4.V. FIGURE LEGENDS

Figure 1. IL-4 promotes viral replication and antagonizes IFN γ suppression of viral replication through the Orf50 promoter (202). (A). RAW264.7 cells were transfected with vectors expressing luciferase under control of four different *gene 50* promoters. Cells were then treated with or without 10ng/ml IL-4 or IL-13 for 24 hours, lysed, and assayed for luciferase activity. (B) Cells were transfected with the N4/N5 promoter luciferase construct and treated with 10ng/ml IL-4, IFN γ , or both. (C) N4/N5 luciferase mutants were transfected into RAW264.7 cells and assayed for sensitivity to IL-4.

Figure 2. G50E1SaKo virus displays a growth defect *in vitro* when IFN α is present. (A). Multistep growth curve of 3T12 fibroblast infected with WT, G50N4/N5pKo, G50E0SdKo, G50E1SaKo, or Orf47.Stop at an MOI of 0.01. (B) Multistep growth curve of Vero-Cre cells infected with WT, G50N4/N5pKo, G50E0SdKo, G50E1SaKo, or Orf47.Stop at an MOI of 0.01.

Figure 3. G50N4/N5pKo virus exhibits a reactivation defect while the Orf47.Stop virus displays a hyper reactivation defect *in vivo*. Female C57BL/6 mice were infected with 1,000 PFU i.n. and 16 days post-infection splenocytes were assessed for reactivation from latency utilizing a limiting-dilution CPE assay. Splenocytes were plated in serial dilutions onto a MEF monolayer, and at 21 days postplating wells were individually scored for CPE. The percentage of these wells was used to calculate frequency of virally reactivating cells.

Figure 4. G50DbIKo virus displays a growth defect in vitro when PKR or RNaseL is functional. A multistep growth curve on C57BL/6 MEFs or PKR/RNaseL^{-/-} MEFs infected with WT or G50DbIKo virus at an MOI of 0.01.

Figure 5. Immunoblot analysis of eIF α phosphorylation levels in WT or G50DbIKo virus infected NIH 3T12 fibroblasts. 3T12 cells were infected with wild-type MHV68 or the G50DbIKo mutant at an MOI of 5, and cells were harvested at 24 hours postinfection. Cells were lysed, and 30 μ g of protein was used for the immunoblot analyses to assess eIF α phosphorylation levels. Immunoblots were stripped and then reprobbed for β -actin levels to ensure equal protein loading. Quantification of expression levels is represented as fold change of eIF α phosphorylation levels over uninfected controls normalized to β -actin.

Figure 6. Generation and infection of 129S2/SvPas.IFN α / β R^{-/-} chimeric mice. (A). Diagram representation of the protocol used to generate 129S2/SvPas.IFN α / β R^{-/-} chimeric mice. Bone marrow from 129S2/SvPas.IFN α / β R^{-/-} mice was injected into irradiate 129S2/SvPas mice and bone marrow from 129S2/SvPas mice was injected into irradiate 129S2/SvPas.IFN α / β R^{-/-} mice to generate two distinct mice. (B) Kaplan-Meier curve depicting survival of chimeric mice when challenged with 1,000 PFU i.n of WT virus. (C). Limiting dilution CPE assay showing percentage of cells reactivating from latency at day 40 post i.n infection for mice that survived challenge.

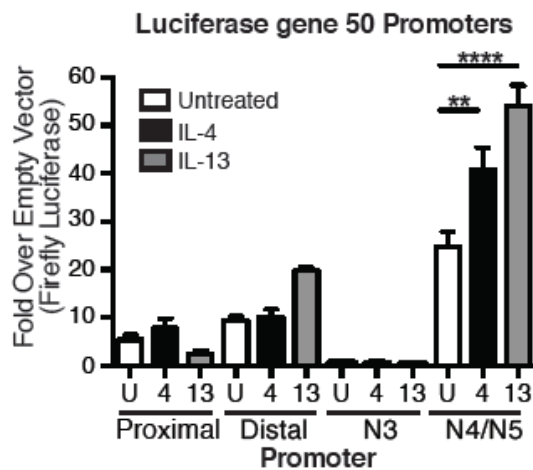
Figure 7. KSHV isoform 1 and isoform 4 RTA show varying transactivation potential on viral promoters. A chart representing fold change in promoter induction when in the presences of

either isoform 1 RTA or isoform 4 RTA. Red indicates a higher induction by isoform 1, green indicates a higher induction by isoform 4, and yellow indicates a similar level of induction between both isoforms.

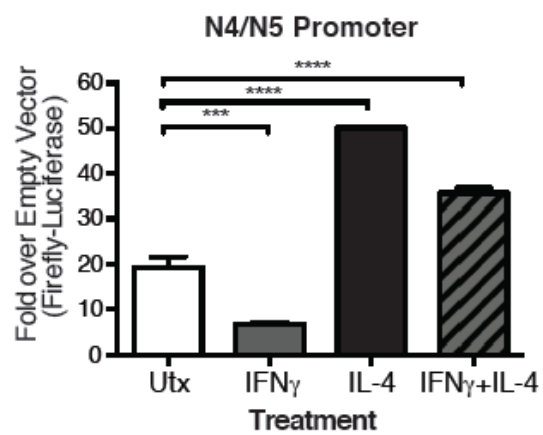
4.VI. FIGURES

1. IL-4 promotes viral replication and antagonizes IFN γ suppression of viral replication through the Orf50 promoter
2. G50E1SaKo virus displays a growth defect *in vitro* when IFN α is present
3. G50N4/N5pKo virus exhibits a reactivation defect while the Orf47.Stop virus displays a hyper reactivation defect *in vivo*
4. G50DbIKo virus displays a growth defect *in vitro* when PKR or RNaseL is functional
5. Immunoblot analysis of eIF α phosphorylation levels in WT or G50DbIKo virus infected NIH 3T12 fibroblasts
6. Generation and infection of 129S2/SvPas.IFN α / β R $^{-/-}$ chimeric mice.
7. KSHV isoform 1 and isoform 4 RTA show varying transactivation potential on viral promoters

A.



B.



C.

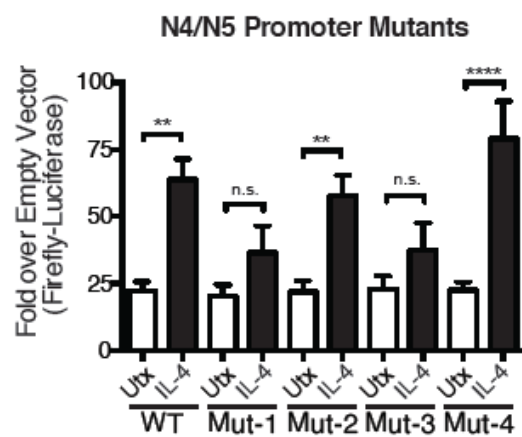
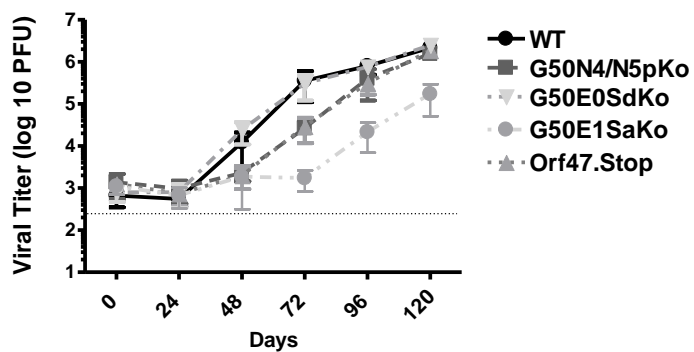


Figure 1

A.



B.

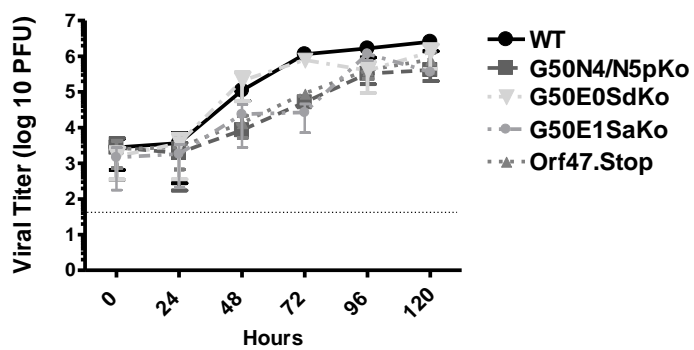


Figure 2

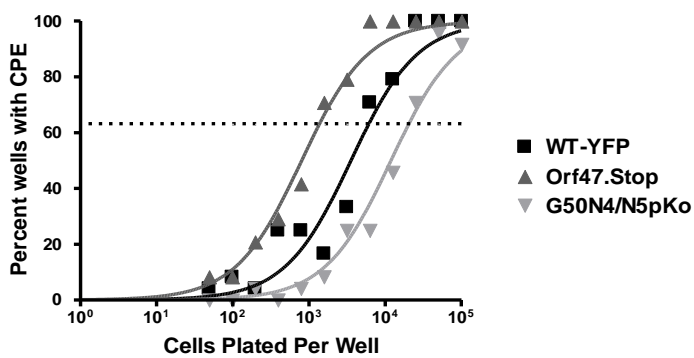


Figure 3

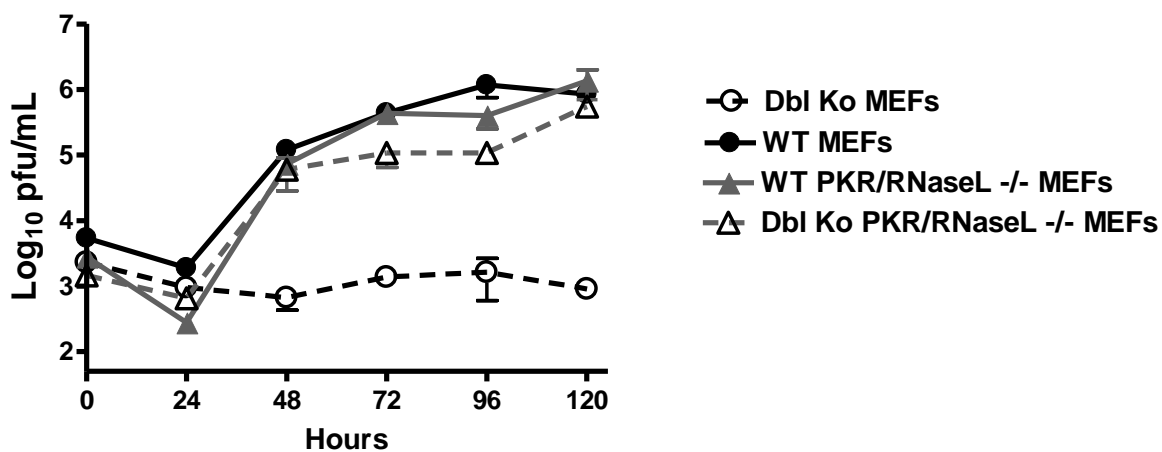


Figure 4

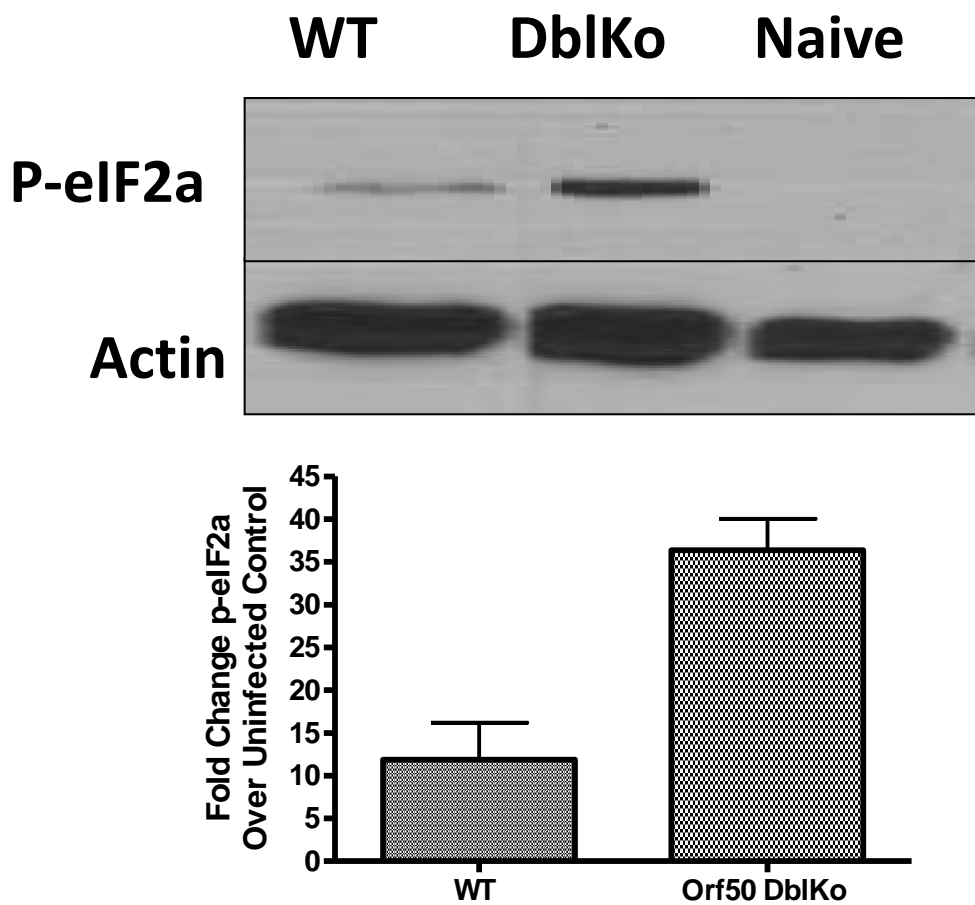


Figure 5

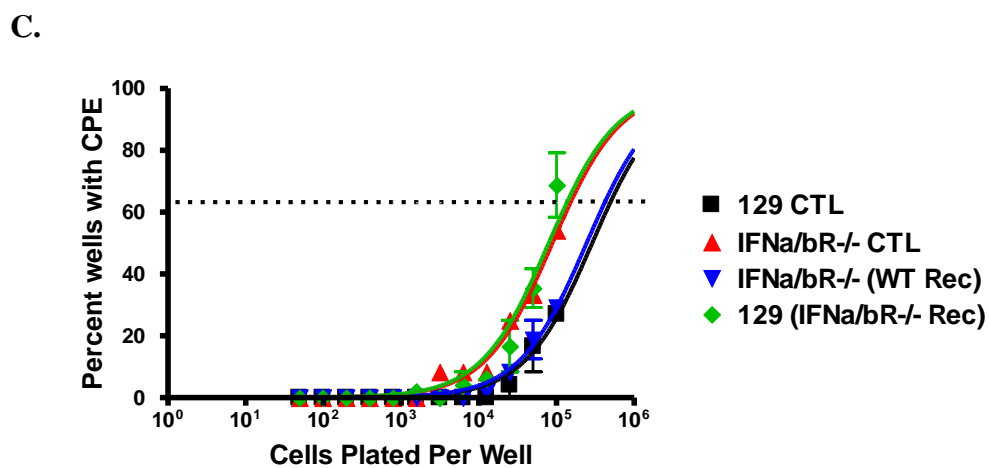
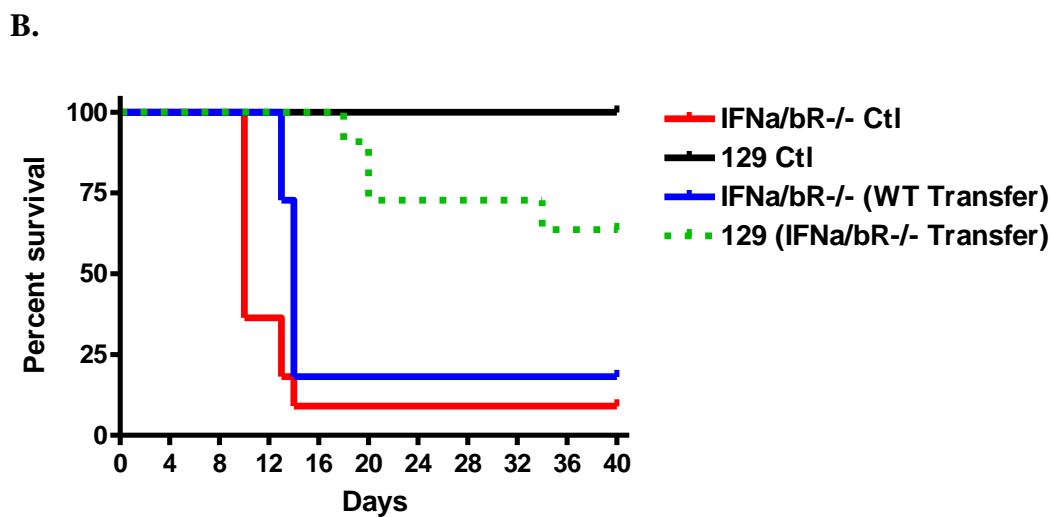
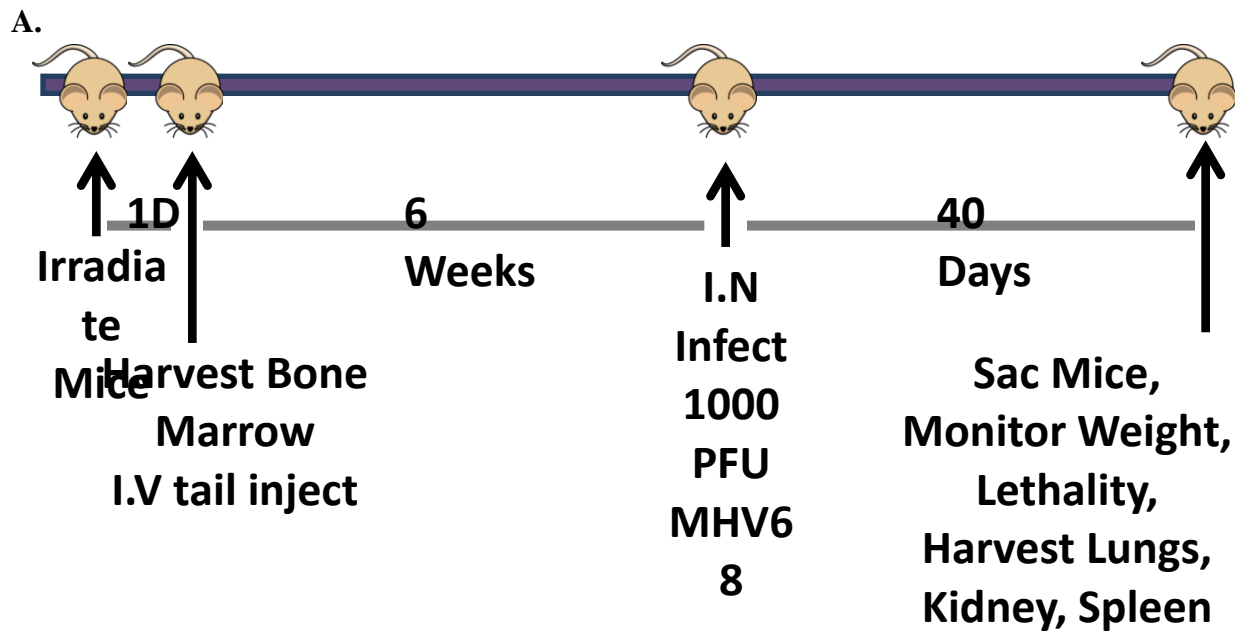


Figure 6

Orfs	K1	4	6	7	8	9	10	11	K2	2	70	K12	57	59	Pan	kbZIP
Isoform1	5	129	120	38	690	68	30	6	34	577	3	17	172	84	115	204
Isoform4	-6	1	13	-3	6	2	2	1	5	390	-4	32	68	61	124	28

Figure 7

LITERATURE CITED

1. **Ablashi, D. V., and G. R. Pearson.** 1974. Animal models: herpesvirus saimiri, a nonhuman primate model for herpesvirus-associated neoplasia of man. *Cancer research* **34**:1232-1236.
2. **Adler, H., M. Messerle, and U. H. Koszinowski.** 2001. Virus reconstituted from infectious bacterial artificial chromosome (BAC)-cloned murine gammaherpesvirus 68 acquires wild-type properties in vivo only after excision of BAC vector sequences. *J Virol* **75**:5692-5696.
3. **Ahmad, H., R. Gubbels, E. Ehlers, F. Meyer, T. Waterbury, R. Lin, and L. Zhang.** 2011. Kaposi sarcoma-associated herpesvirus degrades cellular Toll-interleukin-1 receptor domain-containing adaptor-inducing beta-interferon (TRIF). *J Biol Chem* **286**:7865-7872.
4. **Allen, R. D., M. N. DeZalia, and S. H. Speck.** 2007. Identification of an Rta responsive promoter involved in driving γ HV68 v-cyclin expression during virus replication. *Virology* **365**:250-259.
5. **Areste, C., M. Mutocheluh, and D. J. Blackbourn.** 2009. Identification of caspase-mediated decay of interferon regulatory factor-3, exploited by a Kaposi sarcoma-associated herpesvirus immunoregulatory protein. *J Biol Chem* **284**:23272-23285.
6. **Arico, E., K. A. Robertson, F. Belardelli, M. Ferrantini, and A. A. Nash.** 2004. Vaccination with inactivated murine gammaherpesvirus 68 strongly limits viral replication and latency and protects type I IFN receptor knockout mice from a lethal infection. *Vaccine* **22**:1433-1440.
7. **Arvanitakis, L., E. A. Mesri, R. G. Nador, J. W. Said, A. S. Asch, D. M. Knowles, and E. Cesarman.** 1996. Establishment and characterization of a primary effusion (body cavity-based) lymphoma cell line (BC-3) harboring kaposi's sarcoma-associated herpesvirus (KSHV/HHV-8) in the absence of Epstein-Barr virus. *Blood* **88**:2648-2654.
8. **Babcock, G. J., L. L. Decker, M. Volk, and D. A. Thorley-Lawson.** 1998. EBV persistence in memory B cells in vivo. *Immunity* **9**:395-404.
9. **Barton, E., P. Mandal, and S. H. Speck.** 2011. Pathogenesis and Host Control of Gammaherpesviruses: Lessons from the Mouse. *Annual Review of Immunology* **29**:351-397.
10. **Barton, E. S., M. L. Lutzke, R. Rochford, and H. W. t. Virgin.** 2005. Alpha/beta interferons regulate murine gammaherpesvirus latent gene expression and reactivation from latency. *J Virol* **79**:14149-14160.
11. **Barton, E. S., D. W. White, J. S. Cathelyn, K. A. Brett-McClellan, M. Engle, M. S. Diamond, V. L. Miller, and H. W. t. Virgin.** 2007. Herpesvirus latency confers symbiotic protection from bacterial infection. *Nature* **447**:326-329.
12. **Barton, G. M., J. C. Kagan, and R. Medzhitov.** 2006. Intracellular localization of Toll-like receptor 9 prevents recognition of self DNA but facilitates access to viral DNA. *Nature immunology* **7**:49-56.

13. **Bauer, S.** 2013. Toll-like receptor 9 processing: the key event in Toll-like receptor 9 activation? *Immunology letters* **149**:85-87.
14. **Bechtel, J. T., Y. Liang, J. Hvidding, and D. Ganem.** 2003. Host range of Kaposi's sarcoma-associated herpesvirus in cultured cells. *J Virol* **77**:6474-6481.
15. **Belanger, C., A. Gravel, A. Tomoiu, M. E. Janelle, J. Gosselin, M. J. Tremblay, and L. Flamand.** 2001. Human herpesvirus 8 viral FLICE-inhibitory protein inhibits Fas-mediated apoptosis through binding and prevention of procaspase-8 maturation. *Journal of human virology* **4**:62-73.
16. **Berry, M. P., C. M. Graham, F. W. McNab, Z. Xu, S. A. Bloch, T. Oni, K. A. Wilkinson, R. Banchereau, J. Skinner, R. J. Wilkinson, C. Quinn, D. Blankenship, R. Dhawan, J. J. Cush, A. Mejias, O. Ramilo, O. M. Kon, V. Pascual, J. Banchereau, D. Chaussabel, and A. O'Garra.** 2010. An interferon-inducible neutrophil-driven blood transcriptional signature in human tuberculosis. *Nature* **466**:973-977.
17. **Bisson, S. A., A. L. Page, and D. Ganem.** 2009. A Kaposi's sarcoma-associated herpesvirus protein that forms inhibitory complexes with type I interferon receptor subunits, Jak and STAT proteins, and blocks interferon-mediated signal transduction. *J Virol* **83**:5056-5066.
18. **Blasdel, K., C. McCracken, A. Morris, A. A. Nash, M. Begon, M. Bennett, and J. P. Stewart.** 2003. The wood mouse is a natural host for Murid herpesvirus 4. *The Journal of general virology* **84**:111-113.
19. **Blaskovic, D., M. Stancekova, J. Svobodova, and J. Mistrikova.** 1980. Isolation of 5 Strains of Herpesviruses from 2 Species of Free-Living Small Rodents. *Acta Virol* **24**:468-468.
20. **Bodescot, M., M. Perricaudet, and P. J. Farrell.** 1987. A promoter for the highly spliced EBNA family of RNAs of Epstein-Barr virus. *J Virol* **61**:3424-3430.
21. **Bohlius, J., M. Maskew, M. A. Davies, and M. Egger.** 2015. HHV-8 seroprevalence in HIV-positive and HIV-negative populations. *Int J Cancer* **136**:1243.
22. **Bortz, E., J. P. Whitelegge, Q. Jia, Z. H. Zhou, J. P. Stewart, T. T. Wu, and R. Sun.** 2003. Identification of proteins associated with murine gammaherpesvirus 68 virions. *J Virol* **77**:13425-13432.
23. **Breslin, M. B., C. D. Geng, and W. V. Vedeckis.** 2001. Multiple promoters exist in the human GR gene, one of which is activated by glucocorticoids. *Mol Endocrinol* **15**:1381-1395.
24. **Bruni, D., M. Chazal, L. Sinigaglia, L. Chauveau, O. Schwartz, P. Despres, and N. Jouvenet.** 2015. Viral entry route determines how human plasmacytoid dendritic cells produce type I interferons. *Science signaling* **8**:ra25.
25. **Byun, H., Y. Gwack, S. Hwang, and J. Choe.** 2002. Kaposi's sarcoma-associated herpesvirus open reading frame (ORF) 50 transactivates K8 and ORF57 promoters via heterogeneous response elements. *Molecules and cells* **14**:185-191.
26. **Cai, Q., K. Lan, S. C. Verma, H. Si, D. Lin, and E. S. Robertson.** 2006. Kaposi's sarcoma-associated herpesvirus latent protein LANA interacts with HIF-1 alpha to upregulate RTA expression during hypoxia: Latency control under low oxygen conditions. *J Virol* **80**:7965-7975.

27. **Callan, M. F., N. Steven, P. Krausa, J. D. Wilson, P. A. Moss, G. M. Gillespie, J. I. Bell, A. B. Rickinson, and A. J. McMichael.** 1996. Large clonal expansions of CD8+ T cells in acute infectious mononucleosis. *Nat Med* **2**:906-911.
28. **Carroll, K. D., F. Khadim, S. Spadavecchia, D. Palmeri, and D. M. Lukac.** 2007. Direct interactions of Kaposi's sarcoma-associated herpesvirus/human herpesvirus 8 ORF50/Rta protein with the cellular protein octamer-1 and DNA are critical for specifying transactivation of a delayed-early promoter and stimulating viral reactivation. *J Virol* **81**:8451-8467.
29. **Cavallin, L. E., P. Goldschmidt-Clermont, and E. A. Mesri.** 2014. Molecular and cellular mechanisms of KSHV oncogenesis of Kaposi's sarcoma associated with HIV/AIDS. *PLoS Pathog* **10**:e1004154.
30. **Cesarman, E.** 2011. Gammaherpesvirus and lymphoproliferative disorders in immunocompromised patients. *Cancer Lett* **305**:163-174.
31. **Cesarman, E., Y. Chang, P. S. Moore, J. W. Said, and D. M. Knowles.** 1995. Kaposi's sarcoma-associated herpesvirus-like DNA sequences in AIDS-related body-cavity-based lymphomas. *N Engl J Med* **332**:1186-1191.
32. **Chaganti, S., E. M. Heath, W. Bergler, M. Kuo, M. Buettner, G. Niedobitek, A. B. Rickinson, and A. I. Bell.** 2009. Epstein-Barr virus colonization of tonsillar and peripheral blood B-cell subsets in primary infection and persistence. *Blood* **113**:6372-6381.
33. **Chakrabarti, A., B. K. Jha, and R. H. Silverman.** 2011. New insights into the role of RNase L in innate immunity. *J Interferon Cytokine Res* **31**:49-57.
34. **Chang, P. J., and S. T. Liu.** 2001. Function of the intercistronic region of BRLF1-BZLF1 bicistronic mRNA in translating the zta protein of Epstein-Barr virus. *J Virol* **75**:1142-1151.
35. **Chang, P. J., D. Shedd, L. Gradoville, M. S. Cho, L. W. Chen, J. Chang, and G. Miller.** 2002. Open reading frame 50 protein of Kaposi's sarcoma-associated herpesvirus directly activates the viral PAN and K12 genes by binding to related response elements. *J Virol* **76**:3168-3178.
36. **Chang, Y., E. Cesarman, M. S. Pessin, F. Lee, J. Culpepper, D. M. Knowles, and P. S. Moore.** 1994. Identification of herpesvirus-like DNA sequences in AIDS-associated Kaposi's sarcoma. *Science* **266**:1865-1869.
37. **Chang, Y., H. H. Lee, S. S. Chang, T. Y. Hsu, P. W. Wang, Y. S. Chang, K. Takada, and C. H. Tsai.** 2004. Induction of Epstein-Barr virus latent membrane protein 1 by a lytic transactivator Rta. *J Virol* **78**:13028-13036.
38. **Chawla-Sarkar, M., D. J. Lindner, Y. F. Liu, B. R. Williams, G. C. Sen, R. H. Silverman, and E. C. Borden.** 2003. Apoptosis and interferons: role of interferon-stimulated genes as mediators of apoptosis. *Apoptosis : an international journal on programmed cell death* **8**:237-249.
39. **Chen, J., F. Ye, J. Xie, K. Kuhne, and S. J. Gao.** 2009. Genome-wide identification of binding sites for Kaposi's sarcoma-associated herpesvirus lytic switch protein, RTA. *Virology* **386**:290-302.
40. **Clemens, M. J.** 2003. Interferons and apoptosis. *J Interferon Cytokine Res* **23**:277-292.
41. **Coleman, C. B., M. S. Nealy, and S. A. Tibbetts.** 2010. Immature and transitional B cells are latency reservoirs for a gammaherpesvirus. *J Virol* **84**:13045-13052.

42. **Collins, C. M., J. M. Boss, and S. H. Speck.** 2009. Identification of infected B-cell populations by using a recombinant murine gammaherpesvirus 68 expressing a fluorescent protein. *J Virol* **83**:6484-6493.
43. **Colonna, M., B. Pulendran, and A. Iwasaki.** 2006. Dendritic cells at the host-pathogen interface. *Nature immunology* **7**:117-120.
44. **Coscoy, L., and D. Ganem.** 2000. Kaposi's sarcoma-associated herpesvirus encodes two proteins that block cell surface display of MHC class I chains by enhancing their endocytosis. *Proc Natl Acad Sci U S A* **97**:8051-8056.
45. **Cox, M. A., J. Leahy, and J. M. Hardwick.** 1990. An enhancer within the divergent promoter of Epstein-Barr virus responds synergistically to the R and Z transactivators. *J Virol* **64**:313-321.
46. **D'Antonio, A., A. Boscaino, M. Adesso, M. A. Piris, and O. Nappi.** 2007. KSHV- and EBV-associated germinotropic lymphoproliferative disorder: a rare lymphoproliferative disease of HIV patient with plasmablastic morphology, indolent course and favourable response to therapy. *Leuk Lymphoma* **48**:1444-1447.
47. **da Silva, S. R., and D. E. de Oliveira.** 2011. HIV, EBV and KSHV: viral cooperation in the pathogenesis of human malignancies. *Cancer Lett* **305**:175-185.
48. **Dalton-Griffin, L., S. J. Wilson, and P. Kellam.** 2009. X-box binding protein 1 contributes to induction of the Kaposi's sarcoma-associated herpesvirus lytic cycle under hypoxic conditions. *J Virol* **83**:7202-7209.
49. **Darnell, J. E., Jr.** 2007. Interferon research: impact on understanding transcriptional control. *Curr Top Microbiol Immunol* **316**:155-163.
50. **Darnell, J. E., Jr., I. M. Kerr, and G. R. Stark.** 1994. Jak-STAT pathways and transcriptional activation in response to IFNs and other extracellular signaling proteins. *Science* **264**:1415-1421.
51. **Davis, K. L., M. Korom, and L. A. Morrison.** 2014. Herpes simplex virus 2 ICP34.5 confers neurovirulence by regulating the type I interferon response. *Virology* **468-470**:330-339.
52. **Delaloy, C., J. Lu, A. M. Houot, S. Disse-Nicodeme, J. M. Gasc, P. Corvol, and X. Jeunemaitre.** 2003. Multiple promoters in the WNK1 gene: one controls expression of a kidney-specific kinase-defective isoform. *Mol Cell Biol* **23**:9208-9221.
53. **Deng, H., J. T. Chu, M. B. Rettig, O. Martinez-Maza, and R. Sun.** 2002. Rta of the human herpesvirus 8/Kaposi sarcoma-associated herpesvirus up-regulates human interleukin-6 gene expression. *Blood* **100**:1919-1921.
54. **Deng, H., Y. Liang, and R. Sun.** 2007. Regulation of KSHV lytic gene expression. *Curr Top Microbiol Immunol* **312**:157-183.
55. **Deng, H., A. Young, and R. Sun.** 2000. Auto-activation of the rta gene of human herpesvirus-8/Kaposi's sarcoma-associated herpesvirus. *The Journal of general virology* **81**:3043-3048.
56. **Der, S. D., A. Zhou, B. R. Williams, and R. H. Silverman.** 1998. Identification of genes differentially regulated by interferon alpha, beta, or gamma using oligonucleotide arrays. *Proc Natl Acad Sci U S A* **95**:15623-15628.
57. **Diebold, S. S.** 2008. Recognition of viral single-stranded RNA by Toll-like receptors. *Advanced drug delivery reviews* **60**:813-823.

58. **Dong, X., Z. He, D. Durakogluligil, L. Arneson, Y. Shen, and P. Feng.** 2012. Murine gammaherpesvirus 68 evades host cytokine production via replication transactivator-induced RelA degradation. *J Virol* **86**:1930-1941.
59. **Dutia, B. M., D. J. Allen, H. Dyson, and A. A. Nash.** 1999. Type I interferons and IRF-1 play a critical role in the control of a gammaherpesvirus infection. *Virology* **261**:173-179.
60. **El-Guindy, A., M. Ghiassi-Nejad, S. Golden, H. J. Delecluse, and G. Miller.** 2013. Essential role of Rta in lytic DNA replication of Epstein-Barr virus. *J Virol* **87**:208-223.
61. **Eliopoulos, A. G., C. W. Dawson, G. Mosialos, J. E. Floettmann, M. Rowe, R. J. Armitage, J. Dawson, J. M. Zapata, D. J. Kerr, M. J. Wakelam, J. C. Reed, E. Kieff, and L. S. Young.** 1996. CD40-induced growth inhibition in epithelial cells is mimicked by Epstein-Barr Virus-encoded LMP1: involvement of TRAF3 as a common mediator. *Oncogene* **13**:2243-2254.
62. **Ellison, T. J., Y. Izumiya, C. Izumiya, P. A. Luciw, and H. J. Kung.** 2009. A comprehensive analysis of recruitment and transactivation potential of K-Rta and K-bZIP during reactivation of Kaposi's sarcoma-associated herpesvirus. *Virology* **387**:76-88.
63. **Epstein, M. A., B. G. Achong, and Y. M. Barr.** 1964. Virus Particles in Cultured Lymphoblasts from Burkitt's Lymphoma. *Lancet* **1**:702-703.
64. **Evans, A. G., J. M. Moser, L. T. Krug, V. Pozharskaya, A. L. Mora, and S. H. Speck.** 2008. A gammaherpesvirus-secreted activator of Vbeta4+ CD8+ T cells regulates chronic infection and immunopathology. *The Journal of experimental medicine* **205**:669-684.
65. **Farrell, P. J.** 1998. Signal transduction from the Epstein-Barr virus LMP-1 transforming protein. *Trends in microbiology* **6**:175-177; discussion 177-178.
66. **Ficova, M., T. Betakova, P. Pancik, R. Vaclav, P. Prokop, Z. Halasova, and M. Kudelova.** 2011. Molecular detection of murine herpesvirus 68 in ticks feeding on free-living reptiles. *Microbial ecology* **62**:862-867.
67. **Flemington, E., and S. H. Speck.** 1990. Identification of phorbol ester response elements in the promoter of Epstein-Barr virus putative lytic switch gene BZLF1. *J Virol* **64**:1217-1226.
68. **Fowler, P., S. Marques, J. P. Simas, and S. Efstathiou.** 2003. ORF73 of murine herpesvirus-68 is critical for the establishment and maintenance of latency. *The Journal of general virology* **84**:3405-3416.
69. **Francois, S., S. Vidick, M. Sarlet, D. Desmecht, P. Drion, P. G. Stevenson, A. Vanderplasschen, and L. Gillet.** 2013. Illumination of murine gammaherpesvirus-68 cycle reveals a sexual transmission route from females to males in laboratory mice. *PLoS Pathog* **9**:e1003292.
70. **Friborg, J., Jr., W. Kong, M. O. Hottiger, and G. J. Nabel.** 1999. p53 inhibition by the LANA protein of KSHV protects against cell death. *Nature* **402**:889-894.
71. **Fuld, S., C. Cunningham, K. Klucher, A. J. Davison, and D. J. Blackbourn.** 2006. Inhibition of interferon signaling by the Kaposi's sarcoma-associated herpesvirus full-length viral interferon regulatory factor 2 protein. *J Virol* **80**:3092-3097.
72. **Gao, S. J., C. Boshoff, S. Jayachandra, R. A. Weiss, Y. Chang, and P. S. Moore.** 1997. KSHV ORF K9 (vIRF) is an oncogene which inhibits the interferon signaling pathway. *Oncogene* **15**:1979-1985.

73. **Gargano, L. M., J. C. Forrest, and S. H. Speck.** 2009. Signaling through Toll-like receptors induces murine gammaherpesvirus 68 reactivation in vivo. *J Virol* **83**:1474-1482.
74. **Geiger, T. R., and J. M. Martin.** 2006. The Epstein-Barr virus-encoded LMP-1 oncoprotein negatively affects Tyk2 phosphorylation and interferon signaling in human B cells. *J Virol* **80**:11638-11650.
75. **Gill, M. B., L. Gillet, S. Colaco, J. S. May, B. D. de Lima, and P. G. Stevenson.** 2006. Murine gammaherpesvirus-68 glycoprotein H-glycoprotein L complex is a major target for neutralizing monoclonal antibodies. *The Journal of general virology* **87**:1465-1475.
76. **Gill, N., M. J. Chenoweth, E. F. Verdu, and A. A. Ashkar.** 2011. NK cells require type I IFN receptor for antiviral responses during genital HSV-2 infection. *Cellular immunology* **269**:29-37.
77. **Gillet, L., M. Alenquer, D. L. Glauser, S. Colaco, J. S. May, and P. G. Stevenson.** 2009. Glycoprotein L sets the neutralization profile of murine herpesvirus 4. *The Journal of general virology* **90**:1202-1214.
78. **Gillet, L., J. S. May, S. Colaco, and P. G. Stevenson.** 2007. Glycoprotein L disruption reveals two functional forms of the murine gammaherpesvirus 68 glycoprotein H. *J Virol* **81**:280-291.
79. **Goodwin, M. M., S. Canny, A. Steed, and H. W. Virgin.** 2010. Murine gammaherpesvirus 68 has evolved gamma interferon and stat1-repressible promoters for the lytic switch gene 50. *J Virol* **84**:3711-3717.
80. **Gradoville, L., J. Gerlach, E. Grogan, D. Shedd, S. Nikiforow, C. Metroka, and G. Miller.** 2000. Kaposi's sarcoma-associated herpesvirus open reading frame 50/Rta protein activates the entire viral lytic cycle in the HH-B2 primary effusion lymphoma cell line. *J Virol* **74**:6207-6212.
81. **Gray, K. S., R. D. Allen, M. L. Farrell, J. C. Forrest, and S. H. Speck.** 2008. Alternatively Initiated Gene 50/RTA Transcripts Expressed during Murine and Human Gammaherpesvirus Reactivation from Latency. *Journal of Virology* **83**:314-328.
82. **Gray, K. S., C. M. Collins, and S. H. Speck.** 2012. Characterization of omental immune aggregates during establishment of a latent gammaherpesvirus infection. *PLoS One* **7**:e43196.
83. **Gray, K. S., J. C. Forrest, and S. H. Speck.** 2010. The de novo methyltransferases DNMT3a and DNMT3b target the murine gammaherpesvirus immediate-early gene 50 promoter during establishment of latency. *J Virol* **84**:4946-4959.
84. **Gredmark, S., C. Schlieker, V. Quesada, E. Spooner, and H. L. Ploegh.** 2007. A functional ubiquitin-specific protease embedded in the large tegument protein (ORF64) of murine gammaherpesvirus 68 is active during the course of infection. *J Virol* **81**:10300-10309.
85. **Große, C.** 2012. Pangaea and the Out-of-Africa Model of Varicella-Zoster Virus Evolution and Phylogeography. *J Virol* **86**:9558-9565.
86. **Gruffat, H., and A. Sergeant.** 1994. Characterization of the DNA-binding site repertoire for the Epstein-Barr virus transcription factor R. *Nucleic Acids Res* **22**:1172-1178.
87. **Guito, J., and D. M. Lukac.** 2012. KSHV Rta Promoter Specification and Viral Reactivation. *Frontiers in microbiology* **3**:30.

88. **Gwack, Y., H. Byun, S. Hwang, C. Lim, and J. Choe.** 2001. CREB-binding protein and histone deacetylase regulate the transcriptional activity of Kaposi's sarcoma-associated herpesvirus open reading frame 50. *J Virol* **75**:1909-1917.
89. **Hair, J. R., P. A. Lyons, K. G. Smith, and S. Efstathiou.** 2007. Control of Rta expression critically determines transcription of viral and cellular genes following gammaherpesvirus infection. *The Journal of general virology* **88**:1689-1697.
90. **Haque, M., D. A. Davis, V. Wang, I. Widmer, and R. Yarchoan.** 2003. Kaposi's sarcoma-associated herpesvirus (human herpesvirus 8) contains hypoxia response elements: relevance to lytic induction by hypoxia. *J Virol* **77**:6761-6768.
91. **Hardwick, J. M., P. M. Lieberman, and S. D. Hayward.** 1988. A new Epstein-Barr virus transactivator, R, induces expression of a cytoplasmic early antigen. *J Virol* **62**:2274-2284.
92. **Hearing, J., Y. Mulhaupt, and S. Harper.** 1992. Interaction of Epstein-Barr virus nuclear antigen 1 with the viral latent origin of replication. *J Virol* **66**:694-705.
93. **Henle, G., W. Henle, and V. Diehl.** 1968. Relation of Burkitt's tumor-associated herpes-type virus to infectious mononucleosis. *Proc Natl Acad Sci U S A* **59**:94-101.
94. **Henle, W., V. Diehl, G. Kohn, H. Zur Hausen, and G. Henle.** 1967. Herpes-type virus and chromosome marker in normal leukocytes after growth with irradiated Burkitt cells. *Science* **157**:1064-1065.
95. **Herskowitz, J. H., A. M. Siegel, M. A. Jacoby, and S. H. Speck.** 2008. Systematic mutagenesis of the murine gammaherpesvirus 68 M2 protein identifies domains important for chronic infection. *J Virol* **82**:3295-3310.
96. **Hochberg, D., T. Souza, M. Catalina, J. L. Sullivan, K. Luzuriaga, and D. A. Thorley-Lawson.** 2004. Acute infection with Epstein-Barr virus targets and overwhelms the peripheral memory B-cell compartment with resting, latently infected cells. *J Virol* **78**:5194-5204.
97. **Hofelmayr, H., L. J. Strobl, G. Marschall, G. W. Bornkamm, and U. Zimmer-Strobl.** 2001. Activated Notch1 can transiently substitute for EBNA2 in the maintenance of proliferation of LMP1-expressing immortalized B cells. *J Virol* **75**:2033-2040.
98. **Hoge, A. T., S. B. Hendrickson, and W. H. Burns.** 2000. Murine gammaherpesvirus 68 cyclin D homologue is required for efficient reactivation from latency. *J Virol* **74**:7016-7023.
99. **Holley-Guthrie, E. A., E. B. Quinlivan, E. C. Mar, and S. Kenney.** 1990. The Epstein-Barr virus (EBV) BMRF1 promoter for early antigen (EA-D) is regulated by the EBV transactivators, BRLF1 and BZLF1, in a cell-specific manner. *J Virol* **64**:3753-3759.
100. **Hong, Y., J. Qi, D. Gong, C. Han, and H. Deng.** 2011. Replication and transcription activator (RTA) of murine gammaherpesvirus 68 binds to an RTA-responsive element and activates the expression of ORF18. *J Virol* **85**:11338-11350.
101. **Horenstein, M. G., R. G. Nador, A. Chadburn, E. M. Hyjek, G. Inghirami, D. M. Knowles, and E. Cesarman.** 1997. Epstein-Barr virus latent gene expression in primary effusion lymphomas containing Kaposi's sarcoma-associated herpesvirus/human herpesvirus-8. *Blood* **90**:1186-1191.

102. **Hsu, D. H., R. de Waal Malefyt, D. F. Fiorentino, M. N. Dang, P. Vieira, J. de Vries, H. Spits, T. R. Mosmann, and K. W. Moore.** 1990. Expression of interleukin-10 activity by Epstein-Barr virus protein BCRF1. *Science* **250**:830-832.
103. **Hughes, D. J., A. Kipar, S. G. Milligan, C. Cunningham, M. Sanders, M. A. Quail, M. A. Rajandream, S. Efstathiou, R. J. Bowden, C. Chastel, M. Bennett, J. T. Sample, B. Barrell, A. J. Davison, and J. P. Stewart.** 2010. Characterization of a novel wood mouse virus related to murid herpesvirus 4. *The Journal of general virology* **91**:867-879.
104. **Hurley, E. A., and D. A. Thorley-Lawson.** 1988. B cell activation and the establishment of Epstein-Barr virus latency. *The Journal of experimental medicine* **168**:2059-2075.
105. **Hwang, S., K. S. Kim, E. Flano, T. T. Wu, L. M. Tong, A. N. Park, M. J. Song, D. J. Sanchez, R. M. O'Connell, G. Cheng, and R. Sun.** 2009. Conserved herpesviral kinase promotes viral persistence by inhibiting the IRF-3-mediated type I interferon response. *Cell host & microbe* **5**:166-178.
106. **Hwang, S., T. T. Wu, L. M. Tong, K. S. Kim, D. Martinez-Guzman, A. D. Colantonio, C. H. Uittenbogaart, and R. Sun.** 2008. Persistent gammaherpesvirus replication and dynamic interaction with the host in vivo. *J Virol* **82**:12498-12509.
107. **Inn, K. S., S. H. Lee, J. Y. Rathbun, L. Y. Wong, Z. Toth, K. Machida, J. H. Ou, and J. U. Jung.** 2011. Inhibition of RIG-I-mediated signaling by Kaposi's sarcoma-associated herpesvirus-encoded deubiquitinase ORF64. *J Virol* **85**:10899-10904.
108. **Ivashkiv, L. B., and L. T. Donlin.** 2014. Regulation of type I interferon responses. *Nature reviews. Immunology* **14**:36-49.
109. **Izumiya, Y., S. F. Lin, T. Ellison, L. Y. Chen, C. Izumiya, P. Luciw, and H. J. Kung.** 2003. Kaposi's sarcoma-associated herpesvirus K-bZIP is a coregulator of K-Rta: physical association and promoter-dependent transcriptional repression. *J Virol* **77**:1441-1451.
110. **Jacoby, M. A., H. W. t. Virgin, and S. H. Speck.** 2002. Disruption of the M2 gene of murine gammaherpesvirus 68 alters splenic latency following intranasal, but not intraperitoneal, inoculation. *J Virol* **76**:1790-1801.
111. **Jennings, R. N., J. M. Grayson, and E. S. Barton.** 2014. Type I interferon signaling enhances CD8+ T cell effector function and differentiation during murine gammaherpesvirus 68 infection. *J Virol* **88**:14040-14049.
112. **Jiang, J. H., N. Wang, A. Li, W. T. Liao, Z. G. Pan, S. J. Mai, D. J. Li, M. S. Zeng, J. M. Wen, and Y. X. Zeng.** 2006. Hypoxia can contribute to the induction of the Epstein-Barr virus (EBV) lytic cycle. *J Clin Virol* **37**:98-103.
113. **Jones, T., S. Ramos da Silva, R. Bedolla, F. Ye, F. Zhou, and S. J. Gao.** 2014. Viral cyclin promotes KSHV-induced cellular transformation and tumorigenesis by overriding contact inhibition. *Cell cycle* **13**:845-858.
114. **Joo, C. H., Y. C. Shin, M. Gack, L. Wu, D. Levy, and J. U. Jung.** 2007. Inhibition of interferon regulatory factor 7 (IRF7)-mediated interferon signal transduction by the Kaposi's sarcoma-associated herpesvirus viral IRF homolog vIRF3. *J Virol* **81**:8282-8292.
115. **Kapatai, G., and P. Murray.** 2007. Contribution of the Epstein Barr virus to the molecular pathogenesis of Hodgkin lymphoma. *J Clin Pathol* **60**:1342-1349.
116. **Karamanou, M., C. Antoniou, A. J. Stratigos, Z. Saridaki, and G. Androutsos.** 2013. The eminent dermatologist Moriz Kaposi (1837-1902) and the first description of idiopathic

- multiple pigmented sarcoma of the skin. *Journal of B.U.ON. : official journal of the Balkan Union of Oncology* **18**:1101-1105.
117. **Katano, H., Y. Sato, and T. Sata.** 2001. Expression of p53 and human herpesvirus-8 (HHV-8)-encoded latency-associated nuclear antigen with inhibition of apoptosis in HHV-8-associated malignancies. *Cancer* **92**:3076-3084.
 118. **Katze, M. G.** 1995. Regulation of the interferon-induced PKR: can viruses cope? *Trends in microbiology* **3**:75-78.
 119. **Kaufer, B. B., and L. Flamand.** 2014. Chromosomally integrated HHV-6: impact on virus, cell and organismal biology. *Current opinion in virology* **9**:111-118.
 120. **Kedes, D. H., E. Operskalski, M. Busch, R. Kohn, J. Flood, and D. Ganem.** 1996. The seroepidemiology of human herpesvirus 8 (Kaposi's sarcoma-associated herpesvirus): distribution of infection in KS risk groups and evidence for sexual transmission. *Nat Med* **2**:918-924.
 121. **Kelly, G. L., A. E. Milner, G. S. Baldwin, A. I. Bell, and A. B. Rickinson.** 2006. Three restricted forms of Epstein-Barr virus latency counteracting apoptosis in c-myc-expressing Burkitt lymphoma cells. *Proc Natl Acad Sci U S A* **103**:14935-14940.
 122. **Kenney, S., E. Holley-Guthrie, E. C. Mar, and M. Smith.** 1989. The Epstein-Barr virus BMLF1 promoter contains an enhancer element that is responsive to the BZLF1 and BRLF1 transactivators. *J Virol* **63**:3878-3883.
 123. **Kenney, S., J. Kamine, E. Holley-Guthrie, J. C. Lin, E. C. Mar, and J. Pagano.** 1989. The Epstein-Barr virus (EBV) BZLF1 immediate-early gene product differentially affects latent versus productive EBV promoters. *J Virol* **63**:1729-1736.
 124. **Kim, J. D., C. H. Kim, and B. S. Kwon.** 2011. Regulation of mouse 4-1BB expression: multiple promoter usages and a splice variant. *Molecules and cells* **31**:141-149.
 125. **Klein, E., N. Teramoto, P. Gogolak, N. Nagy, and M. Bjorkholm.** 1999. LMP-1, the Epstein-Barr virus-encoded oncogene with a B cell activating mechanism similar to CD40. *Immunology letters* **68**:147-154.
 126. **Koenigsberger, C., J. J. Chicca, 2nd, M. C. Amoureux, G. M. Edelman, and F. S. Jones.** 2000. Differential regulation by multiple promoters of the gene encoding the neuron-restrictive silencer factor. *Proc Natl Acad Sci U S A* **97**:2291-2296.
 127. **Kristiansen, H., H. H. Gad, S. Eskildsen-Larsen, P. Despres, and R. Hartmann.** 2011. The oligoadenylate synthetase family: an ancient protein family with multiple antiviral activities. *J Interferon Cytokine Res* **31**:41-47.
 128. **Krug, L. T., C. M. Collins, L. M. Gargano, and S. H. Speck.** 2009. NF-kappaB p50 plays distinct roles in the establishment and control of murine gammaherpesvirus 68 latency. *J Virol* **83**:4732-4748.
 129. **Krug, L. T., A. G. Evans, L. M. Gargano, C. R. Paden, and S. H. Speck.** 2013. The absence of M1 leads to increased establishment of murine gammaherpesvirus 68 latency in IgD-negative B cells. *J Virol* **87**:3597-3604.
 130. **Kuhn, K., A. Weihe, and T. Borner.** 2005. Multiple promoters are a common feature of mitochondrial genes in Arabidopsis. *Nucleic Acids Res* **33**:337-346.
 131. **Kulkarni, A. B., K. L. Holmes, T. N. Fredrickson, J. W. Hartley, and H. C. Morse, 3rd.** 1997. Characteristics of a murine gammaherpesvirus infection immunocompromised mice. *In Vivo* **11**:281-291.

132. **Leang, R. S., T. T. Wu, S. Hwang, L. T. Liang, L. Tong, J. T. Truong, and R. Sun.** 2011. The anti-interferon activity of conserved viral dUTPase ORF54 is essential for an effective MHV-68 infection. *PLoS Pathog* **7**:e1002292.
133. **Lee, H., J. Guo, M. Li, J. K. Choi, M. DeMaria, M. Rosenzweig, and J. U. Jung.** 1998. Identification of an immunoreceptor tyrosine-based activation motif of K1 transforming protein of Kaposi's sarcoma-associated herpesvirus. *Mol Cell Biol* **18**:5219-5228.
134. **Lee, H., R. Veazey, K. Williams, M. Li, J. Guo, F. Neipel, B. Fleckenstein, A. Lackner, R. C. Desrosiers, and J. U. Jung.** 1998. Deregulation of cell growth by the K1 gene of Kaposi's sarcoma-associated herpesvirus. *Nat Med* **4**:435-440.
135. **Lee, H. R., M. H. Kim, J. S. Lee, C. Liang, and J. U. Jung.** 2009. Viral interferon regulatory factors. *J Interferon Cytokine Res* **29**:621-627.
136. **Lee, M. A., M. E. Diamond, and J. L. Yates.** 1999. Genetic evidence that EBNA-1 is needed for efficient, stable latent infection by Epstein-Barr virus. *J Virol* **73**:2974-2982.
137. **Lee, S., H. J. Cho, J. J. Park, Y. S. Kim, S. Hwang, R. Sun, and M. J. Song.** 2007. The ORF49 protein of murine gammaherpesvirus 68 cooperates with RTA in regulating virus replication. *J Virol* **81**:9870-9877.
138. **Lefort, S., A. Soucy-Faulkner, N. Grandvaux, and L. Flamand.** 2007. Binding of Kaposi's sarcoma-associated herpesvirus K-bZIP to interferon-responsive factor 3 elements modulates antiviral gene expression. *J Virol* **81**:10950-10960.
139. **Lennette, E. T., D. J. Blackbourn, and J. A. Levy.** 1996. Antibodies to human herpesvirus type 8 in the general population and in Kaposi's sarcoma patients. *Lancet* **348**:858-861.
140. **Li, H., T. Komatsu, B. J. Dezube, and K. M. Kaye.** 2002. The Kaposi's sarcoma-associated herpesvirus K12 transcript from a primary effusion lymphoma contains complex repeat elements, is spliced, and initiates from a novel promoter. *J Virol* **76**:11880-11888.
141. **Li, Q., M. He, F. Zhou, F. Ye, and S. J. Gao.** 2014. Activation of Kaposi's sarcoma-associated herpesvirus (KSHV) by inhibitors of class III histone deacetylases: identification of sirtuin 1 as a regulator of the KSHV life cycle. *J Virol* **88**:6355-6367.
142. **Li, X., J. Feng, S. Chen, L. Peng, W. W. He, J. Qi, H. Deng, and R. Sun.** 2010. Tpl2/AP-1 enhances murine gammaherpesvirus 68 lytic replication. *J Virol* **84**:1881-1890.
143. **Liang, Q., B. Fu, F. Wu, X. Li, Y. Yuan, and F. Zhu.** 2012. ORF45 of Kaposi's sarcoma-associated herpesvirus inhibits phosphorylation of interferon regulatory factor 7 by IKKepsilon and TBK1 as an alternative substrate. *J Virol* **86**:10162-10172.
144. **Liang, X., C. M. Collins, J. B. Mendel, N. N. Iwakoshi, and S. H. Speck.** 2009. Gammaherpesvirus-driven plasma cell differentiation regulates virus reactivation from latently infected B lymphocytes. *PLoS Pathog* **5**:e1000677.
145. **Liang, X., R. L. Crepeau, W. Zhang, S. H. Speck, and E. J. Usherwood.** 2013. CD4 and CD8 T cells directly recognize murine gammaherpesvirus 68-immortalized cells and prevent tumor outgrowth. *J Virol* **87**:6051-6054.
146. **Liang, X., C. R. Paden, F. M. Morales, R. P. Powers, J. Jacob, and S. H. Speck.** 2011. Murine gamma-herpesvirus immortalization of fetal liver-derived B cells requires both the viral cyclin D homolog and latency-associated nuclear antigen. *PLoS Pathog* **7**:e1002220.

147. **Liang, X., Y. C. Shin, R. E. Means, and J. U. Jung.** 2004. Inhibition of interferon-mediated antiviral activity by murine gammaherpesvirus 68 latency-associated M2 protein. *J Virol* **78**:12416-12427.
148. **Lin, R., P. Genin, Y. Mamane, M. Sgarbanti, A. Battistini, W. J. Harrington, Jr., G. N. Barber, and J. Hiscott.** 2001. HHV-8 encoded vIRF-1 represses the interferon antiviral response by blocking IRF-3 recruitment of the CBP/p300 coactivators. *Oncogene* **20**:800-811.
149. **Liu, S., I. V. Pavlova, H. W. t. Virgin, and S. H. Speck.** 2000. Characterization of gammaherpesvirus 68 gene 50 transcription. *J Virol* **74**:2029-2037.
150. **Liu, Y., Y. Cao, D. Liang, Y. Gao, T. Xia, E. S. Robertson, and K. Lan.** 2008. Kaposi's sarcoma-associated herpesvirus RTA activates the processivity factor ORF59 through interaction with RBP-Jkappa and a cis-acting RTA responsive element. *Virology* **380**:264-275.
151. **Lomonte, P., P. Filee, J. R. Lyaku, M. Bublot, P. P. Pastoret, and E. Thiry.** 1997. Analysis of the biochemical properties of, and complex formation between, glycoproteins H and L of the gamma2 herpesvirus bovine herpesvirus-4. *The Journal of general virology* **78 (Pt 8)**:2015-2023.
152. **Lukac, D. M., R. Renne, J. R. Kirshner, and D. Ganem.** 1998. Reactivation of Kaposi's sarcoma-associated herpesvirus infection from latency by expression of the ORF 50 transactivator, a homolog of the EBV R protein. *Virology* **252**:304-312.
153. **Mack, E. A., L. E. Kallal, D. A. Demers, and C. A. Biron.** 2011. Type 1 interferon induction of natural killer cell gamma interferon production for defense during lymphocytic choriomeningitis virus infection. *mBio* **2**.
154. **Malik, P., D. J. Blackbourn, M. F. Cheng, G. S. Hayward, and J. B. Clements.** 2004. Functional co-operation between the Kaposi's sarcoma-associated herpesvirus ORF57 and ORF50 regulatory proteins. *The Journal of general virology* **85**:2155-2166.
155. **Mandal, P., B. E. Krueger, D. Oldenburg, K. A. Andry, R. S. Beard, D. W. White, and E. S. Barton.** 2011. A gammaherpesvirus cooperates with interferon-alpha/beta-induced IRF2 to halt viral replication, control reactivation, and minimize host lethality. *PLoS Pathog* **7**:e1002371.
156. **Matar, C. G., U. S. Rangaswamy, B. S. Wakeman, N. Iwakoshi, and S. H. Speck.** 2014. Murine gammaherpesvirus 68 reactivation from B cells requires IRF4 but not XBP-1. *J Virol* **88**:11600-11610.
157. **Matsumura, S., Y. Fujita, E. Gomez, N. Tanese, and A. C. Wilson.** 2005. Activation of the Kaposi's sarcoma-associated herpesvirus major latency locus by the lytic switch protein RTA (ORF50). *J Virol* **79**:8493-8505.
158. **McCormick, C., and D. Ganem.** 2005. The kaposin B protein of KSHV activates the p38/MK2 pathway and stabilizes cytokine mRNAs. *Science* **307**:739-741.
159. **McNab, F. W., J. Ewbank, R. Rajsbaum, E. Stavropoulos, A. Martirosyan, P. S. Redford, X. Wu, C. M. Graham, M. Saraiva, P. Tschlis, D. Chaussabel, S. C. Ley, and A. O'Garra.** 2013. TPL-2-ERK1/2 signaling promotes host resistance against intracellular bacterial infection by negative regulation of type I IFN production. *J Immunol* **191**:1732-1743.

160. **Milho, R., C. M. Smith, S. Marques, M. Alenquer, J. S. May, L. Gillet, M. Gaspar, S. Efstathiou, J. P. Simas, and P. G. Stevenson.** 2009. In vivo imaging of murid herpesvirus-4 infection. *The Journal of general virology* **90**:21-32.
161. **Mitsui, S., T. Nakamura, A. Okui, K. Kominami, H. Uemura, and N. Yamaguchi.** 2006. Multiple promoters regulate tissue-specific alternative splicing of the human kallikrein gene, KLK11/hippostasin. *The FEBS journal* **273**:3678-3686.
162. **Miyashita, E. M., B. Yang, K. M. Lam, D. H. Crawford, and D. A. Thorley-Lawson.** 1995. A novel form of Epstein-Barr virus latency in normal B cells in vivo. *Cell* **80**:593-601.
163. **Moghaddam, A., M. Rosenzweig, D. Lee-Parritz, B. Annis, R. P. Johnson, and F. Wang.** 1997. An animal model for acute and persistent Epstein-Barr virus infection. *Science* **276**:2030-2033.
164. **Moore, P. S., C. Boshoff, R. A. Weiss, and Y. Chang.** 1996. Molecular mimicry of human cytokine and cytokine response pathway genes by KSHV. *Science* **274**:1739-1744.
165. **Moore, P. S., and Y. Chang.** 1995. Detection of herpesvirus-like DNA sequences in Kaposi's sarcoma in patients with and without HIV infection. *N Engl J Med* **332**:1181-1185.
166. **Moorman, N. J., C. Y. Lin, and S. H. Speck.** 2004. Identification of candidate gammaherpesvirus 68 genes required for virus replication by signature-tagged transposon mutagenesis. *J Virol* **78**:10282-10290.
167. **Moorman, N. J., D. O. Willer, and S. H. Speck.** 2003. The gammaherpesvirus 68 latency-associated nuclear antigen homolog is critical for the establishment of splenic latency. *J Virol* **77**:10295-10303.
168. **Morgan, D. G.** 1977. Observations on the antigenic relationships between Epstein-Barr virus and herpesvirus saimiri. *The Journal of general virology* **36**:281-287.
169. **Moser, J. M., J. W. Upton, K. S. Gray, and S. H. Speck.** 2005. Ex vivo stimulation of B cells latently infected with gammaherpesvirus 68 triggers reactivation from latency. *J Virol* **79**:5227-5231.
170. **Mounce, B. C., F. C. Tsan, L. Droit, S. Kohler, J. M. Reitsma, L. A. Cirillo, and V. L. Tarakanova.** 2011. Gammaherpesvirus gene expression and DNA synthesis are facilitated by viral protein kinase and histone variant H2AX. *Virology* **420**:73-81.
171. **Munir, M., and M. Berg.** 2013. The multiple faces of protein kinase R in antiviral defense. *Virulence* **4**:85-89.
172. **Murakami, Y., R. Fukui, Y. Motoi, A. Kanno, T. Shibata, N. Tanimura, S. Saitoh, and K. Miyake.** 2014. Roles of the cleaved N-terminal TLR3 fragment and cell surface TLR3 in double-stranded RNA sensing. *J Immunol* **193**:5208-5217.
173. **Nakamura, H., M. Li, J. Zarycki, and J. U. Jung.** 2001. Inhibition of p53 tumor suppressor by viral interferon regulatory factor. *J Virol* **75**:7572-7582.
174. **Naranatt, P. P., S. M. Akula, and B. Chandran.** 2002. Characterization of gamma2-human herpesvirus-8 glycoproteins gH and gL. *Archives of virology* **147**:1349-1370.
175. **Nash, A. A., B. M. Dutia, J. P. Stewart, and A. J. Davison.** 2001. Natural history of murine gamma-herpesvirus infection. *Philosophical transactions of the Royal Society of London. Series B, Biological sciences* **356**:569-579.

176. **Nguyen, Y., B. A. McGuffie, V. E. Anderson, and J. B. Weinberg.** 2008. Gammaherpesvirus modulation of mouse adenovirus type 1 pathogenesis. *Virology* **380**:182-190.
177. **Nicholas, J.** 2005. Human gammaherpesvirus cytokines and chemokine receptors. *J Interferon Cytokine Res* **25**:373-383.
178. **Nicholas, J.** 2003. Human herpesvirus-8-encoded signalling ligands and receptors. *Journal of biomedical science* **10**:475-489.
179. **Niederman, J. C., R. W. McCollum, G. Henle, and W. Henle.** 1968. Infectious mononucleosis. Clinical manifestations in relation to EB virus antibodies. *Jama* **203**:205-209.
180. **Noel, J. C., F. De Thier, M. Heenen, I. Fayt, D. Abramowicz, and J. M. Doutrelepont.** 1997. HHV-8 is associated with recurrent Kaposi's sarcoma in a renal transplant recipient. *Transplant international : official journal of the European Society for Organ Transplantation* **10**:81-82.
181. **Noh, C. W., H. J. Cho, H. R. Kang, H. Y. Jin, S. Lee, H. Deng, T. T. Wu, V. Arumugaswami, R. Sun, and M. J. Song.** 2012. The virion-associated open reading frame 49 of murine gammaherpesvirus 68 promotes viral replication both in vitro and in vivo as a derepressor of RTA. *J Virol* **86**:1109-1118.
182. **O'Flaherty, B. M., T. Soni, B. S. Wakeman, and S. H. Speck.** 2014. The murine gammaherpesvirus immediate-early Rta synergizes with IRF4, targeting expression of the viral M1 superantigen to plasma cells. *PLoS Pathog* **10**:e1004302.
183. **Ogawa, Y., D. Watanabe, K. Hirota, M. Ikuma, K. Yajima, D. Kasai, K. Mori, Y. Ota, Y. Nishida, T. Uehira, M. Mano, T. Yamane, and T. Shirasaka.** 2014. Rapid multiorgan failure due to large B-cell lymphoma arising in human herpesvirus-8-associated multicentric Castleman's disease in a patient with human immunodeficiency virus infection. *Internal medicine* **53**:2805-2809.
184. **Ohto, U., T. Shibata, H. Tanji, H. Ishida, E. Krayukhina, S. Uchiyama, K. Miyake, and T. Shimizu.** 2015. Structural basis of CpG and inhibitory DNA recognition by Toll-like receptor 9. *Nature*.
185. **Ozbun, M. A., and C. Meyers.** 1998. Temporal usage of multiple promoters during the life cycle of human papillomavirus type 31b. *J Virol* **72**:2715-2722.
186. **Paden, C. R., J. C. Forrest, N. J. Moorman, and S. H. Speck.** 2010. Murine gammaherpesvirus 68 LANA is essential for virus reactivation from splenocytes but not long-term carriage of viral genome. *J Virol* **84**:7214-7224.
187. **Paden, C. R., J. C. Forrest, S. A. Tibbetts, and S. H. Speck.** 2012. Unbiased mutagenesis of MHV68 LANA reveals a DNA-binding domain required for LANA function in vitro and in vivo. *PLoS Pathog* **8**:e1002906.
188. **Paulson, E. J., J. D. Fingerroth, J. L. Yates, and S. H. Speck.** 2002. Methylation of the EBV genome and establishment of restricted latency in low-passage EBV-infected 293 epithelial cells. *Virology* **299**:109-121.
189. **Pavlova, I., C. Yulin, and S. Speck.** 2005. Murine gammaherpesvirus 68 Rta-dependent activation of the gene 57 promoter. *Virology* **333**:169-179.

190. **Pavlova, I. V., H. W. Virgin, and S. H. Speck.** 2003. Disruption of Gammaherpesvirus 68 Gene 50 Demonstrates that Rta Is Essential for Virus Replication. *Journal of Virology* **77**:5731-5739.
191. **Perkins, A. S., and J. W. Friedberg.** 2008. Burkitt lymphoma in adults. *Hematology / the Education Program of the American Society of Hematology*. American Society of Hematology. Education Program:341-348.
192. **Perry, S. T., and T. Compton.** 2006. Kaposi's sarcoma-associated herpesvirus virions inhibit interferon responses induced by envelope glycoprotein gpK8.1. *J Virol* **80**:11105-11114.
193. **Pestka, S., C. D. Krause, and M. R. Walter.** 2004. Interferons, interferon-like cytokines, and their receptors. *Immunological reviews* **202**:8-32.
194. **Pestka, S., J. A. Langer, K. C. Zoon, and C. E. Samuel.** 1987. Interferons and their actions. *Annual review of biochemistry* **56**:727-777.
195. **Polcicova, K., Z. Hrabovska, J. Mistrikova, J. Tomaskova, J. Pastorek, S. Pastorekova, and J. Kopacek.** 2008. Up-regulation of Murid herpesvirus 4 ORF50 by hypoxia: possible implication for virus reactivation from latency. *Virus research* **132**:257-262.
196. **Puglielli, M. T., N. Desai, and S. H. Speck.** 1997. Regulation of EBNA gene transcription in lymphoblastoid cell lines: characterization of sequences downstream of BCR2 (Cp). *J Virol* **71**:120-128.
197. **Pyakurel, P., F. Pak, A. R. Mwakigonja, E. Kaaya, and P. Biberfeld.** 2007. KSHV/HHV-8 and HIV infection in Kaposi's sarcoma development. *Infect Agent Cancer* **2**:4.
198. **Raab-Traub, N.** 2002. Epstein-Barr virus in the pathogenesis of NPC. *Seminars in cancer biology* **12**:431-441.
199. **Ragoczy, T., L. Heston, and G. Miller.** 1998. The Epstein-Barr virus Rta protein activates lytic cycle genes and can disrupt latency in B lymphocytes. *J Virol* **72**:7978-7984.
200. **Ragoczy, T., and G. Miller.** 1999. Role of the epstein-barr virus RTA protein in activation of distinct classes of viral lytic cycle genes. *J Virol* **73**:9858-9866.
201. **Rangaswamy, U. S., and S. H. Speck.** 2014. Murine gammaherpesvirus M2 protein induction of IRF4 via the NFAT pathway leads to IL-10 expression in B cells. *PLoS Pathog* **10**:e1003858.
202. **Reese, T. A., B. S. Wakeman, H. S. Choi, M. M. Hufford, S. C. Huang, X. Zhang, M. D. Buck, A. Jezewski, A. Kambal, C. Y. Liu, G. Goel, P. J. Murray, R. J. Xavier, M. H. Kaplan, R. Renne, S. H. Speck, M. N. Artyomov, E. J. Pearce, and H. W. Virgin.** 2014. Coinfection. Helminth infection reactivates latent gamma-herpesvirus via cytokine competition at a viral promoter. *Science* **345**:573-577.
203. **Reikine, S., J. B. Nguyen, and Y. Modis.** 2014. Pattern Recognition and Signaling Mechanisms of RIG-I and MDA5. *Frontiers in immunology* **5**:342.
204. **Rickabaugh, T. M., H. J. Brown, D. Martinez-Guzman, T. T. Wu, L. Tong, F. Yu, S. Cole, and R. Sun.** 2004. Generation of a latency-deficient gammaherpesvirus that is protective against secondary infection. *J Virol* **78**:9215-9223.
205. **Rickabaugh, T. M., H. J. Brown, T. T. Wu, M. J. Song, S. Hwang, H. Deng, K. Mitsouras, and R. Sun.** 2005. Kaposi's sarcoma-associated herpesvirus/human herpesvirus 8 RTA reactivates murine gammaherpesvirus 68 from latency. *J Virol* **79**:3217-3222.
206. **Rickinson, A. B.** 1996. Changing seroepidemiology of HHV-8. *Lancet* **348**:1110-1111.

207. **Rickinson, A. B.** 2014. Co-infections, inflammation and oncogenesis: future directions for EBV research. *Seminars in cancer biology* **26**:99-115.
208. **Roan, F., N. Inoue, and M. K. Offermann.** 2002. Activation of cellular and heterologous promoters by the human herpesvirus 8 replication and transcription activator. *Virology* **301**:293-304.
209. **Robertson, K. A., E. J. Usherwood, and A. A. Nash.** 2001. Regression of a murine gammaherpesvirus 68-positive b-cell lymphoma mediated by CD4 T lymphocytes. *J Virol* **75**:3480-3482.
210. **Rogers, R. P., M. Woisetschlaeger, and S. H. Speck.** 1990. Alternative splicing dictates translational start in Epstein-Barr virus transcripts. *The EMBO journal* **9**:2273-2277.
211. **Rohner, E., N. Wyss, S. Trelle, S. M. Mbulaiteye, M. Egger, U. Novak, M. Zwahlen, and J. Bohlius.** 2014. HHV-8 seroprevalence: a global view. *Systematic reviews* **3**:11.
212. **Rooney, C. M., D. T. Rowe, T. Ragot, and P. J. Farrell.** 1989. The spliced BZLF1 gene of Epstein-Barr virus (EBV) transactivates an early EBV promoter and induces the virus productive cycle. *J Virol* **63**:3109-3116.
213. **Rutgers, J. L., R. Wiczorek, F. Bonetti, K. L. Kaplan, D. N. Posnett, A. E. Friedman-Kien, and D. M. Knowles, 2nd.** 1986. The expression of endothelial cell surface antigens by AIDS-associated Kaposi's sarcoma. Evidence for a vascular endothelial cell origin. *Am J Pathol* **122**:493-499.
214. **Ruvolo, V., L. Navarro, C. E. Sample, M. David, S. Sung, and S. Swaminathan.** 2003. The Epstein-Barr virus SM protein induces STAT1 and interferon-stimulated gene expression. *J Virol* **77**:3690-3701.
215. **Sadler, R., L. Wu, B. Forghani, R. Renne, W. Zhong, B. Herndier, and D. Ganem.** 1999. A complex translational program generates multiple novel proteins from the latently expressed kaposin (K12) locus of Kaposi's sarcoma-associated herpesvirus. *J Virol* **73**:5722-5730.
216. **Safai, B., R. Lynfield, D. A. Lowenthal, and B. Koziner.** 1987. Cancers-associated with HIV infection. *Anticancer research* **7**:1055-1067.
217. **Said, W., K. Chien, S. Takeuchi, T. Tasaka, H. Asou, S. K. Cho, S. de Vos, E. Cesarman, D. M. Knowles, and H. P. Koeffler.** 1996. Kaposi's sarcoma-associated herpesvirus (KSHV or HHV8) in primary effusion lymphoma: ultrastructural demonstration of herpesvirus in lymphoma cells. *Blood* **87**:4937-4943.
218. **Saito, F., T. Ito, J. M. Connett, M. A. Schaller, W. F. t. Carson, C. M. Hogaboam, R. Rochford, and S. L. Kunkel.** 2013. MHV68 latency modulates the host immune response to influenza A virus. *Inflammation* **36**:1295-1303.
219. **Sarawar, S. R., R. D. Cardin, J. W. Brooks, M. Mehrpooya, R. A. Tripp, and P. C. Doherty.** 1996. Cytokine production in the immune response to murine gammaherpesvirus 68. *J Virol* **70**:3264-3268.
220. **Sathish, N., F. X. Zhu, E. E. Golub, Q. Liang, and Y. Yuan.** 2011. Mechanisms of autoinhibition of IRF-7 and a probable model for inactivation of IRF-7 by Kaposi's sarcoma-associated herpesvirus protein ORF45. *J Biol Chem* **286**:746-756.
221. **Schaefer, B. C., J. L. Strominger, and S. H. Speck.** 1997. Host-cell-determined methylation of specific Epstein-Barr virus promoters regulates the choice between distinct viral latency programs. *Mol Cell Biol* **17**:364-377.

222. **Scott, F. M., and S. H. Speck.** 2014. A tissue culture model of murine gammaherpesvirus replication reveals roles for the viral cyclin in both virus replication and egress from infected cells. *PLoS One* **9**:e93871.
223. **Seo, T., J. Park, D. Lee, S. G. Hwang, and J. Choe.** 2001. Viral interferon regulatory factor 1 of Kaposi's sarcoma-associated herpesvirus binds to p53 and represses p53-dependent transcription and apoptosis. *J Virol* **75**:6193-6198.
224. **Siegel, A. M., J. H. Herskowitz, and S. H. Speck.** 2008. The MHV68 M2 protein drives IL-10 dependent B cell proliferation and differentiation. *PLoS Pathog* **4**:e1000039.
225. **Silvennoinen, O., J. N. Ihle, J. Schlessinger, and D. E. Levy.** 1993. Interferon-induced nuclear signalling by Jak protein tyrosine kinases. *Nature* **366**:583-585.
226. **Simas, J. P., and S. Efstathiou.** 1998. Murine gammaherpesvirus 68: a model for the study of gammaherpesvirus pathogenesis. *Trends in microbiology* **6**:276-282.
227. **Sinclair, A. J., M. Brimmell, F. Shanahan, and P. J. Farrell.** 1991. Pathways of activation of the Epstein-Barr virus productive cycle. *J Virol* **65**:2237-2244.
228. **Song, M. J., H. Deng, and R. Sun.** 2003. Comparative study of regulation of RTA-responsive genes in Kaposi's sarcoma-associated herpesvirus/human herpesvirus 8. *J Virol* **77**:9451-9462.
229. **Song, M. J., S. Hwang, W. H. Wong, T. T. Wu, S. Lee, H. I. Liao, and R. Sun.** 2005. Identification of viral genes essential for replication of murine gamma-herpesvirus 68 using signature-tagged mutagenesis. *Proc Natl Acad Sci U S A* **102**:3805-3810.
230. **Soulier, J., L. Grollet, E. Oksenhendler, P. Cacoub, D. Cazals-Hatem, P. Babinet, M. F. d'Agay, J. P. Clauvel, M. Raphael, L. Degos, and et al.** 1995. Kaposi's sarcoma-associated herpesvirus-like DNA sequences in multicentric Castleman's disease. *Blood* **86**:1276-1280.
231. **Speck, S. H., A. Pfitzner, and J. L. Strominger.** 1986. An Epstein-Barr virus transcript from a latently infected, growth-transformed B-cell line encodes a highly repetitive polypeptide. *Proc Natl Acad Sci U S A* **83**:9298-9302.
232. **Speck, S. H., and J. L. Strominger.** 1985. Analysis of the transcript encoding the latent Epstein-Barr virus nuclear antigen I: a potentially polycistronic message generated by long-range splicing of several exons. *Proc Natl Acad Sci U S A* **82**:8305-8309.
233. **Speck, S. H., and H. W. Virgin.** 1999. Host and viral genetics of chronic infection: a mouse model of gamma-herpesvirus pathogenesis. *Curr Opin Microbiol* **2**:403-409.
234. **Stark, G. R.** 2007. How cells respond to interferons revisited: from early history to current complexity. *Cytokine & growth factor reviews* **18**:419-423.
235. **Steed, A., T. Buch, A. Waisman, and H. W. t. Virgin.** 2007. Gamma interferon blocks gammaherpesvirus reactivation from latency in a cell type-specific manner. *J Virol* **81**:6134-6140.
236. **Stewart, J. P., and C. M. Rooney.** 1992. The interleukin-10 homolog encoded by Epstein-Barr virus enhances the reactivation of virus-specific cytotoxic T cell and HLA-unrestricted killer cell responses. *Virology* **191**:773-782.
237. **Sun, C. C., and D. A. Thorley-Lawson.** 2007. Plasma Cell-Specific Transcription Factor XBP-1s Binds to and Transactivates the Epstein-Barr Virus BZLF1 Promoter. *Journal of Virology* **81**:13566-13577.

238. **Sun, Q., L. Sun, H. H. Liu, X. Chen, R. B. Seth, J. Forman, and Z. J. Chen.** 2006. The specific and essential role of MAVS in antiviral innate immune responses. *Immunity* **24**:633-642.
239. **Sun, R., S. F. Lin, L. Gradoville, Y. Yuan, F. Zhu, and G. Miller.** 1998. A viral gene that activates lytic cycle expression of Kaposi's sarcoma-associated herpesvirus. *Proc Natl Acad Sci U S A* **95**:10866-10871.
240. **Sun, R., S. F. Lin, K. Staskus, L. Gradoville, E. Grogan, A. Haase, and G. Miller.** 1999. Kinetics of Kaposi's sarcoma-associated herpesvirus gene expression. *J Virol* **73**:2232-2242.
241. **Sunil-Chandra, N. P., J. Arno, J. Fazakerley, and A. A. Nash.** 1994. Lymphoproliferative disease in mice infected with murine gammaherpesvirus 68. *Am J Pathol* **145**:818-826.
242. **Sunil-Chandra, N. P., S. Efstathiou, J. Arno, and A. A. Nash.** 1992. Virological and pathological features of mice infected with murine gamma-herpesvirus 68. *The Journal of general virology* **73 (Pt 9)**:2347-2356.
243. **Swenson, J. J., E. Holley-Guthrie, and S. C. Kenney.** 2001. Epstein-Barr virus immediate-early protein BRLF1 interacts with CBP, promoting enhanced BRLF1 transactivation. *J Virol* **75**:6228-6234.
244. **Tarakanova, V. L., F. Suarez, S. A. Tibbetts, M. A. Jacoby, K. E. Weck, J. L. Hess, S. H. Speck, and H. W. t. Virgin.** 2005. Murine gammaherpesvirus 68 infection is associated with lymphoproliferative disease and lymphoma in BALB beta2 microglobulin-deficient mice. *J Virol* **79**:14668-14679.
245. **Tibbetts, S. A., L. F. van Dyk, S. H. Speck, and H. W. t. Virgin.** 2002. Immune control of the number and reactivation phenotype of cells latently infected with a gammaherpesvirus. *J Virol* **76**:7125-7132.
246. **Torgbor, C., P. Awuah, K. Deitsch, P. Kalantari, K. A. Duca, and D. A. Thorley-Lawson.** 2014. A multifactorial role for *P. falciparum* malaria in endemic Burkitt's lymphoma pathogenesis. *PLoS Pathog* **10**:e1004170.
247. **Trinchieri, G.** 2010. Type I interferon: friend or foe? *The Journal of experimental medicine* **207**:2053-2063.
248. **Unterholzner, L.** 2013. The interferon response to intracellular DNA: why so many receptors? *Immunobiology* **218**:1312-1321.
249. **Urier, G., M. Buisson, P. Chambard, and A. Sergeant.** 1989. The Epstein-Barr virus early protein EB1 activates transcription from different responsive elements including AP-1 binding sites. *The EMBO journal* **8**:1447-1453.
250. **Usherwood, E. J., J. P. Stewart, and A. A. Nash.** 1996. Characterization of tumor cell lines derived from murine gammaherpesvirus-68-infected mice. *J Virol* **70**:6516-6518.
251. **Usherwood, E. J., J. P. Stewart, K. Robertson, D. J. Allen, and A. A. Nash.** 1996. Absence of splenic latency in murine gammaherpesvirus 68-infected B cell-deficient mice. *The Journal of general virology* **77 (Pt 11)**:2819-2825.
252. **van Boxel-Dezaire, A. H., M. R. Rani, and G. R. Stark.** 2006. Complex modulation of cell type-specific signaling in response to type I interferons. *Immunity* **25**:361-372.
253. **Verpooten, D., Z. Feng, T. Valyi-Nagy, Y. Ma, H. Jin, Z. Yan, C. Zhang, Y. Cao, and B. He.** 2009. Dephosphorylation of eIF2alpha mediated by the gamma134.5 protein of herpes simplex virus 1 facilitates viral neuroinvasion. *J Virol* **83**:12626-12630.

254. **Virgin, H. W., E. J. Wherry, and R. Ahmed.** 2009. Redefining chronic viral infection. *Cell* **138**:30-50.
255. **Virgin, H. W. t., P. Latreille, P. Wamsley, K. Hallsworth, K. E. Weck, A. J. Dal Canto, and S. H. Speck.** 1997. Complete sequence and genomic analysis of murine gammaherpesvirus 68. *J Virol* **71**:5894-5904.
256. **Wakeman, B. S., L. S. Johnson, C. R. Paden, K. S. Gray, H. W. Virgin, and S. H. Speck.** 2014. Identification of alternative transcripts encoding the essential murine gammaherpesvirus lytic transactivator RTA. *J Virol* **88**:5474-5490.
257. **Wang, J. T., S. L. Doong, S. C. Teng, C. P. Lee, C. H. Tsai, and M. R. Chen.** 2009. Epstein-Barr virus BGLF4 kinase suppresses the interferon regulatory factor 3 signaling pathway. *J Virol* **83**:1856-1869.
258. **Wang, S., S. Liu, M. H. Wu, Y. Geng, and C. Wood.** 2001. Identification of a cellular protein that interacts and synergizes with the RTA (ORF50) protein of Kaposi's sarcoma-associated herpesvirus in transcriptional activation. *J Virol* **75**:11961-11973.
259. **Wang, Y., Q. Tang, G. G. Maul, and Y. Yuan.** 2006. Kaposi's sarcoma-associated herpesvirus ori-Lyt-dependent DNA replication: dual role of replication and transcription activator. *J Virol* **80**:12171-12186.
260. **Warming, S.** 2005. Simple and highly efficient BAC recombineering using galk selection. *Nucleic Acids Research* **33**:e36-e36.
261. **Weck, K. E., M. L. Barkon, L. I. Yoo, S. H. Speck, and H. I. Virgin.** 1996. Mature B cells are required for acute splenic infection, but not for establishment of latency, by murine gammaherpesvirus 68. *J Virol* **70**:6775-6780.
262. **Weck, K. E., S. S. Kim, H. I. Virgin, and S. H. Speck.** 1999. B cells regulate murine gammaherpesvirus 68 latency. *J Virol* **73**:4651-4661.
263. **Weck, K. E., S. S. Kim, H. I. Virgin, and S. H. Speck.** 1999. Macrophages are the major reservoir of latent murine gammaherpesvirus 68 in peritoneal cells. *J Virol* **73**:3273-3283.
264. **Weslow-Schmidt, J. L., N. A. Jewell, S. E. Mertz, J. P. Simas, J. E. Durbin, and E. Flano.** 2007. Type I interferon inhibition and dendritic cell activation during gammaherpesvirus respiratory infection. *J Virol* **81**:9778-9789.
265. **West, J. T., and C. Wood.** 2003. The role of Kaposi's sarcoma-associated herpesvirus/human herpesvirus-8 regulator of transcription activation (RTA) in control of gene expression. *Oncogene* **22**:5150-5163.
266. **Whitehouse, A., I. M. Carr, J. C. Griffiths, and D. M. Meredith.** 1997. The herpesvirus saimiri ORF50 gene, encoding a transcriptional activator homologous to the Epstein-Barr virus R protein, is transcribed from two distinct promoters of different temporal phases. *J Virol* **71**:2550-2554.
267. **Willer, D. O., and S. H. Speck.** 2003. Long-term latent murine Gammaherpesvirus 68 infection is preferentially found within the surface immunoglobulin D-negative subset of splenic B cells in vivo. *J Virol* **77**:8310-8321.
268. **Wilson, S. J., E. H. Tsao, B. L. J. Webb, H. Ye, L. Dalton-Griffin, C. Tsantoulas, C. V. Gale, M. Q. Du, A. Whitehouse, and P. Kellam.** 2007. X Box Binding Protein XBP-1s Transactivates the Kaposi's Sarcoma-Associated Herpesvirus (KSHV) ORF50 Promoter,

- Linking Plasma Cell Differentiation to KSHV Reactivation from Latency. *Journal of Virology* **81**:13578-13586.
269. **Woisetschlaeger, M., J. L. Strominger, and S. H. Speck.** 1989. Mutually exclusive use of viral promoters in Epstein-Barr virus latently infected lymphocytes. *Proc Natl Acad Sci U S A* **86**:6498-6502.
 270. **Woisetschlaeger, M., C. N. Yandava, L. A. Furmanski, J. L. Strominger, and S. H. Speck.** 1990. Promoter switching in Epstein-Barr virus during the initial stages of infection of B lymphocytes. *Proc Natl Acad Sci U S A* **87**:1725-1729.
 271. **Wood, B. M., W. P. Mboko, B. C. Mounce, and V. L. Tarakanova.** 2013. Mouse gammaherpesvirus-68 infection acts as a rheostat to set the level of type I interferon signaling in primary macrophages. *Virology* **443**:123-133.
 272. **Wu, T. T., L. Tong, T. Rickabaugh, S. Speck, and R. Sun.** 2001. Function of Rta is essential for lytic replication of murine gammaherpesvirus 68. *J Virol* **75**:9262-9273.
 273. **Wylie, K. M., J. E. Schrimpf, and L. A. Morrison.** 2009. Increased eIF2alpha phosphorylation attenuates replication of herpes simplex virus 2 vhs mutants in mouse embryonic fibroblasts and correlates with reduced accumulation of the PKR antagonist ICP34.5. *J Virol* **83**:9151-9162.
 274. **Xi, X., L. M. Persson, M. W. O'Brien, I. Mohr, and A. C. Wilson.** 2012. Cooperation between viral interferon regulatory factor 4 and RTA to activate a subset of Kaposi's sarcoma-associated herpesvirus lytic promoters. *J Virol* **86**:1021-1033.
 275. **Xin, D., L. Hu, and X. Kong.** 2008. Alternative promoters influence alternative splicing at the genomic level. *PLoS One* **3**:e2377.
 276. **Xu, Y., D. P. AuCoin, A. R. Huete, S. A. Cei, L. J. Hanson, and G. S. Pari.** 2005. A Kaposi's sarcoma-associated herpesvirus/human herpesvirus 8 ORF50 deletion mutant is defective for reactivation of latent virus and DNA replication. *J Virol* **79**:3479-3487.
 277. **Yamaji, K., S. Nabeshima, M. Murata, Y. Chong, N. Furusyo, H. Ikematsu, and J. Hayashi.** 2006. Interferon-alpha/beta upregulate IL-15 expression in vitro and in vivo: analysis in human hepatocellular carcinoma cell lines and in chronic hepatitis C patients during interferon-alpha/beta treatment. *Cancer immunology, immunotherapy : CII* **55**:394-403.
 278. **Yang, Z., H. Tang, H. Huang, and H. Deng.** 2009. RTA promoter demethylation and histone acetylation regulation of murine gammaherpesvirus 68 reactivation. *PLoS One* **4**:e4556.
 279. **Ye, F., and S. J. Gao.** 2011. A novel role of hydrogen peroxide in Kaposi sarcoma-associated herpesvirus reactivation. *Cell cycle* **10**:3237-3238.
 280. **Ye, J., D. Shedd, and G. Miller.** 2005. An Sp1 response element in the Kaposi's sarcoma-associated herpesvirus open reading frame 50 promoter mediates lytic cycle induction by butyrate. *J Virol* **79**:1397-1408.
 281. **Yim, H. C., and B. R. Williams.** 2014. Protein kinase R and the inflammasome. *J Interferon Cytokine Res* **34**:447-454.
 282. **Yoshida, H., Y. Okabe, K. Kawane, H. Fukuyama, and S. Nagata.** 2005. Lethal anemia caused by interferon-beta produced in mouse embryos carrying undigested DNA. *Nature immunology* **6**:49-56.

283. **Young, L., C. Alfieri, K. Hennessy, H. Evans, C. O'Hara, K. C. Anderson, J. Ritz, R. S. Shapiro, A. Rickinson, E. Kieff, and et al.** 1989. Expression of Epstein-Barr virus transformation-associated genes in tissues of patients with EBV lymphoproliferative disease. *N Engl J Med* **321**:1080-1085.
284. **Young, L. S., and A. B. Rickinson.** 2004. Epstein-Barr virus: 40 years on. *Nature Reviews Cancer* **4**:757-768.
285. **Yu, F., J. Feng, J. N. Harada, S. K. Chanda, S. C. Kenney, and R. Sun.** 2007. B cell terminal differentiation factor XBP-1 induces reactivation of Kaposi's sarcoma-associated herpesvirus. *FEBS Lett* **581**:3485-3488.
286. **Yu, Y., S. E. Wang, and G. S. Hayward.** 2005. The KSHV immediate-early transcription factor RTA encodes ubiquitin E3 ligase activity that targets IRF7 for proteasome-mediated degradation. *Immunity* **22**:59-70.
287. **Zalani, S., E. Holley-Guthrie, and S. Kenney.** 1996. Epstein-Barr viral latency is disrupted by the immediate-early BRLF1 protein through a cell-specific mechanism. *Proc Natl Acad Sci U S A* **93**:9194-9199.
288. **Zhang, J., S. C. Das, C. Kotalik, A. K. Pattnaik, and L. Zhang.** 2004. The latent membrane protein 1 of Epstein-Barr virus establishes an antiviral state via induction of interferon-stimulated genes. *J Biol Chem* **279**:46335-46342.
289. **Zhang, L., C. Zhu, Y. Guo, F. Wei, J. Lu, J. Qin, S. Banerjee, J. Wang, H. Shang, S. C. Verma, Z. Yuan, E. S. Robertson, and Q. Cai.** 2014. Inhibition of KAP1 enhances hypoxia-induced Kaposi's sarcoma-associated herpesvirus reactivation through RBP-Jkappa. *J Virol* **88**:6873-6884.
290. **Zhi, H., M. A. Zahoor, A. M. Shudofsky, and C. Z. Giam.** 2015. KSHV vCyclin counters the senescence/G1 arrest response triggered by NF-kappaB hyperactivation. *Oncogene* **34**:496-505.
291. **Zhu, F. X., S. M. King, E. J. Smith, D. E. Levy, and Y. Yuan.** 2002. A Kaposi's sarcoma-associated herpesviral protein inhibits virus-mediated induction of type I interferon by blocking IRF-7 phosphorylation and nuclear accumulation. *Proc Natl Acad Sci U S A* **99**:5573-5578.
292. **Zhu, F. X., N. Sathish, and Y. Yuan.** 2010. Antagonism of host antiviral responses by Kaposi's sarcoma-associated herpesvirus tegument protein ORF45. *PLoS One* **5**:e10573.
293. **Zhu, F. X., and Y. Yuan.** 2003. The ORF45 protein of Kaposi's sarcoma-associated herpesvirus is associated with purified virions. *J Virol* **77**:4221-4230.
294. **Zimber-Strobl, U., and L. J. Strobl.** 2001. EBNA2 and Notch signalling in Epstein-Barr virus mediated immortalization of B lymphocytes. *Seminars in cancer biology* **11**:423-434.